Review of primary frequency control requirements on the GB power system against a background of increasing renewable generation

Vol. 1

Appendix A

Published Papers

Ross Stuart Pearmine

Academic Supervisor: Prof. Yong-Hua Song, Brunel Institute of Power Systems, Brunel University, Uxbridge

Industrial Supervisor: Dr. Ahmad Chebbo, National Grid, Sindlesham

Identification of a load–frequency characteristic for allocation of spinning reserves on the British electricity grid

R. Pearmine, Y.H. Song, T.G. Williams and A. Chebbo

Abstract: The transmission-grid system operator must maintain the system frequency of a synchronous transmission system within legislated tolerances. This task becomes of particular importance during large power imbalances. To establish a frequency-reserve scheme that maintains a healthy system frequency, the exact behaviour of generators and load response must be known. The paper provides details of load behaviour during a number of large infeed losses. These results show that the current load–frequency sensitivity factor of 2%MW/Hz is justified, and can even be extended to a value of 2.5%MW/Hz. Therefore, this value can be substituted in the calculation of reserve schemes on the electricity grid in Great Britain.

1 Introduction

The system frequency of a synchronous transmission system varies with the imbalance between the energy fed into the network from power stations and the electrical energy taken out by consumers [1]. Any short-term imbalance of energy will result in an instantaneous drop in system frequency as system inertia is harnessed to replace the lost energy while reserve is initiated. For isolated island power systems, such as the grid in Great Britain (GB), adequate provision of energy at all times is essential to maintain safe operation of the network. Large power swings, if left unchecked, can lead to extreme frequency excursions outside the working range of generating plant. This can cause undesirable vibration in the machines, shutting down of plant, and in worst case lead to system collapse.

In practice, frequency deviations are limited through scheduling reserve for frequency response. The reserve is composed of dynamic responsive generation (spinning reserve) or nondynamic measures (demand side management) [2]. To manage the levels of reserve for frequency response, a response requirement is employed to ensure that obligations are met under large imbalances of power. It is well known that the interaction between the load characteristics, the generator behaviour and the performance of the transmission system influences the power-system frequency [3]. The formulation of a frequency-response requirement is achieved through modelling of these components against simulated loss scenarios. This paper will concentrate on the influence of the load characteristic.

IEE Proceedings online no. 20050404

doi:10.1049/ip-gtd:20050404

Paper first received 13th September 2005 and in final revised form 9th February 2006

R. Pearmine and Y.H. Song are with Brunel Institute of Power Systems, Brunel University, Uxbridge, Middx UB8 3PH, UK

T.G. Williams and A. Chebbo are with Operations and Trading, National Grid, Wokingham, UK

R. Pearmine is also with the Operations and Trading, National Grid, Wokingham, UK

E-mail: Ross.Pearmine@uk.ngrid.com

A review of existing papers concluded that most research into load–frequency response was concerned mainly with parts of whole systems [4–7] or single composite loads [8]. In both cases the load–frequency response presented covered a considerable range of values with an undefined distribution. Those quantities documented on whole systems were based on estimates [9] or had no supporting evidence [10–12]. Work presented in this paper uses a number of large-generator in-feed losses to quantify a value for the load–frequency sensitivity. This value is a key component in allocating reserve for frequency response on the GB grid.

2 System operation and reserve for frequency response

National Grid is owner of some 14 000 km of overhead transmission lines, and 1000 km of cable circuits in England and Wales. It is responsible for the operation of these circuits in England, Wales and, more recently, the transmission network in Scotland. This includes switching operations in some 447 substations across the country at 400, 275 and 132 kV voltage levels. The system shares a 2000 MW interconnector with France, and Scotland has a 500 MW interconnector with Ireland. Both of these links are DC and do not act as synchronous ties influencing grid frequency, therefore GB can be considered as an isolated grid. It is in the interest of the operator to ensure that the network remains safe and secure at all times, and the GB transmission system is operated to strict quality standards. The Transmission System Security and Quality of Supply Standard [13] explains the frequency obligations of the system which shall be normally 50 Hz and are to be controlled within the limits of 49.5 and 50.5 Hz. For an instantaneous loss of over 1 GW but below 1320 MW, considered an 'abnormal' event, the system may deviate beyond these limits but returning to 49.5 Hz within 1 min. In addition to these safety limits, National Grid imposes its own operating limits of 50 ± 0.2 Hz for losses up to 300 MW, and a maximum deviation of -0.8 Hz on abnormal events.

To ensure that these limits are met, a predetermined amount of reserve is held for frequency response, to recover any lost generation. This reserve is mainly held on spinning units that operate at reduced output (typically 50–90% of rated output) to provide the necessary headroom to act under governor droop. Unlike other network operators [14, 15] frequency response held on the GB system is optimised every 20 min according to the total network demand and the maximum potential loss of generation on the system. On a typical operating day, around 70% of system generators will operate in a limited frequency-sensitive mode, with the remaining units deloaded to provide the frequency-response requirement.

The frequency-response holding is complicated by an artificial distinction whereby the requirement is defined over specific time scales. Primary-response is deliverable at 10 s after an incident has occurred and must be maintained, where necessary, for a further 20 s. Secondary-response is deliverable subsequent to primary time scales and can be required for 30 min after an event. The primary-response requirement is defined to arrest the drop in frequency and the secondary-response requirement restores frequency within operational limits. Both primary- and secondary-response levels are established at each of the optimisation stages during the day. In addition, a level of standing reserve is scheduled on 'warm' or fast-starting units that can be called on within 20 min. This will be instructed under manual action to restore the response holding levels to the prefault state. Figure 1 shows a typical frequency trace following an incident and the associated delivery of reserves.

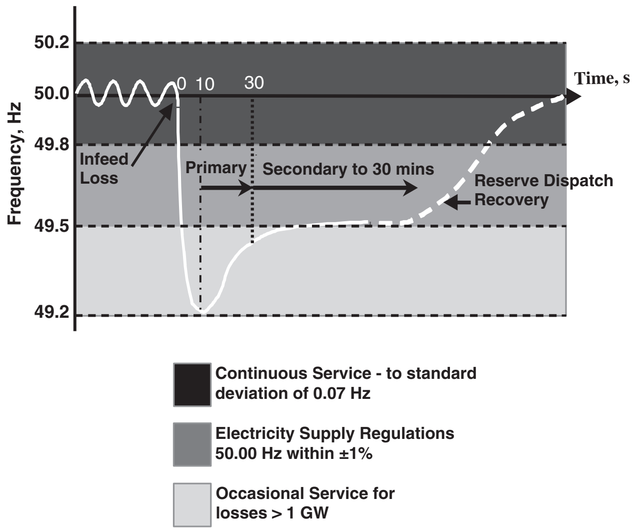

Fig. 1 *Frequency response on the UK grid*

Every generator offering a responsive mode of operation described above (acting under governor droop) that is energised on the UK grid also has a portfolio of response contracts. These contracts define the output in power expected at set frequency deviations and set load levels over secondary and/or primary time scales. The response requirement can thus be met through the commitment of frequency-responsive plant until the sum of contracted primary- and secondary-response levels equals the optimised response-holding level.

2.1 Establishing frequency-response-holding levels

Levels of both primary and secondary-response are established at each of the optimisation stages during the day. This holding level is derived from a set of requirement curves that quantify the recommended frequency-response values at a range of system-demand levels, for a number of loss scenarios.

Primary-response-requirement curve values are calculated from simulations of generation losses using a dynamic simulation package. These simulations establish the required net generator response to limit the drop in frequency to that expressed in the standard. The system-network model is lumped as a single transmission line with all loads connected to one end of the line and all generators connected to the other. All active demand is lumped together and is assumed to have the recommended load–frequency characteristic. The system generators are grouped into different fuel types (i.e. nuclear, coal, gas) with each generator type having its own generic governor and exciter model. The starting frequency is assumed to be at 50 Hz.

The resulting primary requirements, derived through simulations, are multiplied by a margin that is included to cater for the necessary assumptions made to formulate the response requirement. These assumptions include:

(*a*) modelling inaccuracies;
(*b*) variation in the choice of units used to provide response;
(*c*) errors in the system-wide parameters used, such as starting frequency;
(*d*) 100% supply of generator response as agreed in contracts;
(*e*) operation of rate of change of frequency relays;
(*f*) under performance of the load response;
(*g*) increased system losses following the fault; and
(*h*) variation of CCGT output with temperature.

The secondary-response requirement R_{sec} is calculated by considering the level of risk for which response is being calculated 'Risk' together with the required balancing actions to limit the maximum frequency deviation allowed on secondary-response time scales ($\Delta F_{max,sec}$). The recommended load–frequency characteristic α is also included in this calculation. Secondary-response-requirement curves are calculated for a range of system demand levels (D_{GB}) using (1):

$$R_{sec} = (1 + \varepsilon)(\text{Risk} - \alpha.D_{GB}.\Delta f_{max,sec}) \quad (1)$$

A margin ε is again included in the calculation to cater for the necessary assumptions made to formulate the secondary-response requirement.

Optimisation of the response requirements, which includes the load-sensitivity factor, increases the efficiency of the response-holding process. To compare with other grids of similar scale, the Nordic Power System assumes a 200 MW level of self regulation from the load at all times to contain frequency within 0.5 Hz of nominal [15]. At a minimum system load of 24 300 MW, this translates to a frequency-sensitivity of 1.6%/Hz.

2.2 Effect of an in-feed loss on system frequency

Figure 2 illustrates the real-life behaviour of grid-connected generators in England and Wales to a loss of 1050 MW in Scotland on 19th April 2005 at 19:04. The maximum frequency deviation for this example is 0.303 Hz, and the total system demand preloss was 45 275 MW (40 600 MW in England and Wales). Figure 2 shows a total change in output from spinning reserves of 500 MW at the point of minimum frequency. 80 MW of demand-side reserve tripped at 49.7 Hz and frequency reserve in Scotland increased by around 100 MW. In total, nationally,

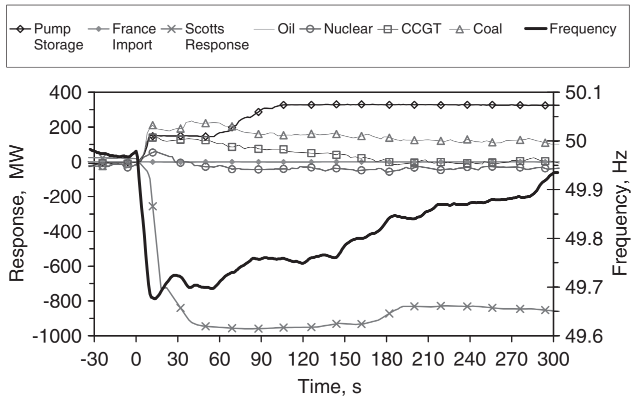

Fig. 2 *Response of generators in England and Wales to a 1050 MW in-feed loss*

680 MW of response was supplied through frequency-responsive services. The shortfall of $1050 - 680 = 370$ MW was supplied by the frequency sensitivity of the load.

The previous example shows how the response requirement is heavily dependent on the load–frequency sensitivity making up 36% of the lost power. The precise quantity of the load sensitivity is determined through the consumer-load mix and behaviour. In calculation of the response requirement, National Grid currently uses a continuous value of 2%MW/Hz for its load–frequency sensitivity, which is derived through earlier investigations [16].

The load sensitivity is largely due to motor loads on the system, and can be affected by semiconductor-controlled power devices that break the synchronous tie between the power grid and equipment. Examples of such devices are found in new generations of industrial drive controllers and switch-mode power supplies, common in most personal computers. As proportions of these devices increase, they are also met with changes in customer behaviour, such as an increased utilisation of air conditioning. Both of these effects may be reflected in changes of the load response. Increasing proportions of distributed renewable generation may also influence the load sensitivity seen by National Grid at supply points. These generators act to displace demand at these connections, and the inertia and dynamic behaviour, as seen by the grid (or not if semiconductor controllers are used), will have a bearing on the load sensitivity experienced. This potential change in load mix since early studies means that investigation is required to confirm if this value is still applicable for reserve studies. A further possibility exists to optimise the continuous value of load–frequency sensitivity against time of day or seasonal variations.

3 Quantifying a system-load-sensitivity factor

A number of literature sources quote the load-sensitivity factor as a percentage value, which is normalised against base frequency and system demand. However, we will keep with the convention adopted by National Grid and quote sensitivity in percentage MW reduction per hertz deviation.

The load–frequency response accounts for a substantial portion of the lost energy and this change in load ΔP_L becomes a self-regulating effect, helping to stabilise frequency. This load response is a function of the frequency deviation Δf, total system demand (P_L) and the variation in supply voltage resulting from the change in impedance of substation components due to frequency (transformers, shunt reactors etc.). Papers that define the voltage component of the load response [17] are valuable for transient and voltage-stability studies, while measurements of the frequency component are essential in frequency-stability studies.

Data on system loads extracted from the National Grid energy-management system are not of the appropriate resolution to capture transient properties of the British grid. However, suitable generation quantities are metered from substations on the transmission system. By considering only the power change, the individual voltage component and frequency component can be incorporated nationally into a single frequency-sensitivity factor k_L, see (2):

$$\frac{\Delta P_L}{P_L} = k_L . \Delta f \tag{2}$$

To investigate the effects of the frequency-sensitivity factor, a record of the national generation totals was established, monitoring values at intervals of 2 s. Local grid frequency was also recorded at a sample rate of 1 s. By using these values, it is possible to monitor the dynamics of the grid during the loss of a generating unit. In order to substitute for system loads, a period of stable frequency is required for the assumption to hold true that prefault load equals the total system generation P_T. Using this hypothesis, the change in load can be represented by the sum of the total change in system generation ΔP_T, the loss of generation P_{Loss} and any frequency control by demand management P_{FCDM} (Fig. 3). The load-sensitivity factor can thus be calculated from the relation given in (3):

$$k_L = \frac{\Delta P_T + P_{Loss} + P_{FCDM}}{\Delta f . P_T} \tag{3}$$

Early trials showed that a meaningful load-sensitivity factor could reliably be established from generator losses greater than 200 MW. Over the course of a year, data were collected for 81 individual system incidents that led to loss of generator supply.

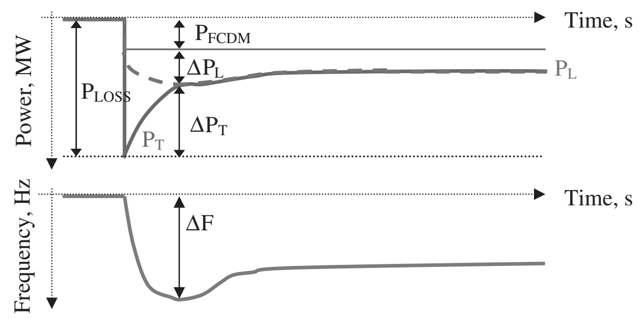

Fig. 3 *Assumed network response used in the calculation of load sensitivity*

3.1 Inertial method of calculating load sensitivity

A second technique [18] was also used to increase confidence in the results calculated from (3), based on a method of establishing a spinning-reserve requirement. The initial rate of decay of frequency is applied to quantify the imbalance between load and generation, effectively the load response. For a known system inertia M, the load-sensitivity factor is given by (4). The data provided by this method were accepted to be of lower significance as they were a measure of the imbalance of load and generation at the instant of loss. As described by Fig. 3, the load response should fall further if frequency continues to drop; results would therefore be conservative. The result is also sensitive to the 1 s sampling interval of the recorded grid frequency used in calculating the initial decay rates

$$M\frac{d(\Delta f)}{dt} + k_L.\Delta f = P_L - P_T = \Delta P_L \quad (4)$$

4 Discussion

Figure 4 shows the calculated sensitivity factors using (3) and the recorded incidents plotted against the time of the day and compared with a typical daily load profile experienced by National Grid. The distribution of values is over a large range between 1.4 and 6.8%MW/Hz; this agrees with a number of sources [19, 20]. This range of values is, in part, due to the changing load mix throughout the day and also in part to seasonal variations. Figure 4 shows low correlation between the sensitivity value and the period of the day, and a low correlation with system demand levels.

Figure 5 shows the annual variation of the sensitivity factor using both (3) and (4). Results from both techniques yield a very similar range of values from the recorded incidents, with a correlation factor of 0.23 between the two methods. Overall, the results from (4) are generally lower than those obtained from (3) for reasons previously discussed. Instances when this is not the case can be attributed to error introduced through the 1 s sampling interval or events when the preloss frequency is not stable. Figure 5 also shows, as expected, that there is no correlation between the size of loss and the sensitivity factor.

Of the 81 incidents monitored, a clear void of values occurred during the months of January, July and September. This impedes a possible trend from being established, given the available data set; however, study of the remaining results would seem to show a lack in seasonal trend for the data.

Figure 6 shows the frequency distribution of results using (3), together with lines of 95% confidence limits. The results indicate a mean value of 3.8%MW/Hz; however, in the interest of security, a worst case must be considered. The 10th percentile from the line of best fit (derived from maximum-likelihood estimation) suggests a load sensitivity of 2.16%MW/Hz, with a 95% confidence that the value lies between 1.86 and 2.5. The results have shown that 93% of values calculated are above a sensitivity of 2%MW/Hz. This gives assurance in using this value as a minimum response expected from the load when used in conjunction

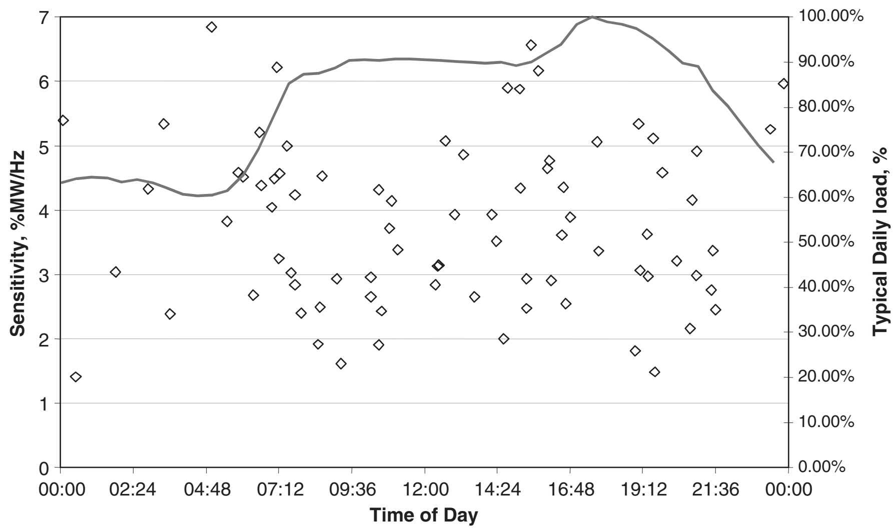

Fig. 4 *Typical daily variation of demand against measured load sensitivity*

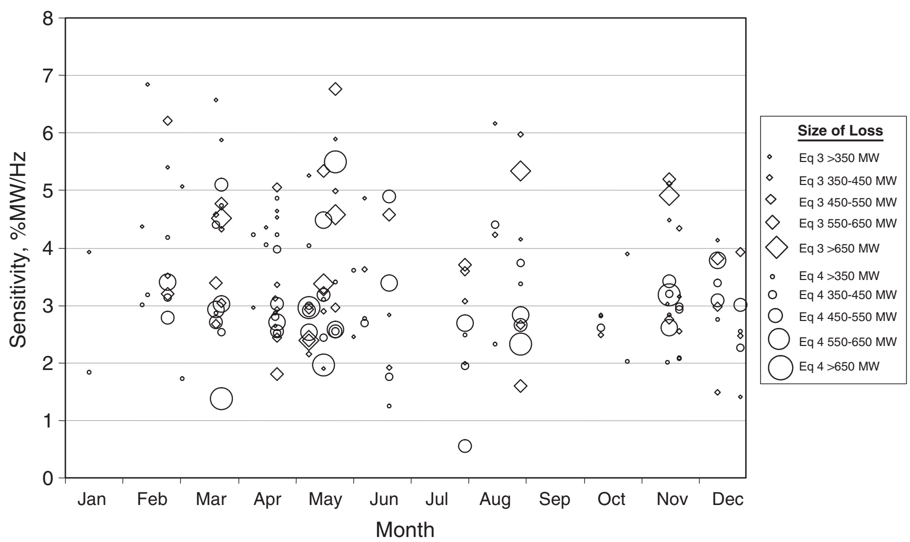

Fig. 5 *Annual variation of load sensitivity to frequency, April 2004 to June 2005*

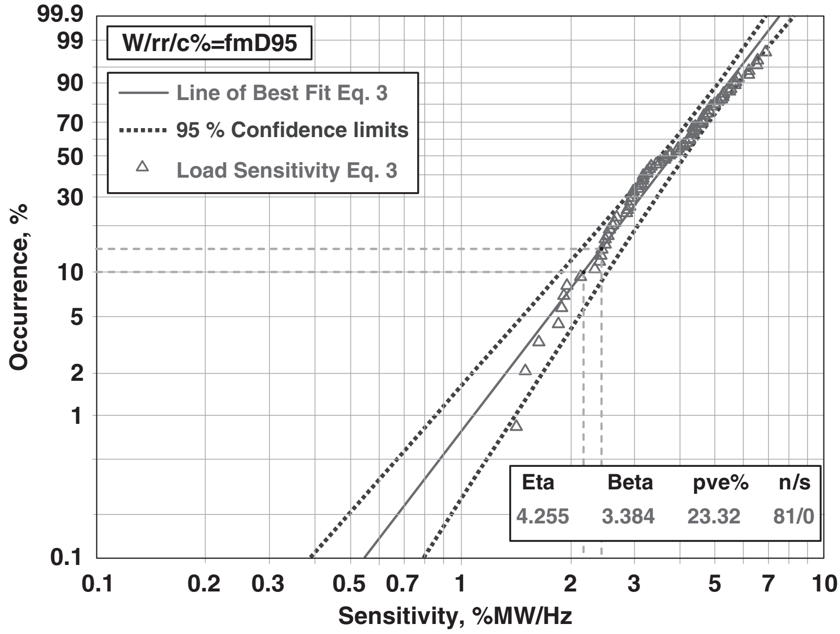

Fig. 6 *Distribution of load sensitivity to frequency*

with the margin offered though response requirement calculations. This additional margin will provide additional security for any instances when full load response is not delivered.

The 15th percentile suggests a load sensitivity of 2.45%MW/Hz, with confidence limits of 2.15–2.8. A load sensitivity of 2.5%MW/Hz is used by a number of system operators [11, 12, 21]. These results suggest the possibility of increasing load response levels from 2 to 2.5%MW/Hz whilst still maintaining a high degree of security. This change would reduce the requirement for spinning reserve held on the system. However, before implementing this change in response calculations, it would be necessary to perform trials so as to confirm operating confidence in using this value.

5 Cost saving through changes in response holding

To translate this change in response holding into simple cost savings, consider that the system is always secured against the worst foreseeable risk, namely 1320 MW. The resulting changes in primary and secondary-response holding levels are shown in Fig. 7 over the course of a day. To simplify this dynamic requirement in calculations, consider a median saving of 72 MW in primary holding and 160 MW for secondary-response. Assume, also, that the plants holding this response capability offer primary and secondary-response, and that holding 160 MW of secondary means that the obligation of holding 72 MW of primary-response is met automatically.

Assuming full delivery of generator response, but with a load response of only 1.3%/Hz, the new frequency-response levels should still contain a 1 GW loss within limits. On average, three system incidents occur per year with an infeed loss that is greater than 1 GW; in the worst case, the load response will under-perform for all three events. In these three events, a supplementary 160 MW of energy (to secure back to the old levels) is required. Based on a balancing mechanism cost of £2500/MWh, this would require expenditure of £600 000 on emergency fast reserve. This cost does not reflect the fact that these fast reserves

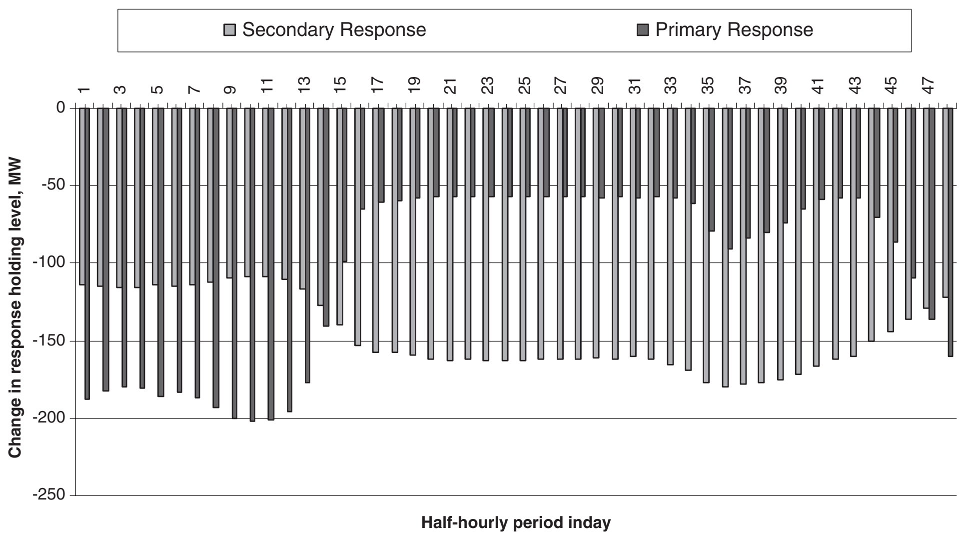

Fig. 7 *Changes in response holding when considering a 0.5% increase in load sensitivity against a 1320 MW loss*

may not be deliverable in time to limit the fall in frequency. The result may be that the frequency breaches 48.8 Hz and automatic disconnection of load begins, to recover the system. If this loss in load exceeds 320 MWh, this could cost up to £16.9 million in incentives and result in damage to the operator reputation that cannot easily be assigned a monetary value.

The emergency-response cost would be offset against a reduced operating expenditure of £2 719 100 per annum. This is due to the response-holding costs based on average costs from the first quarter of 2005. To create headroom for response holding, generators must be deloaded through bids and this energy must be replaced by associated offers on other units in the balancing mechanism. Units do not fully supply all of the power from the load point to maximum output in response, and a return of 55% response is expected on the reduced output. This means that approximately double the volume of bids and offers is required for any volume of response. The differences in system buy and sell price over the period of interest, multiplied by the volume of bids and offers required, is an indication of the cost saving that can be made. The market will therefore see reduced activity on bids and associated offers to the sum of £22 451 083 per annum. This assumes an average cost, but in reality the saving may be greater due to the marginal costing of bids and offers. As the bids and offers are selected by increasing expense, the higher trading costs may be avoided.

The total cost saving through a reduced load–frequency characteristic, provided that no demand disconnection occurs, is therefore £22 451 083 + £2 719 100 − £600 000 = £22 570 183 per annum. These values are speculative and a number of assumptions have been made to simplify the calculation. All costs relating to system-balancing actions are recovered through the Balancing Services Use of System (BSUoS) charge. Each registered balancing mechanism unit (both suppliers and generators) is liable to pay BSUoS charges.

6 Conclusions

This paper has presented a number of incidents where load sensitivity has been calculated during large frequency excursions. This behaviour has given confidence in using a load-sensitivity factor of 2%MW/Hz when deriving a frequency response requirement.

Data show the possibility of considering an increase in the load-sensitivity factor to 2.5%MW/Hz while still maintaining a high degree of security. Moving frequency response holding levels in line with this new value could imply savings of £22 570 183 per annum on system balancing costs. However, this cost saving must be considered against the possible risk that demand disconnection may occur. Further collection of data would increase confidence in establishing this new value. The annual variation of load sensitivity has not been determined from current incidents and it is unlikely that future studies would reveal any operational pattern to the data.

7 Acknowledgments

The authors thank The National Grid Electricity Transmission plc for granting permission to publish this paper. Thanks are also extended to staff at Brunel Institute of Power Systems for their invaluable experience and encouragement and also to the Brunel University/Surrey University Engineering Doctorate programme.

8 References

1 Kundur, P.: 'Power system stability and control' (McGraw-Hill, New York, 1994)
2 Wood, G.F., Hung, W.W., Erinmez, I.A., and Bickers, D.O.: 'NGC experience with frequency control in England and Wales – Provision of frequency response by generators'. Power Engineering Society 1999 Winter Meeting, 1999, Vol. 1, pp. 590–596
3 CIGRE TF 38.02.14: 'Analysis and modelling needs of power systems under major frequency disturbances', December 1997, report no. 148
4 Berg, G.J.: 'System and load behaviour following loss of generation', *Proc. IEE*, 1972, **119**, (10), pp. 1483–1486
5 Concordia, C., and Ihara, S.: 'Load representation in power system stability studies', *IEEE Trans. Power Appl. Syst.*, 1982, **PAS-101**, (4), pp. 136–143
6 Welfonder, E., Hall, B., and Neifer, R.: 'Influence of the frequency and voltage dependence of load part systems on the control behaviour of power systems during emergency conditions'. IFAC 12th Triennial World Congress Conf., Sydney, Australia, 1993, pp. 789–796
7 Welfonder, E., Weber, H., and Hall, B.: 'Investigations of the frequency and voltage dependence of load part systems using a digital self-acting measuring and identification system', *IEEE Trans. Power Syst.*, 1989, **4**, (1), pp. 19–25
8 IEEE task force on load representation for dynamic performance: 'Load representation for dynamic performance analysis', *IEEE Trans. Power Syst.*, 1993, **8**, (2), pp. 472–482
9 O'Sullivan, J.W., and O'Malley, M.J.: 'Identification and validation of dynamic global load model parameters for use in power system frequency simulation', *IEEE Trans. Power Syst.*, 1996, **11**, (2), pp. 851–857
10 Näser, W., and Grebe, E.: 'Kosten von Regelmaßnahmen im Netzbetrieb', *VDI Beri.*, 1996, (1245), pp. 35–49 (in German)
11 Schulz, R.P.: 'Modelling of governing response in the eastern interconnection'. 1999 Winter Power Meeting, Symp. on frequency control requirements, 1999, pp. 561–566
12 National Electricity Market Management Company Limited: 'Discussion paper: generation and load measurement', 15 January 2002, ACN. 072 010 327, version 1.0
13 National Grid: 'GB security and quality of supply standard – version 1', 22 September 2004, Available on-line at http://www.nationalgrid.com/uk/library/documents/pdfs/GB_SQSS_V1.pdf
14 Eltra: 'Eltra's purchases of ancillary services and regulating reserves', 2003, Accessed February 2006 at http://www.eltra.dk/media(15104,1033)/Eltra's_Purchases.pdf
15 Elkraft: 'Summary of recommendation for frequency and time deviation', 1996, Dok id:85210. Available on-line at http://eng.elkraft-system.dk/C1256C790032C72A/(AllDocsByDocId)/F777DBE7BCBC7D9EC1256ED000440AC1?OpenDocument
16 Davies, M., Moran, F., and Bird, J.I.: 'Power/frequency characteristics of the British grid system', *Proc. IEE*, 1958, **105C**, pp. 154–167
17 Baghzouz, Y., and Quist, C.: 'Composite load model derivation from recorded field data'. Power Engineering Society 1999 Winter Meeting, 1999, Vol. 1, pp. 713–718
18 Inoue, T., Ikeguchi, Y., and Yoshida, K.: 'Estimation of power system inertia constant and capacity of spinning reserve support generators using measured frequency transients', *IEEE Trans. Power Syst.*, 1997, **12**, (1), pp. 136–143
19 Machowski, J., Bialek, J., and Bumby, J.R.: 'Power system dynamics and stability' (John Wiley & Sons, London, 1997)
20 Weber, H., Asal, H.P., and Grebe, E.: 'Characteristic numbers of primary control in the UCPTE power system and future requirement'. ETG '97 summer meeting, Berlin, Germany, July 1997
21 Chown, G., Coker, M.: 'Interim report on frequency relaxation project', August 2000. Accessed February 2006 at http://www.sapp.co.zw/docs/frequency%20relaxation.pdf

Available online at www.sciencedirect.com
ScienceDirect
ELSEVIER
Electric Power Systems Research xxx (2006) xxx–xxx
ELECTRIC POWER SYSTEMS RESEARCH
www.elsevier.com/locate/epsr

Experiences in modelling the performance of generating plant for frequency response studies on the British transmission grid

R. Pearmine [a,b,*], Y.H. Song [a], A. Chebbo [b]

[a] *Brunel Institute of Power Systems, Brunel University, Middlesex UB8 3PH, UK*
[b] *Operations and Trading, National Grid, Wokingham, UK*

Received April 2006; received in revised form 25 August 2006; accepted 8 November 2006

Abstract

Significant changes to the generation mix on the British transmission system have occurred in the past 10 years, and this trend is expected to continue in the future with an increase in renewable generation. This change, in conjunction with market changes, has driven the need to establish suitable generator models for thermal plant used in dynamic response studies. These studies are presently used to quantify the dynamic requirement that secures the transmission system against large instantaneous losses of power. This paper provides an account of the experiences gained in modelling the performance of generators based in Great Britain. Established governor models to represent the behaviour of traditional coal and oil fired plant already exist and comments are made on their performance against system incidents. Models of combined cycle units using traditional open cycle gas turbine models have shown poor correspondence with monitored grid data in simulations. A gas and steam turbine governor model to represent combined cycle plant was developed, and is presented, with results from validation trials against recorded test data. Improvements in simulating grid frequency have been demonstrated using the developed models in a full network simulation of a recent generator loss event.

Keywords: Power system control; Dynamic simulation; Frequency reserve; Frequency response; Combined cycle gas turbines; CCGT

1. Introduction

The energy mix of the electricity grid in Great Britain has changed greatly over the last decade, with an increasing proportion of combined cycle gas turbine (CCGT) units now being utilised for ancillary services, such as frequency response. Historically, the provision of frequency response has been dominated by coal fired stations that have proven to be very reliable, but a large number of these units will be retired in the coming decade. With these changes in plant mix and an increase in the proportions of renewable generation expected by 2010 [1], a firm understanding behind the collective dynamic behaviour of generator response is required. The balancing market in Britain has now been liberalised, and there is a growing requirement to optimise the response held on the system in order to reduce the financial impacts of what may become a more volatile market.

Changes in the system frequency of a synchronous AC transmission system are a direct result of the imbalance between the electrical load and the power supplied by system connected generators [2]. Any short-term imbalance of energy will result in an instantaneous change in system frequency as the disturbance is initially offset by the kinetic energy of rotating plant. The power system in Great Britain is linked with Ireland and France through dc interconnectors, these connections do not offer synchronous ties with the external systems. As such, the national grid is operated as an isolated island system and the adequate provision of energy and response at all times is essential to ensure the network is not jeopardised. Significant loss of generating plant without adequate system response can produce extreme frequency excursions outside the working range of plant. This can lead to demand disconnection as the frequency drops below 48.8 Hz and may even cause disconnection of plant if the deviation infringes 47.5–47 Hz, which in an already delicate operating situation may lead to system collapse.

* Corresponding author at: Operations and Trading, National Grid, Wokingham, UK.
E-mail addresses: Ross.Pearmine@uk.ngrid.com, ross.pearmine@brunel.ac.uk (R. Pearmine), Y.H.Song@Brunel.ac.uk (Y.H. Song), Ahmad.Chebbo@uk.ngrid.com (A. Chebbo).

0378-7796/$ – see front matter © 2006 Published by Elsevier B.V.
doi:10.1016/j.epsr.2006.11.004

Deviations from the nominal frequency are managed through scheduling frequency response, this reserve is composed of demand management and dynamic response held on synchronised generators. To schedule the necessary levels of response needed to meet frequency obligations, a frequency response requirement is employed to prevent a breach of limits under large imbalances of power. Studies have shown that the frequency response requirement is influenced by the interactions between the generator performance, the transmission system characteristics and load behaviour [3]. The frequency response requirement is formulated through modelling the performance of these components in simulated loss scenarios. It is essential that these models depict the true dynamic behaviour of plant to establish a frequency response scheme that does not compromise the overall security of the system. This paper highlights the experiences that have been gained through the reconstruction of various system incidents in order to validate a proposed model to calculate the system frequency response requirement.

2. Requirements for frequency response

The transmission system in England, Wales and Scotland is managed by National Grid and this network can experience a national demand that ranges between 20 and 60 GW. As system operator, National Grid performs many tasks during the day-to-day running of the transmission system. Among these tasks the real time balancing of the system is crucial to maintain system frequency at 50 Hz. Under instantaneous gains or losses of power, such as a generating station trips, the system can experience large frequency swings. The British grid must cope with conditions whereby the largest potential dimensioning fault on the system can reach 1320 MW. In order to recover any large imbalance of generation or demand National Grid became a world leader to pioneer a process to calculate, monitor and contract for a reserve held for frequency response [4].

To limit the effect of extreme losses the Transmission System Security and Quality of Supply Standard [5] defines control tolerances that are applied to the network to contain grid frequency. National Grid operates under its own limits of ±0.2 Hz which are imposed on the system under normal operation, and these limits should contain step changes in power up to 300 MW. For a step change in power up to 1 GW, the system frequency is controlled within a deviation of ±0.5 Hz. For significant losses greater than 1000 MW but below 1320 MW the system frequency may drop to 49.2 Hz for no longer than 1 min, before returning to 49.5 Hz.

In order to match the dynamic changes in demand a proportion of this frequency response must be held on spinning units. These synchronised generators are deloaded to provide headroom to operate under governor action. The response may also be partly held by non-dynamic measures, which includes frequency triggered demand management and hydro-generation on frequency sensitive relays. The total frequency response held on the system is optimised every 20 min according to the total network demand and the largest dimensioning fault on the system. This process is significantly different from other network operators [6,7] who can constrain their individual instantaneous disturbance reserves by dividing the requirement between

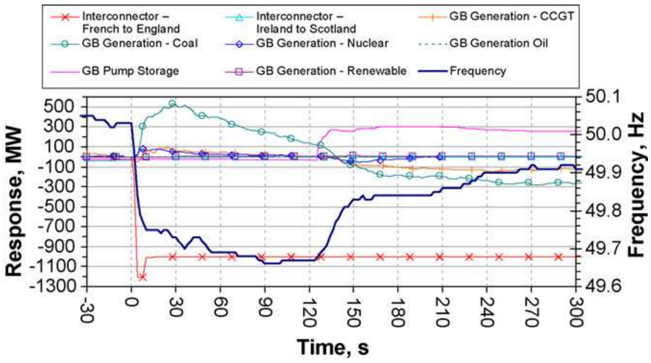

Fig. 1. Frequency response on the GB grid to a 1000 MW bipole trip at a national demand of 42318 MW.

neighbouring interconnected countries. Under these conditions response is commonly establish at a discrete level and not optimised against system conditions as the potential risk is a sustained quantity.

Around seventy percent of the system generators operate as base load plant, with the remaining units providing the frequency response requirement. The concept of a frequency response requirement is complicated by an artificial distinction to define the required system response over two time scales. A primary response requirement is defined to arrest the initial drop in frequency, and is deliverable 10 s after an incident has occurred. This response must be sustained where necessary for a further 20 s. The secondary response requirement is deliverable subsequent to primary time scales and can be required for up to 30 min. The secondary response requirement recovers the frequency to the appropriate limits. To recover the levels of frequency response subject to further incidents, the control room dispatches standing reserve that has been pre-scheduled on warm or fast starting units. Fig. 1 shows a breakdown of system generation following a loss of 1000 MW and the associated delivery of response. The reduction in generating plant output in Fig. 1, even at low frequencies, can be attributed to changes in system loads and some increase in open cycle gas turbine output over the monitored timescales.

Generators that contribute in the balancing mechanism have a portfolio of response contracts that are derived through compliance tests. These contracts quantify the delivery of response expected at set frequency deviations and set load levels over secondary and/or primary time scales. The control room maintains the system frequency response requirement by dispatching balancing units until the sum of contracted primary and secondary response levels equals the optimised response holding level. To ensure the response holding process remains robust supplementary feedback from event monitoring is conducted. This includes in depth analysis of plant performance for all events outside 49.8 or 50.2 Hz for more than 2 min.

3. The frequency response model

Unlike similar techniques used to establish a response requirement [8,9] the method proposed by National Grid involves the utilisation of a full transmission system model

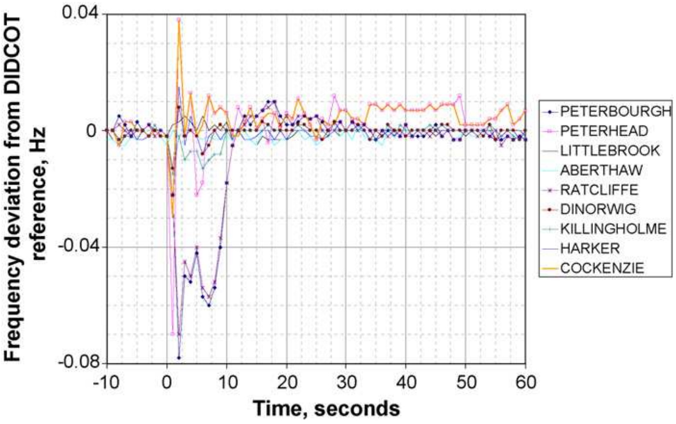

Fig. 2. System-wide frequency deviations on the GB grid following 1110 MW of lost generation (frequency fell by 0.373 Hz).

down to 275 kV nodes in England, Wales and Scotland. The method provides a set of lookup tables that are calculated off-line using the transmission model. This representation allows for the influence of network losses through the geographic position of generators dispatched to provide frequency response. The model also differs from other techniques by allowing for a non-homogeneous grid frequency across the network. Fig. 2 highlights a typical frequency profile experienced across the network recorded on monitoring equipment following an incident. Most of the network remains within a tight ±0.005 Hz tolerance of the reference frequency. Substations local to the fault however experience a significant variation of up to 0.08 Hz for the initial 10 s before stabilising.

Simulation studies carried out using the Eurostag package developed by Tractebel and EDF provide the basis for analysis. System active loads are lumped at each grid supply point and assumed to be frequency dependent at a rate of 2%/Hz, it is assumed that all voltage dependent effects are subsumed by this value [10]. Reactive loads are assumed to be voltage and frequency independent in the study, any contributing influence on frequency is satisfied by the active load frequency sensitivity. Frequency responsive plant in the simulation is equipped with an exciter model submitted for in-house stability studies, and a unit specific governor model. Non-responsive plant, operating as base load is represented with a similar exciter model and a generic governor model developed to meet grid code requirements.

Using monitored output data during a range of real incidents, each generating unit response can be compared against a simulated response based on its governor model behaviour. By injecting the changes in grid frequency experienced during historic events into the model and analysing the response, validation of the governor model can be conducted. This type of analysis offers the ability to change droop settings and time constants in the models to meet inline with past historic performances. In the case of responsive coal and oil fired plant during incidents where the system frequency remains within operational levels, implementing a standard governor model [11,12] with associated steam delays [13] provides an adequate representation of performance. However, in the interests of frequency

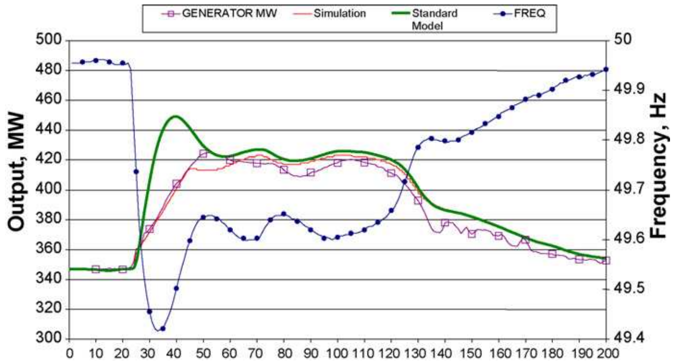

Fig. 3. Frequency response of a rate-limited generator during an actual incident and the simulated response.

response, the possibilities exist of reaching excursions down to 49.2 Hz. Analysis of historic incidents with much larger losses revealed that a degree of model tuning was required to match the performance seen in actual events.

A number of coal fired generators in the study operated with a rate-limited response that was seemingly triggered when the system frequency (ω) breached 49.8 Hz (Fig. 3). These rate-limits ranged from 0.01 to 0.003 pu s^{-1} among the generating stations that operated under this strategy. The chief reasoning behind operating plant in this manner is to reduce thermal loading in steam pipes and boiler waterwalls. While limiting response during large frequency deviations, this practice still offers a high degree of frequency regulation within the operating frequency band. Operating under this methodology prolongs component life and reduces refurbishment costs for generating stations. A modification can be made to the load speed control section in the governor model to represent this behaviour (Fig. 4).

The remaining coal and oil fired stations that did not respond inline with the previous or standard model during large frequency excursions operated with a limited peak output. This output was related to the machine load point. This mode is illustrated in Fig. 5 against the simulated response of the same unit operating with a standard governor model. Again, a simple modification to the existing governor can be implemented to account for this based on load reference (P_0) (Fig. 6). Adequate models for pump storage and hydro-generation are widely available from a number of sources [12,14,15] and the same tuning process can be applied to these units. Most nuclear generation is not called upon to supply frequency response in Great Britain, so these units are equipped with generic non-responsive models.

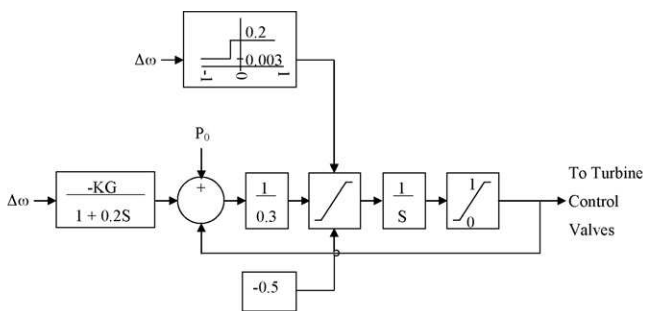

Fig. 4. Modification to coal governor to allow frequency triggered rate-limit.

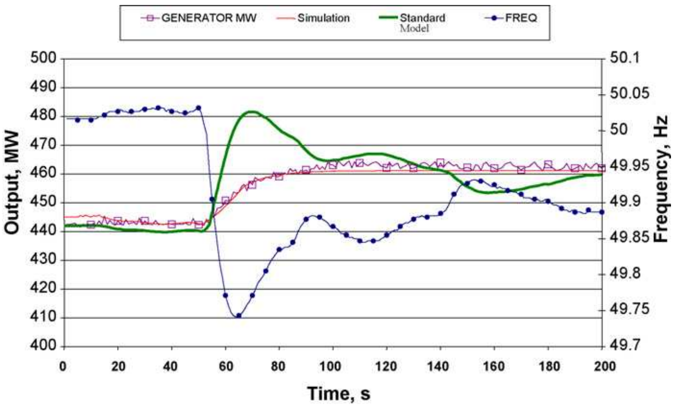

Fig. 5. Frequency response of an output-limited generator during an actual incident and the simulated response.

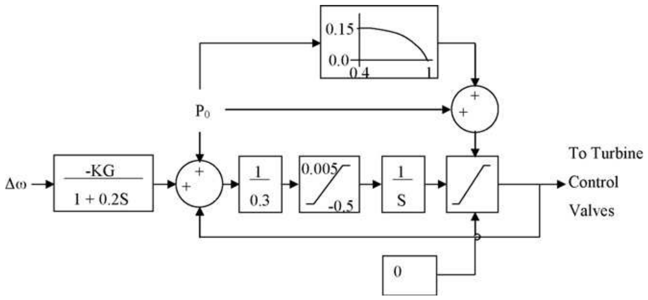

Fig. 6. Modification to coal governor to allow an output-limit.

A generic open cycle gas turbine model developed for long-term dynamic transmission studies was employed for all grid-connected CCGT generators in initial studies. National Grid, along with other system operators [16], identified concerns over representing gas turbine sections in CCGT modules with a simplified open cycle model. Assessment against the larger frequency excursions showed that the model could not adequately represent the nature of the gas plant. Fig. 7 shows an exaggerated example of this behaviour. The combined cycle unit in question is operated with a high degree of temperature limiting, apparent from the initial 30 s of the trip. This prompted the development of a single governor model that could be parameterised to represent all the CCGT units in the system.

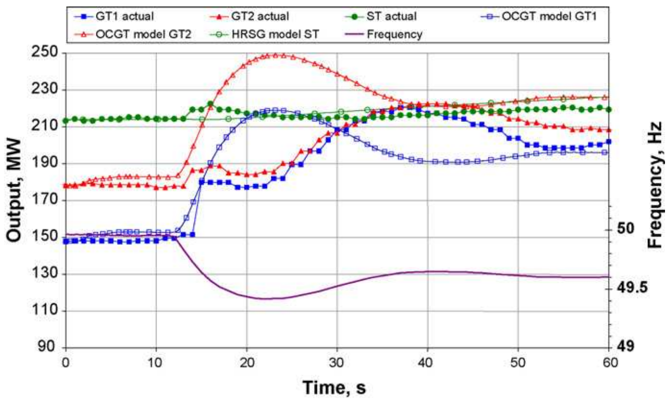

Fig. 7. Frequency response of a CCGT gas turbine module during an actual incident and the simulated response using OCGT representation.

4. Response from combined cycle units

Initially, CCGT units where developed to provide maximum efficiency and hence expected to operate as base load plant. In the early stages of deployment National Grid entered discussions with a number of CCGT manufactures to encourage the improvement of part load performance, and to ensure that plant could offer a frequency response capability. CCGT units employ inlet guide vanes to control the mass of air flowing through the plant at part load and thus maintain a high output exhaust temperature, keeping efficiencies high. These guide vanes are not modelled in the basic open cycle models and for this reason the model brings an inaccuracy in the control of the exhaust temperature profile. The exhaust gases are subsequently feed into heat recovery steam generator (HRSG) to raise steam to drive further steam turbine modules. The open cycle model only offers an output power signal to feed into the steam section. In conjunction with inlet guide vanes the exhaust temperature is also controlled through limiting the fuel flow to the combustion chamber, influencing the turbine power. To keep the HRSG temperature stable, some of the larger CCGT units operate under an almost uniform exhaust temperature profile, which directly influences the control strategy employed. Fig. 8 shows a selection of CCGT units, at different operating points, with the associated gas turbine variables. It identifies the differences in profiles employed by manufactures.

A large number of models representing CCGT units already exist, some of these models are developed for small sub-100 MW units [17–19]. Other models [20–26] are essentially tuned versions of the established models developed by Rowen [27,28], that assume a constant exhaust temperature. An implementation of the Rowen model is available in the Eurostag governor library, but studies with this model have provided poor simulation results except for with some specific machines. Further models of large-scale units require detailed turbine parameters [29] or have difficulties coding into the Eurostag macroblock language [30,31]. Papers that show promising results [17,32] lack the detail necessary to reproduce full control systems in a model.

4.1. CCGT model

To provide a single CCGT model that could be tuned for used with a range of different gas turbine manufactures, and plant

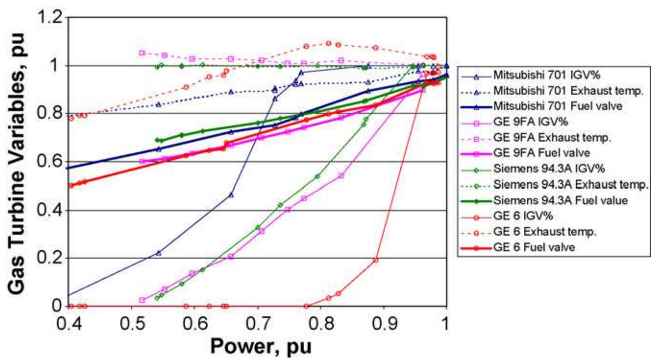

Fig. 8. Exhaust temperature, IGV position and fuel valve position of a number of combined cycle gas turbines.

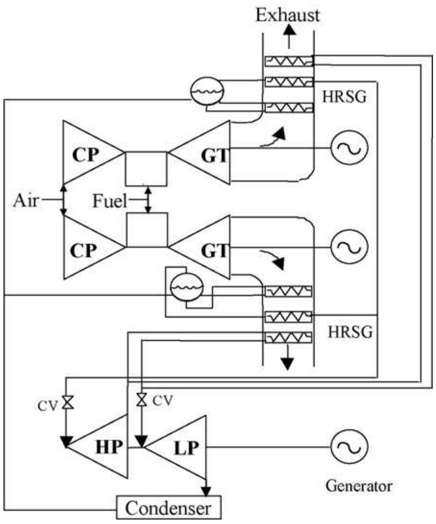

Fig. 9. A typical combined cycle gas turbine arrangement. CP: compressor; GT: gas turbine; LP: low pressure turbine; HP: high pressure turbine; CV: control valve.

frames, a simple model was developed. The basic gas turbine engine (Fig. 9) consists of a combustion chamber, compressor and a gas turbine. Variables of interested in terms of temperature control can be calculated though a set of three basic equations, whose derivation can be found in [33]. Air at atmospheric temperature (T_a) is adiabatically compressed by a pressure ratio (Cpr) to reach a discharge temperature (T_d) according to Eq. (1). The pressure ratio here is assumed to be a constant and the rated value. Some reduction in compressor pressure ratio would result from reduced shaft speed; however, it is assumed that the change is negligible over the frequency response range:

$$T_d = T_a\left(1 + \frac{(\mathrm{Cpr}\,W_a)^{(\gamma-1)/\gamma} - 1}{\eta_c}\right) \quad (1)$$

The per unit airflow (W_a) through the machine can be controlled by the inlet guide vanes and is also dependent on the ambient temperature and pressure, assumed to be 303 K and 1 Pa, respectively. The compression process is not perfect, and the isentropic efficiency of the compressor (η_c) is included to calculate the work done by the compressor. The ratio of specific heats (γ) is assumed to be 1.4. The combustion firing temperature (T_f) can be calculated from the combustor heat balance, Eq. (2). The fuel flow (W_f) is in per unit of the rated value. The rated firing (T_{fr}) and discharge temperature (T_{dr}) of the turbine is used to calculate the design combustor rise temperature:

$$T_f = T_d + (T_{fr} - T_{dr})\frac{W_f}{W_a} \quad (2)$$

The exhaust temperature (T_e) can be calculated from Eq. (3), where the exhaust gas flow is assumed to be equal to the airflow, and the isentropic efficiency of the turbine (η_t) is also included. All above temperatures are expressed in K.

$$T_e = T_f\left(1 - \eta_t\left[1 - \frac{1}{(\mathrm{Cpr}\,W_a)^{(\gamma-1)/\gamma}}\right]\right) \quad (3)$$

Integrating this basic gas turbine engine model with a control system provides the required governor model for use in frequency response simulation studies. Fig. 10 shows the complete governor control diagrams that can be used in Eurostag simulations. In Fig. 10a the speed droop (KG) is implemented to provide the fuel demand signal (FD) according to the load reference (P_0) and machine speed (OMEGA). To supply the minimum expected response against the registered capacity of the station, gas turbine modules are generally set with a higher than normal droop so that the net station droop is in the order of 4%. The demand signal is rate limited and position limited.

In Fig. 10b a low value selection occurs between fuel demand and temperature limit (LIMIT), this signal feeds into the fuel control blocks. It is possible to include frequency dependence in the fuel supply, this is a result of mechanical or electrical pumps with rotational speeds tied into the unit, for most instances no frequency dependence is assumed, and the block can be omitted. The demand is then adjusted inline with the minimum fuel demand at no load and the result is the fuel flow signal (WF).

The calculated exhaust temperature (T) from the gas turbine engine model Fig. 10c is compared to a reference temperature based on fuel valve position. This error signal is then feed to the exhaust temperature limiter (Fig. 10d) and the inlet guide vane control (Fig. 10e). The inlet guide vane control is adjusted so that the required exhaust temperature is attained. The guide vanes operate to control the airflow at a rate (IGVRATE) slower than the fuel valves, which results in preliminary intervention by the temperature fuel limit under large power fluctuations. The airflow is adjustable between maximum and minimum limits (WAMAX/MIN). By altering the exhaust profile function and adjusting turbine parameters to design values it is possible to represent alternative machines and manufactures. With the compressor directly coupled to the electric generator the airflow (WA) will be influenced by system frequency and will therefore be proportional to the rotor speed. The mechanical torque (TORQUE) derived from the gas turbine (Fig. 10f), is assumed as a linear function with respect to the fuel flow over the rotor speed range [27]. A speed dependant term is also included in the machine torque block to represent the friction acting on the shaft when fuel flow is stopped.

If large frequency deviations below 49.2 Hz are incurred the output power from a gas turbine is significantly reduced due to diminished compressor speed and pressure ratio. To overcome this natural power reduction and meet with grid code requirements a degree of overfiring is employed to maintain power levels within limits. If studies are intended to simulate plant behaviour outside the frequency response operating range additional modifications to the temperature controls must be made to include this effect.

The HRSG module can be modelled based on the output exhaust temperature and the airflow through the gas engine(s). Steam turbine modules are generally operated in sliding pressure mode on the British grid, meaning that the steam is not throttled as in coal based plant, and steam control valves are set fully

Please cite this article in press as: R. Pearmine et al., Experiences in modelling the performance of generating plant for frequency response studies on the British transmission grid, Electr. Power Syst. Res. (2006), doi:10.1016/j.epsr.2006.11.004

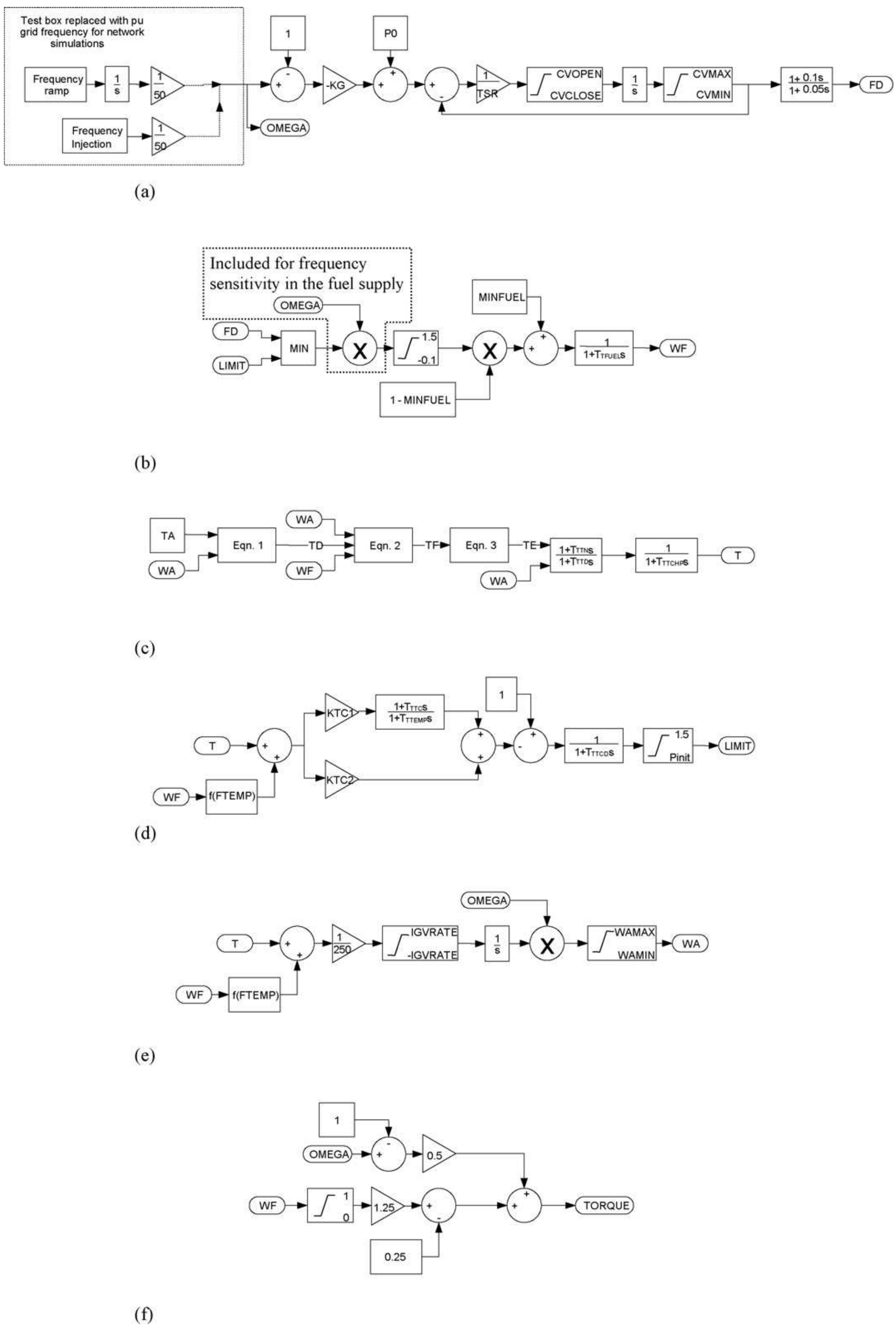

Fig. 10. CCGT model: (a) governor; (b) fuel offset/delay; (c) gas turbine engine model; (d) temperature limiter; (e) inlet guide vane controls; (f) output torque.

open. This practise reduces the control scheme complexity in the model, and a basic block diagram is given in Fig. 11. The function FHRSG is introduced to account for boiler and turbine efficiency on steam unit output, in the simulation the function reflects unity efficiency. Large boiler time constants mean that generally the steam turbine module supplies a small percentage of the overall station response.

4.2. CCGT model validation

The developed model for CCGT plant was validated against tests carried out on an existing unit. These tests form a basis to demonstrate compliance with the grid code and are conducted on all grid-connected and large embedded plant. A frequency injection signal is provided to the governor to simulate the grid

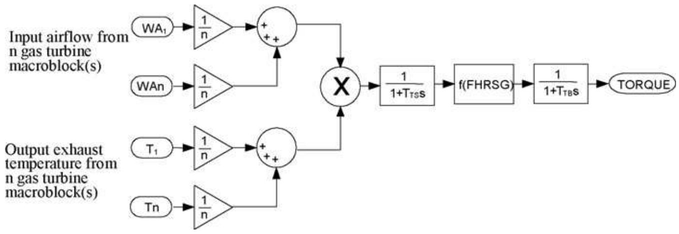

Fig. 11. CCGT model—heat recovery steam generator.

frequency during a real transient. Various injection shapes are tested; the one chosen to validate against is the 0.8 Hz ramp over 10 s, returning to 0.5 Hz at a load set point of 60%. Power output, inlet guide vane position, exhaust temperature and fuel valve positions are monitored during the test at sampling intervals of 0.1 s. As in the original tests the unit under simulation is synchronised to the full network model as was experienced on the day of tests. A frequency injection signal is supplied to the governor model as depicted in Fig. 10a. The response of the simulation is shown in Fig. 12 against compliance test results.

The fuel valve position signal from tests shows an opening from 60 to 73% as frequency is injected, this is met by a rise from 60 to 87% in the model. However, despite this difference the overall power output of the model remains within a tolerance of actual unit, suggesting a supplementary fuel valve that was not monitored during tests. The actual test frequency injection is the summation of grid frequency and injection signal, hence, the signal is not as crisp as the simulation injection due to minor fluctuations in the grid frequency. Fig. 13 shows the change in power for the same CCGT unit and model at a slightly higher loading point.

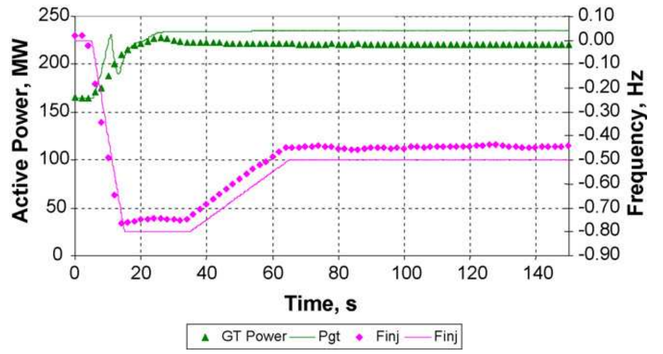

Fig. 13. Power output from combined cycle gas turbine governor model at 73% load.

Marginal differences between the simulation of inlet guide vane position and exhaust temperature from the test results bring attention to inaccuracies in the modelling of temperature limit controls. This is also noticeable in the simulated power output curve as it reaches peak output. The output power as simulated by the model, provides a close match to the compliance test in the initial 30 s of the trip. This time scale is critical for establishing response levels that curtail the drop in frequency. Response on secondary time scales whilst important to restore system operation back to normality does not critically influence the risks of demand disconnection provided it is sustained from primary levels. Whilst these results show a marked improvement in comparison with the results obtained from open cycle gas turbines there remains an opportunity to improve the model further. The addition of a fuel limit to prevent more than a 70 MW change in output would improve the long-term performance of the model.

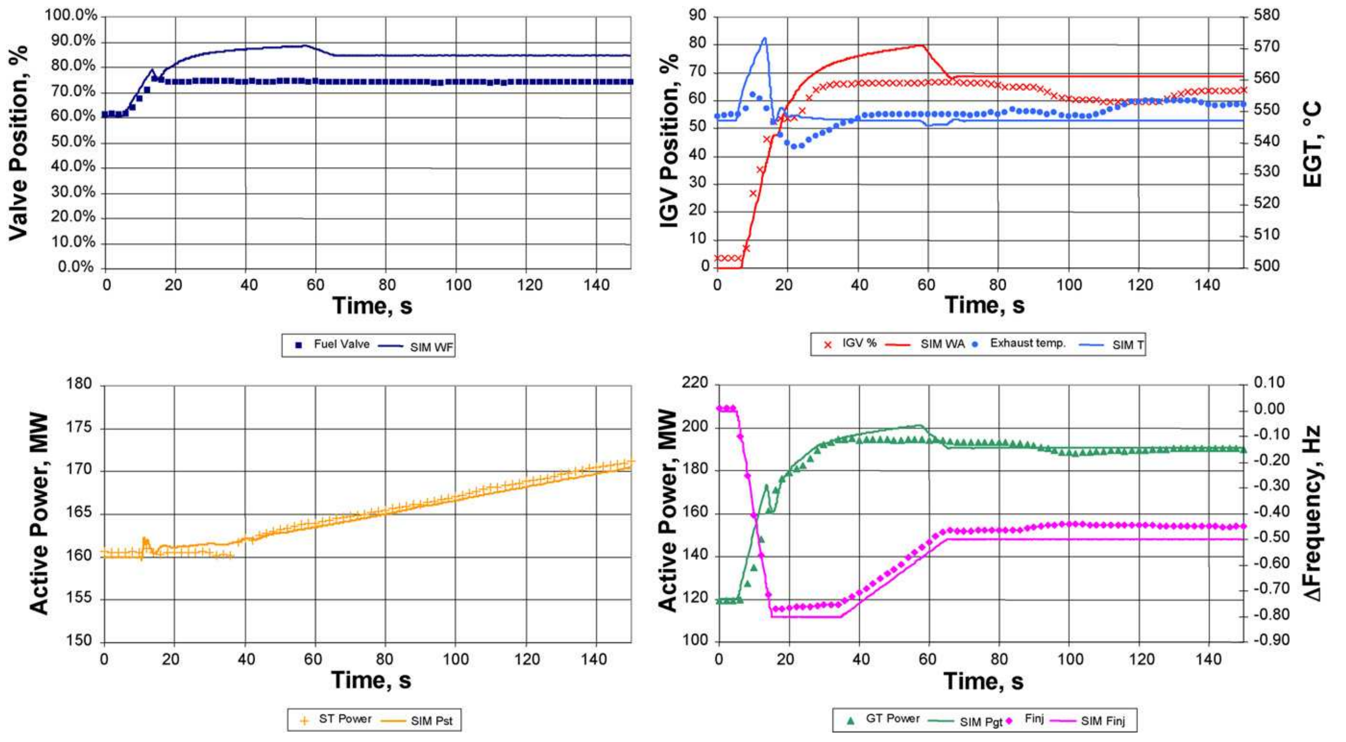

Fig. 12. Validation of a combined cycle gas turbine governor model at 60% load.

Please cite this article in press as: R. Pearmine et al., Experiences in modelling the performance of generating plant for frequency response studies on the British transmission grid, Electr. Power Syst. Res. (2006), doi:10.1016/j.epsr.2006.11.004

5. Full network frequency simulation

The different operational behaviour of generators can have significant impact on the curtailment of a frequency drop. If the initial output power from machines under primary response time scales is much reduced the demand-generator imbalance remains high, consequently, the frequency will decay at a faster rate than would otherwise be experienced. Conversely, early frequency simulation studies using untuned governor models on a complete system provided exaggerated generation results. These results confirmed that the frequency that did not fall to the experienced levels especially in primary response time scales, and reinforced the importance of tuning models. Accurate representation of generator output in generator governor models is essential during the simulation of system frequency swings. Ensuring these models are tuned and validated is paramount in establishing frequency response schemes that do not compromise system security. At a system frequency of 48.2 Hz demand disconnection begins to prevent full system collapse. In order to prevent a breach of this limit on the actual network, simulations must not be conservative in representing the deviation in frequency.

Fig. 14 shows a simulation of grid frequency and the associated generator response during an event from May 2004. This incident was one of the largest of recent years with a total plant loss in the order of 1260 MW. This study utilises the developed CCGT model together with tuned versions of the coal fired plant models discussed. These models used in conjunction with the generic models for non-responsive plant provide a superior recreation of the network dynamics. In the example of Fig. 14, the simulation provides a peak response error of 5%, with a frequency mismatch of only 0.022 Hz. The slight mismatch between the real and simulated grid frequency is mainly due to the representation of the system load. In the real system the loads are dynamic, however, under these studies they are represented as frequency dependant static loads.

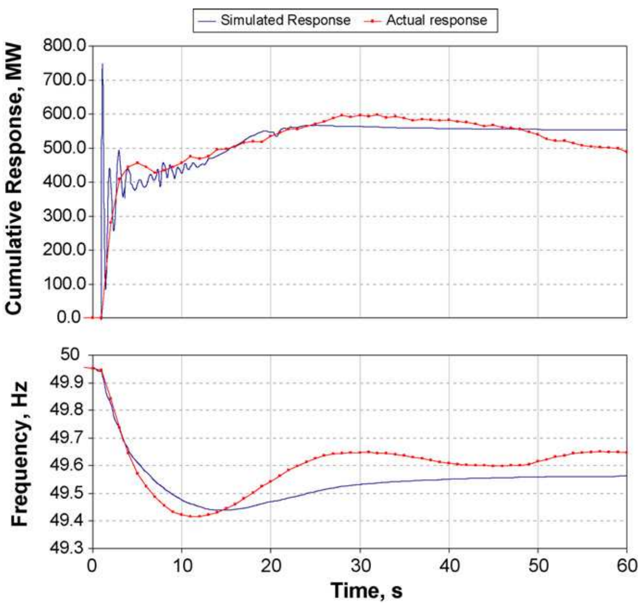

Fig. 14. Network simulation of a 1260 MW loss.

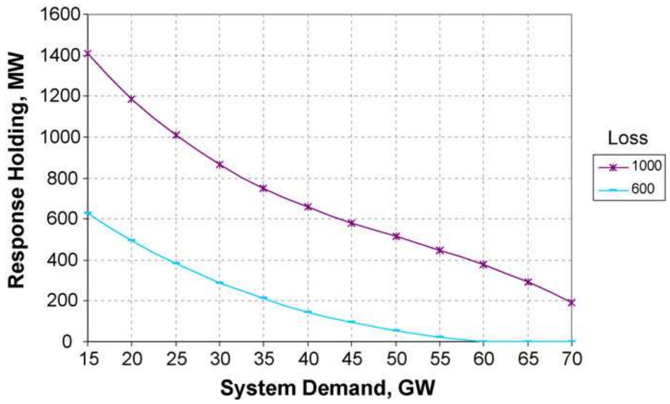

Fig. 15. Primary response requirement curves.

By implementing this full network model at various system demand levels and varying magnitudes of plant loss, a set of response requirements can be identified. A set of response requirements curves can be established through iterative adjustment of the response held until set frequency limits are met. Fig. 15 shows and example of two curves under primary response time-scales.

6. Conclusions

Responsive models of traditional hydro, coal and oil fired plant are well established and validation for real units proves to be a simple exercise. Data from grid code compliance tests and historic events can be used to match simulation models against actual plant behaviour. The nature of combine cycle gas turbines in providing frequency responsive services is more complex. Temperature control provides a critical factor for large frequency deviations and limits the output power from units during primary response time-scales. These controls are unit specific and vary widely according to manufacturer and turbine frame.

Presented is a gas turbine model for use in the simulation of combined cycle modules. This model was validated against test data recorded during grid compliance tests. It provides a detailed long-term dynamic model for use in post-event analysis and in studies for identification of frequency response holding levels. While representation is accurate under primary response time scales this model would benefit from further refinement to improve the temperature control system. This weakness in the model highlights the complexities in determining the exact temperature controls found in gas turbine sections of a CCGT.

The developed CCGT governor, rate-limited and limited coal fired governor models can provide an accurate tool to establish a set of frequency response requirements as demonstrated through simulation of a recent generator loss event.

Acknowledgements

This work is published by permission of The National Grid Electricity Transmission plc, and gratitude is specifically extended to William Hung and Rachel Morfill for their advice regarding the research. Any views expressed are those of the authors, who would also like to thank staff at Brunel Institute of

Power Systems and also to the Brunel University/University of Surrey Engineering Doctorate Programme.

Appendix A

Variables used in the gas turbine governor model

Variable	Description	Value
KG	1/droop	31
TSM	Servo time constant	0.1
CVOPEN	Governor valve open rate limit	0.02
CVCLOSE	Governor valve close rate limit	−0.1
CVMAX	Governor valve open limit	1.0
CVMIN	Governor valve close limit	0.0
MINFUEL	Minimum fuel demand at no load	0.2
TA	Ambient temperature (K)	303
TD	Rate compressor discharge temperature (K)	660
TR	Rated exhaust temperature (K)	850
TF	Rated firing temperature (K)	1598
TFUEL	Fuel system time constant	0.1
THLEAD	Heat transfer lead time constant	15
THLAG	Heat transfer lag time constant	20
TTCD	Temperature controller delay	5
TTHCP	Thermocouple time constant	1.0
KTC1	Temperature controller gain	0.2
KTC2	Temperature controller gain	0.01
TTC	Temperature controller time constant	5
MUCOMP	Compressor efficiency	0.88
MUTURB	Turbine efficiency	0.85
TTEMP	Temperature control time constant	200
IGVRATE	Inlet guide vane open/closing rate	0.018
WAMAX	Maximum airflow	1.0
WAMIN	Minimum airflow	0.7
CPR	Compressor ratio	16.6
UG	Load set point	0.6
%FTEMP	Exhaust temperature profile function	WF: 0.0, EXLIM: 1; WF: 0.5, EXLIM: 1; WF: 1.0, EXLIM: 1

Variables used in the HRSG and steam turbine governor model

Variable	Description	Value
TS	Steam pipe time constant	20
TB	Boiler storage time constant	550
%FHRSG	Exhaust energy steam turbine output function	In: 0.0, out: 0.0; In: 0.5, out: 0.5; In: 0.8, out: 0.8; In: 1.0, out: 1.0

Appendix B. List of symbols

Cpr pressure ratio (%)
T_a atmospheric temperature (K)
T_d discharge temperature (K)
T_{dr} rated discharge temperature (K)
T_e exhaust temperature (K)
T_f firing temperature (K)
T_{fr} rated firing temperature (K)
W_a airflow (%)
W_f fuel flow (%)

Greek symbols
γ ratio of specific heats (%)
η_c isentropic compressor efficiency (%)
η_t isentropic turbine efficiency (%)

References

[1] HMSO, Renewables obligation order (Statutory Instrument No. 914), 2002. Available online http://www.opsi.gov.uk/si/si2002/20020914.htm.
[2] P. Kundur, Power System Stability and Control, McGraw-Hill, 1994.
[3] CIGRE TF 38.02.14, Analysis and modelling needs of power systems under major frequency disturbances, Report No. 148, 1997.
[4] G.F. Wood, W.W. Hung, I.A. Erinmez, D.O. Bickers, Frequency control in England and Wales—generating plant frequency control services, in: Proceedings of the 11th CEPSI, Kuala Lumpur, Malaysia, October 21–25, 1996.
[5] National Grid, GB Security and Quality of Supply Standard, version 1, 2004. Available online http://www.nationalgrid.com/uk/library/documents/pdfs/GB_SQSS_V1.pdf.
[6] Eltra, Eltra's Purchases of ancillary services and regulating reserves, 2003. Available online http://www.eltra.dk/media(15104,1033)/Eltra's_Purchases.pdf.
[7] Elkraft, Summary of recommendation for frequency and time deviation, Dok id: 85210, 1996. Available online http://eng.elkraft-system.dk/C1256C790032C72A/(AllDocsByDocId)/F777DBE7BCBC7D9EC125-6ED000440AC1?OpenDocument.
[8] E. Welfonder, Least-cost dynamic interaction of power plants and power systems, Control Eng. Practice 5 (9) (1997) 1203–1216.
[9] R. Doherty, G. Lalor, M.J. O'Malley, Frequency control in competitive electricity market dispatch, IEEE Trans. Power Syst. 20 (2005) 1588–1596.
[10] R.S. Pearmine, Y.H. Song, A. Chebbo, T.G. Williams, Identification of a load frequency characteristic for allocation of spinning reserves on the UK electricity grid, IEE Proc. GTD, in press.
[11] Working Group on prime mover and energy supply models for system dynamic performance studies, Dynamic models for fossil fuelled steam units in power system studies, IEEE Trans. Power Syst. 6 (2) (1991) 753–761.
[12] IEEE Committee Report, Dynamic models for steam and hydro turbines in power system studies, IEEE Trans. Power Appl. Syst. PAS-92 (6) (1973) 1904–1915.
[13] F.P. de Mello, Boiler models for system dynamic performance studies, IEEE Trans. Power Syst. 6 (1) (1991) 66–74.
[14] Working Group on prime mover and energy supply models for system dynamic performance studies: Hydraulic turbine and turbine control models for system dynamic studies, IEEE Trans. Power Syst. 7 (1) (1992) 167–179.
[15] C.D. Vournas, Second order hydraulic turbine models for multimachine stability studies, IEEE Trans. Energy Convers. 5 (2) (1990) 239–244.
[16] M. Nagpal, A. Moshref, G.K. Morison, P. Kundur, Experience with testing and modeling of gas turbines, IEEE PES Winter Meeting 2 (2001) 652–656.
[17] K. Kunitomi, A. Kurita, Y. Tada, S. Ihara, W.W. Price, L.M. Richardson, G. Smith, Modelling combined-cycle power plant for simulation of frequency excursions, IEEE Trans. Power Syst. 18 (2) (2003) 724–729.
[18] L.N. Hannett, J.W. Feltes, Testing and model validation for combined-cycle power plants, IEEE PES Winter Meeting 2 (2001) 664–670.
[19] Working Group on prime mover and energy supply models for system dynamic performance studies: dynamic models for combined cycle plants in power system studies, IEEE Trans. Power Syst. 9 (3) (1994) 1698–1707.
[20] Q. Zhang, P.L. So, Dynamic modelling of a combined cycle plant for power system stability studies, IEEE PES Winter Meeting 2 (2000) 1538–1543.
[21] L.N. Hannett, A.H. Khan, Combustion turbine dynamic model validation from tests, IEEE Trans. Power Syst. 8 (1) (1993) 152–158.
[22] A. Bagnasco, B. Delfino, G.B. Denegri, S. Massucco, Management and dynamic performances of combined cycle power plants during parallel and islanding operation, IEEE Trans. Energy Convers. 13 (2) (1998) 194–201.

Please cite this article in press as: R. Pearmine et al., Experiences in modelling the performance of generating plant for frequency response studies on the British transmission grid, Electr. Power Syst. Res. (2006), doi:10.1016/j.epsr.2006.11.004

[23] L.M. Hajagos, G.R. Berube, Utility experience with gas turbine testing and modeling, IEEE PES Winter Meeting 2 (2001) 671–677.
[24] J.H. Kim, T.W. Song, T.S. Kim, S.T. Ro, Model development and simulation of transient behavior of heavy duty gas turbines, ASME J. Eng. Gas Turbines Power 123 (2001) 589–594.
[25] G. Lalor, J. Ritchie, D. Flynn, M.J. O'Malley, The impact of combined cycle gas turbine short term dynamics on frequency control, IEEE Trans. Power Syst. 20 (2005) 1456–1464.
[26] G. Lalor, M. O'Malley, Frequency control on an island power system with increasing proportions of combined cycle gas turbines, in: Proceedings of the IEEE Power Tech, Bologna, Italy, 2003.
[27] W.I. Rowen, Simplified mathematical representations of heavy-duty gas turbines, ASME J. Eng. Power 105 (1983) 865–869.
[28] W.I. Rowen, Simplified mathematical representations of single shaft gas turbines in mechanical drive service, International Gas Turbine and Aero-engine Congress and Exposition, ASME PAPER 92-GT-22, Cologne, Germany, June 1–4, 1992.
[29] S. Suzaki, K. Kawata, M. Sekoguchi, M. Goto, Mathematical model for a combined cycle plant and its implementation in an analogue power system simulator, IEEE PES Winter Meeting 1 (2000) 416–421.
[30] J.L. Aguero, M. Beroqui, R. Molina, Combined cycle plants: models and in-situ reliability tests, IEEE PES Summer Meeting 3 (2001) 1788–1793.
[31] N. Kakimoto, K. Baba, Performance of gas turbine-based plants during frequency drops IEEE Trans, Power Syst. 18 (3) (2003) 1110–1115.
[32] J. Undrill, A. Garmendia, Modeling of combined cycle plants in grid simulation studies, IEEE PES Winter Meeting 2 (2001) 657–663.
[33] H.I.H. Saravanamuttoo, G.F.C. Rogers, H. Cohen, Gas Turbine Theory, 5th ed., Pearson Education Ltd., 2001.

Please cite this article in press as: R. Pearmine et al., Experiences in modelling the performance of generating plant for frequency response studies on the British transmission grid, Electr. Power Syst. Res. (2006), doi:10.1016/j.epsr.2006.11.004

Wind power and the UK electricity grid

R. S. Pearmine [1,2], T. G. Williams[1], K.R.W. Bell[3], Y. H. Song[2]

1. **Operations & Trading, National Grid Transco,** Bearwood Rd, Sindlesham
2. **Brunel Institute of Power Systems, Brunel University,** Uxbridge, Middlesex
3. **Network Strategy, National Grid Transco**, Warwick Technology park, Warwick

Abstract

It is expected that an increasing level of wind generation will be available on the GB grid within the next five to ten years. Sufficient system planning is required to ensure the grid infrastructure will be suitable to transmit this renewable source of electricity to demand centres where it is required.

This paper attempts to explain the correlation of output between theoretical wind farm sites across Great Britain. Comparisons are made between the net output from a region and individual farms. A selection of transmission factors has been suggested to allow regional variations in wind farm output to be accommodated in system planning studies.

Keywords: Wind turbines, renewables, GB grid, transmission system planning.

1.0 Introduction

The ideal in transmission system planning is for investment to be made in sufficient network infrastructure such that there are not excessive restrictions on the transmission of power or failure to meet consumers' demand for power. Under present GB 'wholesale' electricity market arrangements, 'congestion' must be paid for by the system operator (in effect, compensating generators for lack of access to the market); failure to meet demand may also be represented by some cost.

Excessive congestion or failure to meet demand could be prevented by transmission that permits transport of all possible patterns of power production and all demand at all times. However, significant investment would be required to commission and maintain a system at this level of capability, for conditions that may in reality only occur one or two hours a year. A balance must be found that allows a reasonable level of extraction of, for example, wind power while at the same time managing the total costs of transmission. Transmission planning can thus be seen as a minimisation of the sum of the costs of system infrastructure, congestion and supply unreliability. To fully quantify these dimensions is extremely difficult, so the system planner is accustomed to making use of rules to identify specific conditions that should be met by investment in system infrastructure. A key part of this concerns the assumptions that should be made about the outputs from different types of generating plant.

Over the next 15 years the power sector can expect a dramatic increase in the level of renewable generation used to supply electricity in the UK. The Renewables Obligation Order (2002) has provided the UK government with a legislative tool to encourage the uptake of renewable energy technologies. Wind farms in particular are expected to provide much of the added renewable capacity required because of the economic and technological viability in comparison with other forms of renewable generation.

With the current share of wind generation at 1.3 % of the total GB capacity, the order calls to increase this proportion to 10% by 2010, and a possible 15% by 2015. The impact this level of change will have on the GB electricity market and the physical transmission system is yet unclear. To plan the system for the increase in wind generation, allow the wind generation to be utilised and the power to be transmitted to electricity consumers, behaviour of wind generation patterns across Great Britain is needed.

2.0 Previous Work

This paper follows, previous work [1], to calculate a capacity factor that was to be used in transmission planning studies when taking account of the possible net output of a number wind farms spread across some geographical area. The capacity contribution factor is required to facilitate the calculation of a required transmission capacity to allow for import of power to meet the imbalance between demand and generation within an area. Or conversely, to export power when there is a surplus of generation over demand so that a deficit in a neighbouring area can be met. In order to avoid over-investment in network capacity, account needs to be taken of the fact that wind farms will not operate at their maximum output all of the time, they are constrained by wind speed, maintenance outages and even operated at owner discretion.

One of the keys to deriving an appropriate capacity factor for a group of wind farms is an understanding of the correlation between the outputs of different farms. In [1], data was used from feasibility analysis of a proposed off-shore wind farm development in the Irish Sea. This wind farm had an average output of 41% of its capacity and an 8% chance of operating at maximum output. Probability density functions were then estimated to describe the net output of a number of geographically separated wind farms that had a load-duration curve the same as that of this same wind farm. It was concluded that the 90th percentile of the net output from six such wind farms ranged between 60% of the total installed capacity and 100%. This was dependant on the correlation of outputs between them (i.e. the P90 output level was 60% of capacity when there was no correlation and 100% when all the wind farms' outputs were fully correlated).

Previous work suggested the capacity factor should be taken as 60% of the maximum electrical output.

3.0 Turbine Model and Test Data

The data used in these studies has been made available courtesy of the UK Meteorological Office. Wind speed frequency data has been collected from 43 weather stations at various sites across Great Britain, details are shown in Figure 1. The data consists of hourly average wind speed from a three-year period between 1997 and 2001, to half a meter-per-second resolution. The wind speed is measured as close to ten meters above ground level as the sites permit. The data sets where typically greater than 95% complete. In order to obtain a representation of wind farm output data is passed through a model of a wind turbine.

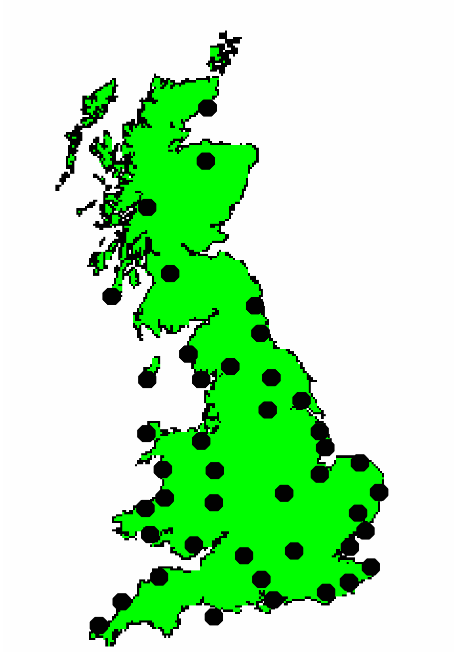

Fig. 1 - Geographic distribution of UK Met Office weather stations used in studies

The turbine output model is based on the general formula for calculating the extracted power from the wind (1), taken from [2]. Here the output power (P), is a function of coefficient of performance (C_P) the density of air (ρ_{air}) the swept area of the turbine blades (A) and the wind speed (v)

$$P = \frac{C_P . \rho_{air} . A . v^3}{2} \quad (1)$$

The coefficient of performance in this equation can be thought of as the efficiency of the turbine in extracting power from the wind. The value of C_P varies with different wind speeds and is also dependent on the designs of wind turbines. For this study a typical C_P-λ curve was used to calculate the power extracted by the turbines where λ is the tip speed ratio (2), Figure 2. In (2), Ω is the rate of rotation and R is the turbine blade radius.

$$\lambda = \frac{\Omega R}{v} \quad (2)$$

The turbine model limits operation of the turbine to between a lower cut-in wind speed of 4 ms^{-1} and an upper out-cut speed of 20 ms^{-1}. The turbine capacity was taken at each site as the maximum output experienced for the data set if wind speeds did not exceed 20 ms^{-1}. This is a reasonable assumption as most turbines are specifically selected based on the weather conditions at sites where they operate.

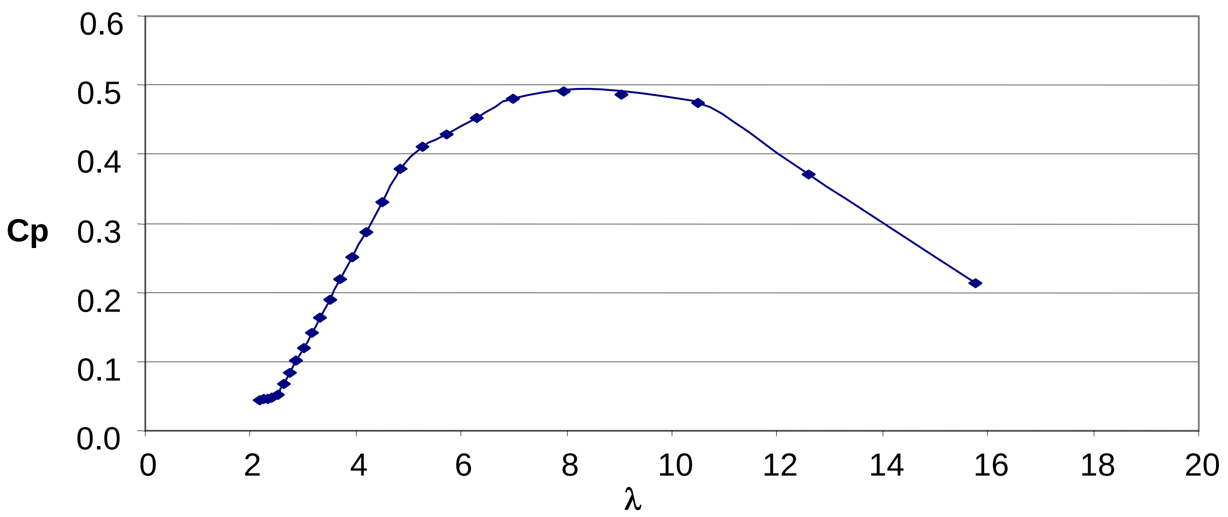

Fig. 2 - Typical C_P-λ curve used in studies to calculate turbine output

4.0 GB Wind Characteristics

Wind patterns in and around the UK allow a favorable amount of wind energy extraction to be realized. Figure 3 shows the average wind speed across the UK. The West Coast of England and Scotland has the highest mean wind speeds, which make them desirable sites for wind farms. Compiled data [3] shows the European coastline closest to Great Britain experiences similar wind speeds to those seen across England and Wales. It is only the Nordic countries that have speeds that reach as high as those found in Scotland.

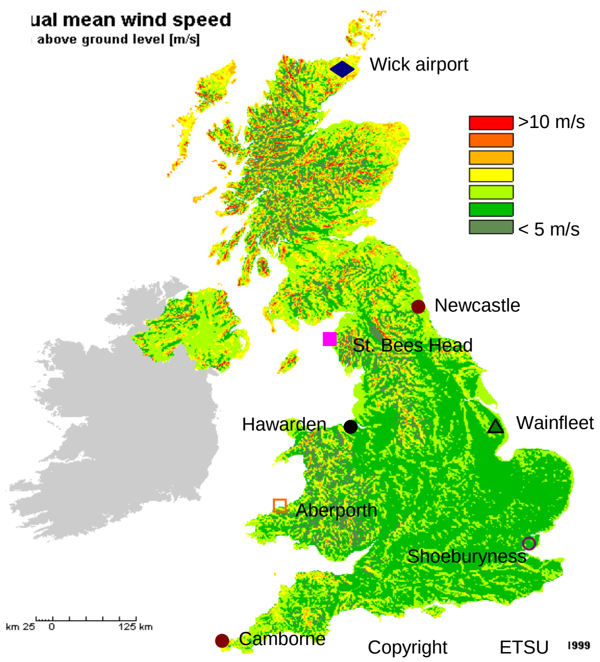

Fig. 3 - Annual mean wind speed at 25m above ground level ms^{-1}

Using Met office data and the wind turbine model a theoretical Power output duration curve can be calculated for each of the stations. Figure 4 shows these curves for a selection of sites across Great Britain as highlighted in figure 3.

Figure 4 illustrates how the difference in the wind characteristics across the country has a dramatic effect on the output power that can be expected from the wind farms. It also demonstrates the strong link between the high mean wind speeds in the north and the higher load factor of wind farms in these areas. In general the wind speed across Great Britain cannot be represented as a single mean value at any instant. The differences in power output across the country are best described due to part or regional weather systems on a micro scale.

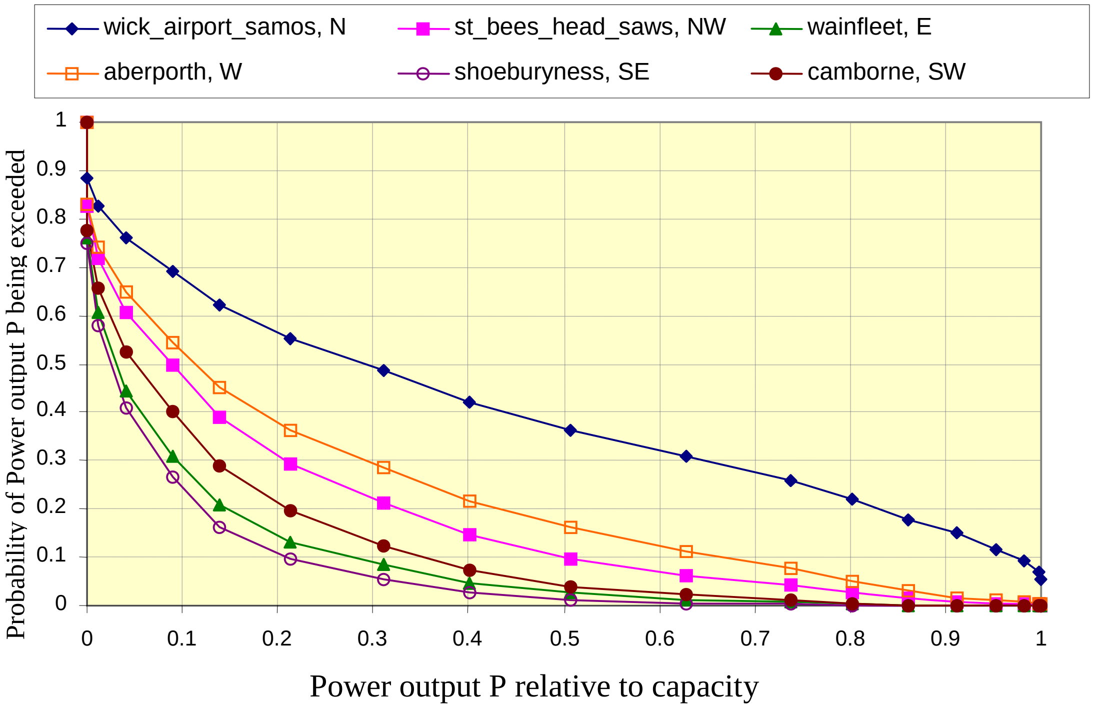

Fig. 4 - Load duration curves for a selection of sites across Great Britain

To establish the size of these weather regions the correlation of output from pairs of the sites must be calculted. The Pearson's correlation coefficent is caculated for every two sets of data and the distance between sites can be calculated from geographic bearings. If the pairs of data are realisations of two truly independent radom variables then the expected correlation value will be zero.

The correlation of sites suggests that we cannot simply assume that the outputs of all wind farms around Great Britain would be at the same output regardless of location. Figure 5 looks at the variation of wind speed as we move away from individual sites. The loss of correlation as distance increases is clearly visible in the curves. What is also noticeable is the noisiness of the graphs, this again highlights the regional weather systems, which are causing distinct differences in wind speed even though geographic separation of sites is of the same distance.

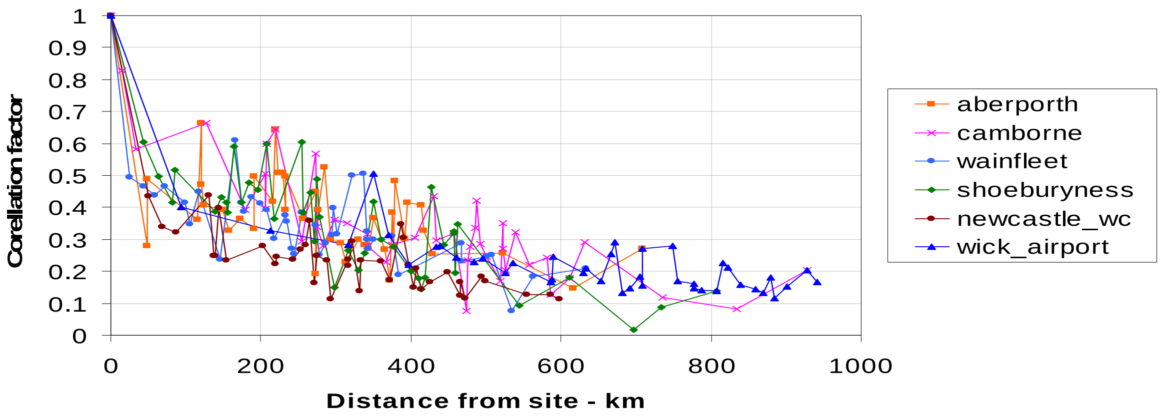

Fig. 5 - Correlation of hourly wind at various distances for specific sites in Great Britain (see fig. 3 for location)

Looking at the difference between site wind speeds we can estimate the distance at which the outputs from two wind farms become independent. For the fitted curve in figure 6, at distances above 200km the correlation factor is below 0.5, this implies that the correlation between sites is weak above this distance. In similar studies [4], it was found that the correlation between Nordic wind farm sites is also weak at distances greater than 200 km. This suggests that operation of British wind farms would have similar experiences to the Nordic electricity grid in terms of aggregated output.

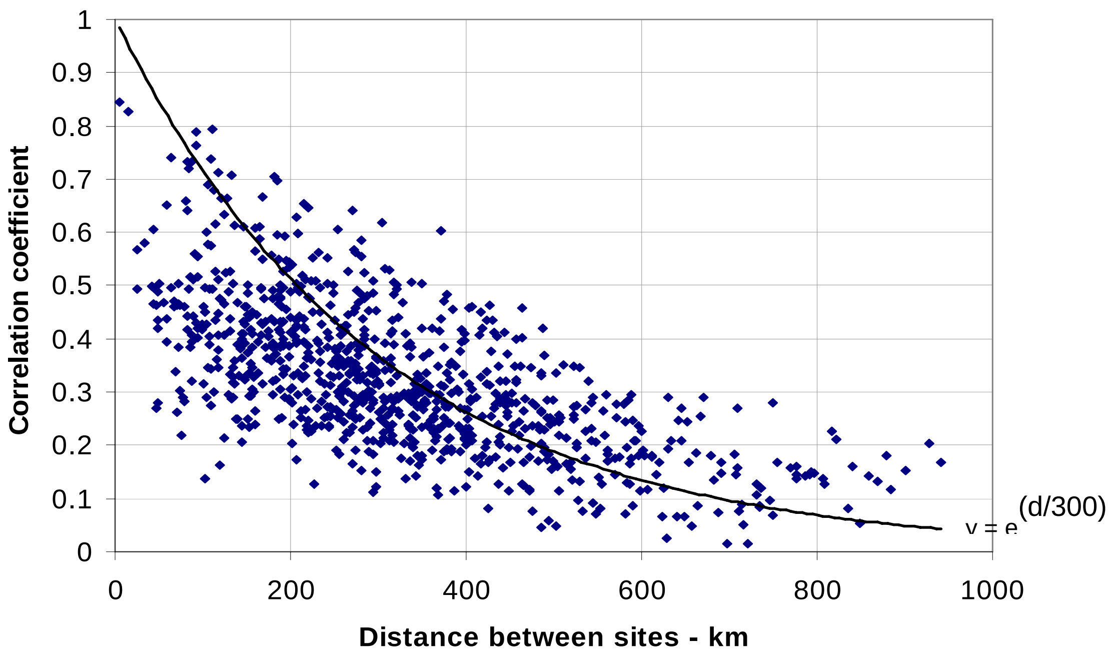

Fig. 6 - Correlation of hourly wind at various distances between sites

For system planning studies Great Britain is divided by a set of 13 boundaries, the main boundaries of concern are given in figure 7. Planning studies require a transmission factor be assigned to generator plants across these boundaries. This factor gives a realistic estimate of the percentage of total capacity in that area that would be generating electricity. Once this value is established the net transfer across the boundary can be calculated. This transfer can then be interpreted as how much extra network reinforcement would be necessary to cope with the import or export of power across the boundary in question.

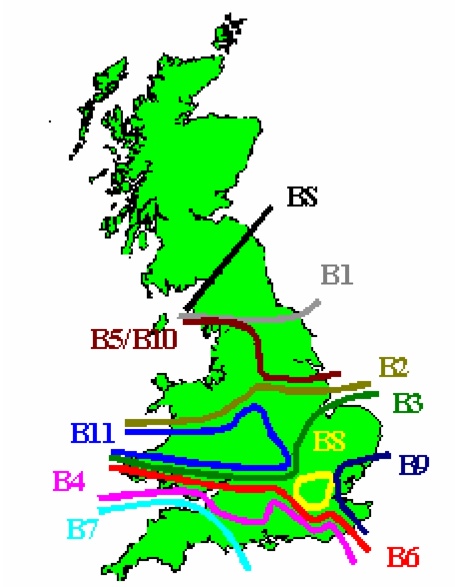

Fig. 7 - Main boundaries of the British grid used in planning studies [5]

Fig. 8 - Operational GB wind farms

4.0 Wind Transmission Factors

Table 1 shows the ninetieth and seventieth percentile outputs for wind farms in the different regions of GB separated by the boundaries shown in fig. 7. The values range from 0.26 to 0.43 at the ninetieth percentile interval. The cumulative output from wind turbines in Great Britain at a national level is in the order of 0.28 at the ninetieth percentile.

	All	BS		B1		B2		B3		B4	
		N	S	N	S	N	S	N	S	N	S
90th Percentile	0.28	0.42	0.27	0.39	0.27	0.35	0.26	0.26	0.26	0.28	0.40
70th Percentile	0.18	0.29	0.18	0.23	0.18	0.16	0.18	0.17	0.18	0.18	0.15

N = North S = South I = inside O = Outside

	B6		B7		B9		B10 / B5		B11	
	N	S	N	S	O	I	N	S	O	I
90th Percentile	0.33	0.28	0.29	0.43	0.26	0.27	0.33	0.27	0.27	0.26
70th Percentile	0.17	0.17	0.18	0.21	0.17	0.11	0.11	0.18	0.17	0.19

Table 1 - Wind transmission factors at boundaries of the GB grid

E.ON has published similar curves for the cumulative output of German turbines [6]. At the ninetieth percentile outputs are at a level of 0.45. The system operator in West Denmark, Eltra, has provided a set of duration curves for onshore and offshore wind installations [7]. The onshore data suggests a factor of 0.52 at the same interval level, although this is for a single farm output. A study commissioned by the Irish Wind Energy Association [8] suggests a value of 0.78 is a reasonable assumption.

5.0 Discussion

There is a large discrepancy between the cumulative outputs of turbines given for the Irish, German and West Denmark systems in comparison to the estimated outputs in Table 1. This is in part due to the assumption made about the geographic dispersion of wind turbines in Great Britain. The data is determined assuming an even distribution as given in figure 1. In reality the current distribution of turbines is concentrated mainly around the West Coast of the Britain. In particular Cornwall, Wales and Northern England where wind speeds are higher (Figure 8). It is also worth mentioning that the geographic siting of the Met office weather stations may not be ideal sites for wind turbines, and as such only serve as an indication of the wind speed in the area.

To provide a more realistic geographic distribution of turbines a weighting factor could be added to areas where turbines are already in operation. These sites are generally in areas that offer higher than average wind speeds and so provide higher outputs. With this addition it is likely that the aggregated GB output would be brought in line with the values experienced by other system operators in Europe.

The study itself was limited to the use of only three years of data, ideally more current data up to 2003/4 would increase the confidence in the wind distributions. Without using up to date data sets the data could be misrepresenting any changing trends to current weather patterns.

One final shortfall to note in the calculated output data is that the model does not take account of turbine hub height. Wind installations are typically 40 to 80 meters above ground level, data used in this study is collected at 10 meters. This has the effect of increasing wind speeds as seen by the turbines. A simple modification could be made to the calculation to include a surface layer model to calculate the wind speed at the required height (3). Here, u is the wind speed at a given height, k is the Von Karmen constant, h is the required height and z_0 is the roughness length (taken as 0.03m).

$$u(h_1) = \frac{u(0)}{k}.\ln\left(\frac{h_1}{z_0}\right) \quad (3)$$

However, translating a sample of the collected data in this fashion would increase wind speeds by a factor of 1.3. As the measuring instruments are placed over level, open terrain it is highly possible that the measurements are an accurate enough representation of the wind speeds in that particular area. Therefore, applying this modification may not bring any further improvement to the data.

Regardless of the height scaling factor or any potential inadequacies of the geographic distribution chosen, this model does show the regional significance of aggregating wind farm outputs. Figure 9 shows the output from two sites in the Wales area, and an aggregated total of all the Welsh sites. If we were to take the 90^{th} percentile in each case the cumulative value would be 0.3, whereas for the two individual sites the values are 0.18 and 0.69. Both sites have a distinctly different wind distribution pattern even though they are located in the same region. However, the sites are 216 km apart, which as has been shown to be above the distance at which we can consider the two sites to be independent. This explains why the outputs from the individual farms are different.

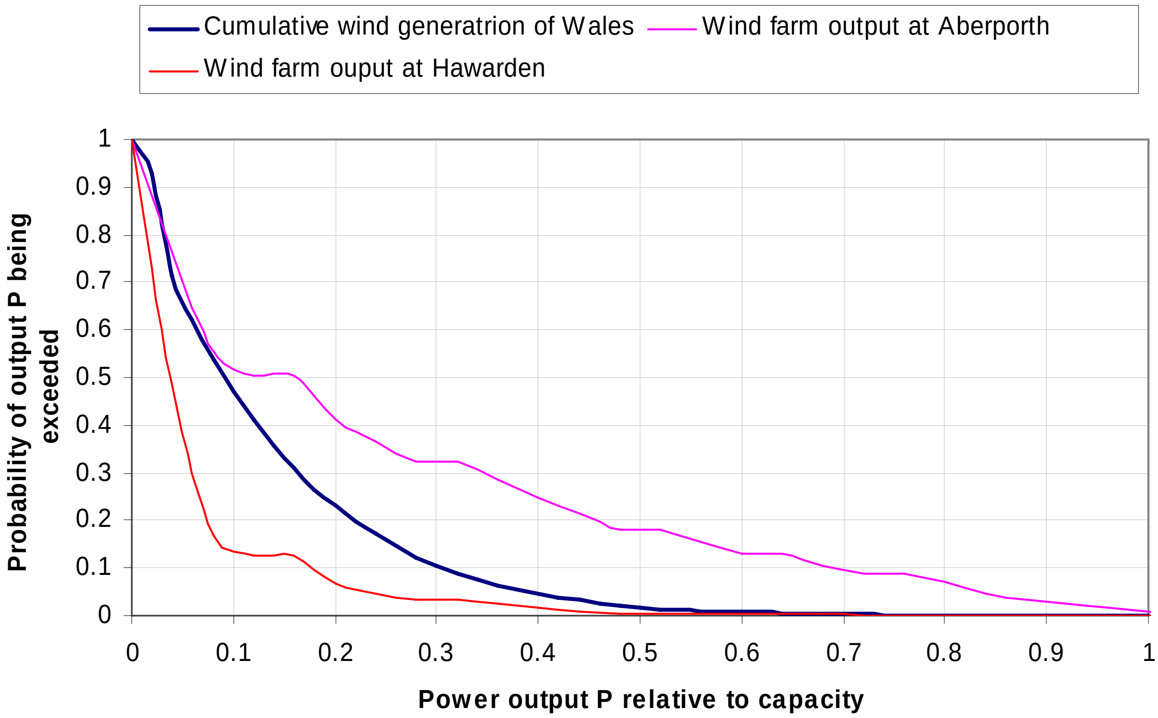

Fig. 9 - Duration curves for single turbines in Wales and cumulative total of 7 sites within the region

6.0 Conclusion

The results of this paper highlight some of the potential problems in planning for large amounts wind turbines in Great Britain. It is clear that the effects of wind speed cannot be assumed as constant over the entire length of the country. In the case of wind generation it is necessary to provide a specific transmission factor to represent the regional variations in actual wind farm output. This paper has suggested transmission factors in the range of 0.26 to 0.43 for use in system planning studies. This is considerably less than the 0.6 factor suggested in previous studies.

The geographic siting of wind farms also has a significant impact on the values of transmission factor within the system boundaries. A distinct correlation exists between sites that are less than 200 km part, whilst sites at greater distances can be considered as independent. In order to enhance the accuracy of the transmission factors it is suggested that further calculations be made using weighting factors for areas of existing turbines and possibly even potential sites.

There is need for further work to investigate how to aggregate the wind distributions at individual sites whilst taking into account any correlation factors. If a simple method can be developed this method would be of great benefit to planning studies and also for forecasting wind turbine outputs.

Acknowledgement

The author wishes to acknowledge the UK Met. Office for supplying data used in this paper, and also for its assistance in answering questions regarding the acquisition of the data.

References

[1] Civil J., "Assumed load factors for distributed wind generation", Internal Report, National Grid, Dec 2003
[2] Burton T., Sharpe D., Jenkins N., Bossyani E.,"Wind Energy Handbook", Wiley, New York, 2001
[3] Risø Laboratory, "European wind resource map", Denmark.
[4] Holttinen H.,Norgaard,P., "A multi-turbine power curve approach", Nordic wind power conference, Chalmers university of technology, Mar 2004
[5] "Seven Year Statement", National grid, March 2004 http://www.nationalgrid.com/uk/library/documents/sys_04/default.asp?action=&sNode=SYS&Exp=Y
[6] E.ON, "E.ON netz Wind report", 2004 www.eon-energie.de/bestellsystem/frameset_eng.php?choosenBu=eonenergie&choosenId=405
[7] Eltra (Kent Søbrink), "The challenge of wind power" http://www.owen.eru.rl.ac.uk/workshop_4/pdfs/owen_KSobrink_The%20challenge%20of%20wind%20power.pdf
[8] Coelingh J.P., "Geographical dispersion of wind power output in Ireland", IWEA report, December 1999 http://www.iwea.com/publications/Ecofys2.pdf

Review of primary frequency control requirements on the GB power system against a background of increasing renewable generation

Vol. 1

Appendix B

Network Model and Parameters

Ross Stuart Pearmine

Academic Supervisor: Prof. Yong-Hua Song, Brunel Institute of Power Systems, Brunel University, Uxbridge

Industrial Supervisor: Dr. Ahmad Chebbo, National Grid, Sindlesham

Network Diagram

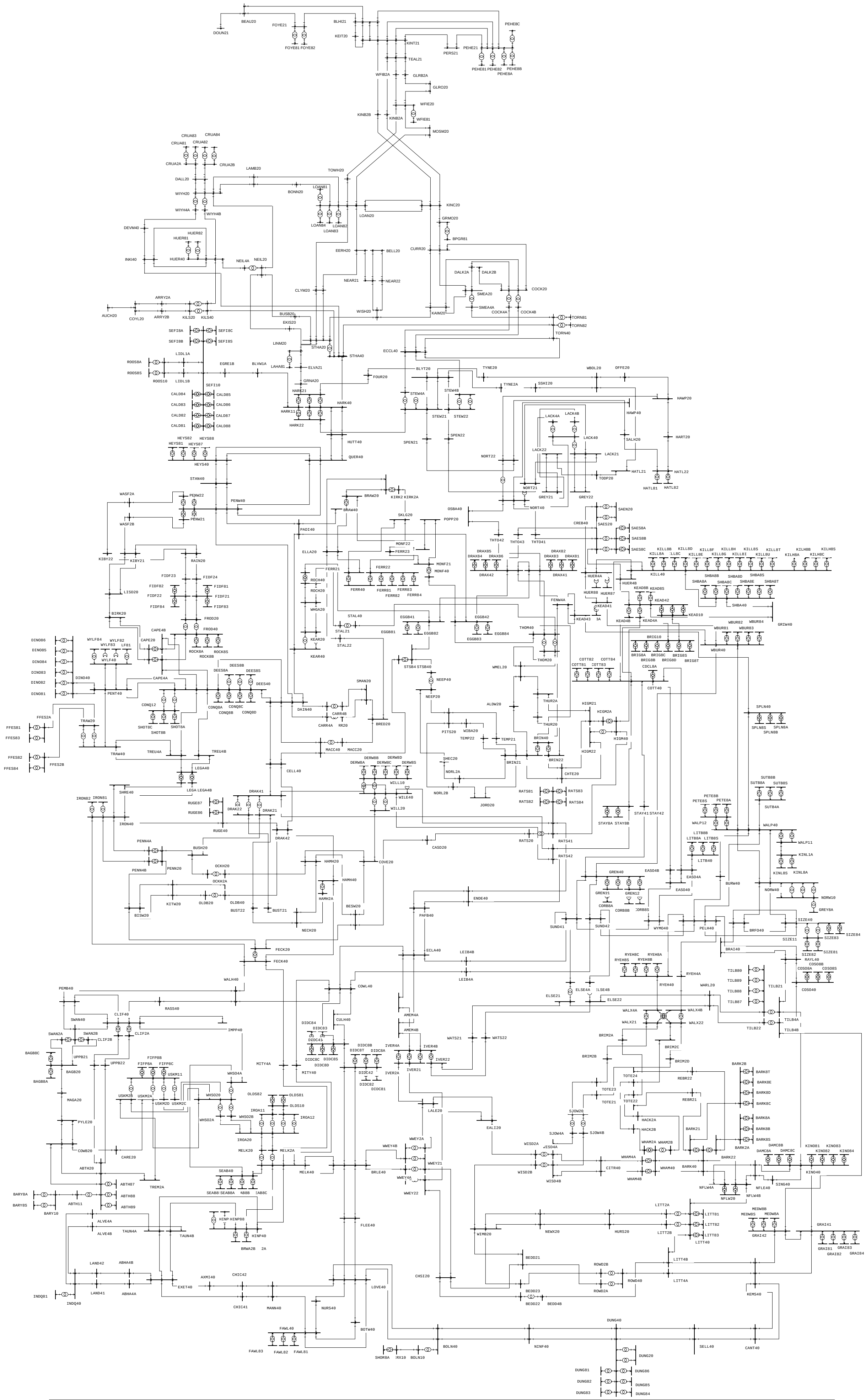

Area	Node	Voltage	Area	Node	Voltage	Area	Node	Voltage	Area	Node	Voltage
1A1	CHIC42	400	1E7	BRWA2B	275	1M5	CONQ8C	22	1Q4	HAWP40	400
1A1	KEMS40	400	1E7	BRWA2A	275	1M5	FROD40	400	1Q4	HAWP20	275
1A1	TOTE22	275	1E7	TAUN4B	400	1M5	DEES40	400	1Q4	NORT22	275
1A1	BEDD23	275	1E7	TAUN4A	400	1M5	LEGA4A	400	1Q4	WBOL20	275
1A1	BEDD4B	400	1F6	ABHA4B	400	1M6	DINO86	22	1Q4	TYNE2A	275
1A1	TOTE23	275	1F6	INDQ81	22	1M6	DINO40	400	1Q4	TYNE20	275
1A1	TOTE24	275	1F6	INDQ40	400	1M6	PENT40	400	1Q4	NORT21	275
1A1	ELSE22	275	1F6	ABHA4A	400	1M6	DINO85	22	1Q5	STEW22	275
1A1	CLIF40	400	1F6	ALVE4B	400	1M6	WYLF81	22	1Q5	STEW4A	400
1A1	CLIF2B	275	1F6	ALVE4A	400	1M6	WYLF82	22	1Q5	STEW4B	400
1A1	CULH40	400	1G1	WALH40	400	1M6	WYLF83	22	1Q5	STEW21	275
1A1	CLIF2A	275	1G6	MELK40	400	1M6	DINO84	22	1Q7	SPEN22	275
1A1	BRAI40	400	1G6	MELK2A	275	1M6	WYLF84	22	1Q7	SPEN21	275
1A1	TEMP22	275	1G6	MITY40	400	1M6	DINO81	22	1Q8	FOUR20	275
1A1	ELSE4B	400	1G6	MITY4A	400	1M6	WYLF10	132	1Q8	HARK11	132
1A1	MONF40	400	1G6	IROA20	275	1S1	SHRU2B	275	1Q8	HARK21	275
1A1	CHIC41	400	1G6	IROA11	132	1M6	DINO83	22	1Q8	HARK22	275
1A1	HACK2A	275	1G6	MELK20	275	1M6	WYLF40	400	1Q8	HARK40	400
1A1	HACK2B	275	1G6	SEAB8S	22	1M6	DINO82	22	1Q8	HARK13	132
1A1	HAMH20	275	1G6	OLDS10	132	1M7	FFES84	22	1Q8	EGRE1B	132
1A1	WHAM2A	275	1G6	OLDS82	22	1M7	FFES83	22	1Q8	BLVW1A	132
1A1	WHAM2B	275	1G6	OLDS81	22	1M7	FFES82	22	1R5	HEYS82	22
1A1	WHAM40	400	1G6	IROA12	132	1M7	FFES81	22	1R5	HEYS40	400
1A1	WHAM4A	400	1G6	SEAB8C	22	1M7	FFES2B	275	1R5	HEYS87	22
1A1	WHAM4B	400	1G6	SEAB8B	22	1M7	FFES2A	275	1R5	HEYS88	22
1A1	HUTT40	400	1G6	SEAB8A	22	1M7	TRAW20	275	1R5	HEYS81	22
1A1	LAND42	400	1G6	SEAB40	400	1M7	TRAW40	400	1R6	CALD88	22
1A1	LAND41	400	1H1	BAGB8C	22	1N1	RAIN20	275	1R6	FELL81	22
1A1	ELSE4A	400	1H1	COWB20	275	1N1	FIDF22	275	1R6	CALD86	22
1A1	BARK21	275	1H1	BAGB20	275	1N1	FIDF23	275	1R6	SEFI10	132
1A1	REBR21	275	1H1	PYLE20	275	1N1	FIDF24	275	1R6	SEFI8A	22
1A1	REBR22	275	1H1	BAGB8A	22	1N1	FIDF81	22	1R6	SEFI8B	22
1A1	RATS20	275	1H1	BARY8S	22	1N1	FIDF82	22	1R6	SEFI8C	22
1A1	QUER40	400	1H1	BARY10	132	1N1	FIDF83	22	1R6	LIDL1B	132
1A1	PENW40	400	1H1	BARY8A	22	1N1	FIDF84	22	1R6	CALD87	22
1A1	PENW22	275	1H1	UPPB22	275	1N1	WASF2A	275	1R6	CALD84	22
1A1	PENW21	275	1H1	UPPB21	275	1N1	WASF2B	275	1R6	FELL84	22
1A1	PAFB40	400	1H1	MAGA20	275	1N1	FIDF21	275	1R6	FELL83	22
1A1	SING40	400	1H2	WHSO20	275	1N1	LISD20	275	1R6	FELL82	22
1A1	NFLW4B	400	1H2	ABTH88	22	1N1	KIBY22	275	1R6	SEFI8S	22
1A1	STAN40	400	1H2	TREM2A	275	1N1	KIBY21	275	1R6	CALD82	22
1A1	NFLW4A	400	1H2	ABTH11	132	1N2	CARR4A	400	1R6	CALD85	22
1A1	TOTE21	275	1H2	ABTH20	275	1N2	BRED20	275	1R6	ROOS10	132
1A1	ELSE21	275	1H2	ABTH89	22	1N2	CARR20	275	1R6	ROOS8A	22
1A1	BLYT20	275	1H2	FIFP8B	22	1N2	SMAN20	275	1R6	LIDL1A	132
1A1	BARK22	275	1H2	WHSO4A	400	1N2	CARR4B	400	1R6	ROOS8S	22
1A1	BARK2A	275	1H2	WHSO2A	275	1N3	CAPE4A	400	1R6	CALD81	22
1A1	BARK2B	275	1H2	USKM2D	275	1N3	FROD20	275	1R6	CALD83	22

Area	Node	Voltage	Area	Node	Voltage	Area	Node	Voltage	Area	Node	Voltage
1A1	BARK40	400	1H2	ABTH87	22	1N3	CAPE20	275	1S1	WIYH4C	400
1A1	BARK8A	22	1H2	FIFP8A	22	1N3	ROCK8S	22	1S1	PEHE2C	275
1A1	BARK8B	22	1H2	USKM11	132	1N3	BIRK20	275	1S1	PEHE2B	275
1A1	BARK8C	22	1H2	USKM2A	275	1N3	CAPE4B	400	1S1	KINB21	275
1A1	BARK8D	22	1H2	USKM2B	275	1N3	ROCK8B	22	1S1	PEHE21	275
1A1	BARK8E	22	1H2	FIFP8C	22	1N3	ROCK8A	22	1S1	NEIL4B	400
1A1	BARK8S	22	1H2	USKM2C	275	1N4	KEAR20	275	1S1	LOAN87	22
1A1	BARK8T	22	1H2	WHSO2B	275	1N4	WHGA20	275	1S1	LOAN88	22
1A1	NEEP40	400	1H2	CARE20	275	1N4	KEAR40	400	1S1	MOSM2B	275
1A1	NFLW20	275	1H2	USKM83	22	1N4	ROCH20	275	1S1	MOSM2E	275
1A3	BRIM2C	275	1H2	USKM84	22	1N4	ROCH40	400	1S1	NEAR2B	275
1A3	WALX21	275	1H2	USKM85	22	1N5	PADI40	400	1S1	NEAR2C	275
1A3	WALX22	275	1H6	IMPP40	400	1N6	MACC40	400	1S1	NEIL20	275
1A3	WALX4B	400	1H6	SWAN2A	275	1N6	MACC20	275	1S1	WHHO2C	275
1A3	WALX4A	400	1H6	RASS40	400	1N6	DAIN40	400	1S1	NEIL4C	400
1A3	BRIM2B	275	1H6	SWAN40	400	1N7	STAL21	275	1S1	PEHE22	275
1A3	BRIM2D	275	1H6	SWAN2B	275	1N7	STAL22	275	1S1	TEAL2D	275
1A3	BRIM8A	22	1H6	PEMB40	400	1N7	STAL40	400	1M6	WYLF1AAL	132
1A3	BRIM2A	275	1J4	LITB40	400	1P1	BRAW40	400	1S1	TORN81	22
1A4	WIMB20	275	1J4	EASO4B	400	1P1	BRAW20	275	1S1	SHRU2C	275
1A4	NEWX20	275	1J4	LITB8B	22	1P1	SKLG20	275	1S1	SIGH2B	275
1A6	LALE20	275	1J4	LITB8S	22	1P1	ELLA20	275	1S1	SIGH2C	275
1A6	IVER22	275	1J4	EASO4A	400	1P1	KIRK20	275	1S1	SMEA20	275
1A6	WATS22	275	1J4	LITB8A	22	1P1	KIRK2A	275	1S1	WIYH20	275
1A6	WATS21	275	1J4	EASO40	400	1P2	POPP20	275	1S1	TORN40	400
1A6	IVER2A	275	1J5	BRFO40	400	1P3	TEMP21	275	1S1	RAVE2B	275
1A6	IVER4A	400	1J5	SIZE82	22	1P3	NORL2A	275	1S1	TEAL2C	275
1A6	IVER21	275	1J5	SIZE83	22	1P3	SHEC20	275	1S1	TEAL2B	275
1A6	IVER4B	400	1J5	SIZE84	22	1P3	NORL2B	275	1S1	TEAL22	275
1A6	AMEM4A	400	1J5	SIZE40	400	1P3	JORD20	275	1S1	TEAL21	275
1A6	AMEM4B	400	1J5	SIZE11	132	1P3	STSB40	400	1S1	STHA40	400
1A7	WISD4B	400	1J5	SIZE81	22	1P3	ALDW20	275	1S1	STHA20	275
1A7	SJOW20	275	1J6	CORB8S	22	1P3	WMEL20	275	1S1	SMEA4C	400
1A7	SJOW4A	400	1J6	GREN11	132	1P3	CHTE20	275	1S1	SMEA4B	400
1A7	SJOW4B	400	1J6	CORB8B	22	1P3	BRIN22	275	1S1	PEHE82	22
1A7	WISD2A	275	1J6	GREN40	400	1P3	WIBA20	275	1S1	WISH20	275
1A7	WISD4A	400	1J6	GREN12	132	1P3	THUR2A	275	1S1	WHHO2B	275
1A7	CITR40	400	1J6	CORB8A	22	1P3	NEEP20	275	1S1	WGEO2C	275
1A7	EALI20	275	1J7	NORW10	132	1P3	STSB4A	400	1S1	WGEO2B	275
1A7	WISD2B	275	1J7	WALP40	400	1P3	THUR20	275	1S1	WFIE20	275
1A8	LITT2A	275	1J7	WALP12	132	1P3	PITS20	275	1S1	WFIB20	275
1A8	LITT40	400	1J7	WALP11	132	1P3	BRIN21	275	1S1	PEHE2D	275
1A8	LITT4A	400	1J7	KINL1A	132	1P3	BRIN40	400	1S1	TORN82	22
1A8	LITT4B	400	1J7	SUTB8S	22	1P4	DRAX81	22	1S1	PEHE81	22
1A8	LITT81	22	1J7	NORW40	400	1P4	DRAX82	22	1S1	RAVE2C	275
1A8	LITT82	22	1J7	PETE8B	22	1P4	DRAX83	22	1S1	PERS2B	275
1A8	LITT83	22	1J7	SUTB8B	22	1P4	DRAX84	22	1S1	PERS2C	275
1A8	LITT2B	275	1J7	SUTB4A	400	1P4	DRAX85	22	1S1	POOB2B	275

Area	Node	Voltage	Area	Node	Voltage	Area	Node	Voltage	Area	Node	Voltage
1A8	BEDD22	275	1J7	GREY22	275	1P4	DRAX86	22	1S1	POOB2C	275
1A8	CHSI20	275	1J7	GREY21	275	1P4	DRAX42	400	1S1	PORD2B	275
1A8	ROWD40	400	1J7	PETE8S	22	1P4	DRAX41	400	1S1	PORD2C	275
1A8	ROWD2B	275	1J7	KINL8S	22	1P5	FERR81	22	1S1	WIYH4B	400
1A8	ROWD2A	275	1J7	PETE8A	22	1P5	FERR21	275	1S1	PEHE2E	275
1A8	HURS20	275	1J7	GREY8A	22	1P5	FERR22	275	1S1	AUCH20	275
1A8	WWEY4B	400	1J7	SUTB8A	22	1P5	MONF21	275	1S1	DEWP2C	275
1A8	WWEY21	275	1J7	KINL8A	22	1P5	MONF22	275	1S1	COCK84	22
1A8	WWEY4A	400	1J7	BURW40	400	1P5	FERR40	400	1S1	COYL20	275
1A8	BEDD21	275	1K1	SPLN8A	22	1P5	FERR82	22	1S1	COYW2D	275
1A8	WWEY2A	275	1K1	SPLN40	400	1P5	FERR83	22	1S1	COYW2E	275
1A8	WWEY22	275	1K1	SPLN8B	22	1P5	FERR84	22	1S1	CRUA2B	275
1A9	RYEH8A	22	1K1	SPLN8S	22	1P5	FERR23	275	1S1	CRUA2C	275
1A9	RYEH8S	22	1K2	HIGM21	275	1P6	THTO43	400	1S1	CRUA2D	275
1A9	RYEH8B	22	1K2	HIGM22	275	1P6	THTO42	400	1S1	AYR-2C	275
1A9	RYEH40	400	1K2	HIGM2A	275	1P6	THTO41	400	1S1	CRUA81	22
1A9	RYEH8C	22	1K5	STAY41	400	1P6	THOM40	400	1S1	BEAU21	275
1A9	RYEH4A	400	1K5	COTT84	22	1P6	THOM20	275	1S1	ARDR2B	275
1B1	SERX10	132	1K5	STAY42	400	1P6	EGGB81	22	1S1	CRUA82	22
1B1	BOLN40	400	1K5	COTT83	22	1P6	EGGB42	400	1S1	CRUA83	22
1B1	SHOR8A	22	1K5	COTT82	22	1P6	EGGB41	400	1S1	CRUA84	22
1B1	NINF40	400	1K5	COTT81	22	1P6	FENW4A	400	1S1	CURR20	275
1B1	BOLN10	132	1K5	STAY8A	22	1P6	EGGB84	22	1S1	DALL20	275
1B2	NURS40	400	1K5	STAY8B	22	1P6	EGGB83	22	1S1	DALM2B	275
1B2	LOVE40	400	1K5	COTT40	400	1P6	OSBA40	400	1S1	KINC20	275
1B2	FAWL40	400	1K5	CDCL8A	22	1P6	EGGB82	22	1S1	DEVM40	400
1B2	FAWL8C	22	1K6	WBUR81	22	1P7	KILL8I	22	1S1	CRUA2E	275
1B2	BOTW40	400	1K6	HIGM40	400	1P7	KILL8U	22	1S1	CHAS2C	275
1B2	FAWL8A	22	1K6	WBUR84	22	1P7	GRIW40	400	1S1	LOAN86	22
1B2	FAWL8B	22	1K6	WBUR83	22	1P7	KILH8B	22	1S1	COCK83	22
1B3	FLEE40	400	1K6	WBUR82	22	1P7	KILH8A	22	1S1	COCK82	22
1B4	BRLE40	400	1K6	WBUR40	400	1P7	KILL8S	22	1S1	COCK81	22
1C1	TILB4A	400	1L1	PENN4A	400	1P7	KILL8G	22	1S1	COCK4C	400
1C1	TILB4B	400	1L1	PENN4B	400	1P7	KILL8H	22	1S1	COCK4B	400
1C1	TILB80	22	1L1	PENN20	275	1P7	KILH8C	22	1S1	COCK20	275
1C1	TILB87	22	1L2	OCKH2A	275	1P7	KILH8S	22	1S1	COAL2C	275
1C1	TILB88	22	1L2	OCKH20	275	1P7	KILL40	400	1S1	AYR-2B	275
1C1	COSO8S	22	1L2	BISW20	275	1P7	KILL8A	22	1S1	CLYM20	275
1C1	TILB89	22	1L2	KITW20	275	1P7	KILL8B	22	1S1	DEWP2B	275
1C1	TILB22	275	1L2	OLDB20	275	1P7	KILL8C	22	1S1	CHAS2B	275
1C1	COSO40	400	1L2	OLDB40	400	1P7	KILL8D	22	1S1	CHAP81	22
1C1	COSO8B	22	1L2	DRAK21	275	1P7	KILL8E	22	1S1	BUSB20	275
1C1	COSO8A	22	1L2	BUSH20	275	1P7	KILL8F	22	1S1	BONN20	275
1C1	TILB21	275	1L2	DRAK89	22	1P7	KILL8T	22	1S1	BLHI22	275
1C2	DAMC8C	22	1L2	DRAK22	275	1P7	SHBA40	400	1S1	BLHI21	275
1C2	DAMC8A	22	1L2	DRAK41	400	1P7	SHBA8T	22	1S1	BELL2C	275
1C2	NFLE40	400	1L2	DRAK42	400	1P7	SHBA8S	22	1S1	BELL2B	275
1C2	KINO84	22	1L2	DRAK81	22	1P7	SHBA8E	22	1S1	BEAU22	275

Area	Node	Voltage	Area	Node	Voltage	Area	Node	Voltage	Area	Node	Voltage
1C2	KINO83	22	1L2	DRAK82	22	1P7	SHBA8D	22	1S1	COAL2B	275
1C2	KINO82	22	1L3	NECH20	275	1P7	SHBA8C	22	1S1	KINT2D	275
1C2	KINO81	22	1L3	WILL20	275	1P7	SHBA8A	22	1S1	KILS20	275
1C2	KINO40	400	1L3	HAMH40	400	1P7	SHBA8B	22	1S1	DALM2C	275
1C2	DAMC8B	22	1L3	FECK20	275	1P8	KEAD42	400	1S1	KILS4E	400
1C3	CANT40	400	1L3	FECK40	400	1P8	KEAD43	400	1S1	KILT2B	275
1C3	MEDW8B	22	1L3	DERW8S	22	1P8	KEAD4A	400	1S1	KILT2C	275
1C3	MEDW8S	22	1L3	DERW81	22	1P8	KEAD4B	400	1S1	KINB22	275
1C3	GRAI84	22	1L3	BESW20	275	1P8	KEAD8A	22	1S1	KINT21	275
1C3	GRAI83	22	1L3	DERW84	22	1P8	KEAD8B	22	1S1	KINT22	275
1C3	GRAI82	22	1L3	DERW83	22	1P8	KEAD41	400	1S1	DOUN20	275
1C3	GRAI81	22	1L3	DERW82	22	1P8	KEAD8S	22	1S1	KINT2C	275
1C3	GRAI42	400	1L3	HAMH2A	275	1P8	KEAD8C	22	1S1	KEIT2C	275
1C3	GRAI41	400	1L3	DERW8C	22	1P8	SAES8C	22	1S1	LAMB20	275
1C3	MEDW8A	22	1L3	DERW8B	22	1P8	BRIG8C	22	1S1	LAMB2E	275
1C4	DUNG86	22	1L3	DERW8A	22	1P8	BRIG10	132	1S1	LINM20	275
1C4	DUNG40	400	1L3	BUST22	275	1P8	BRIG8D	22	1S1	LOAN20	275
1C4	DUNG81	22	1L3	WILL10	132	1P8	BRIG8S	22	1S1	LOAN81	22
1C4	DUNG82	22	1L3	CASD20	275	1P8	BRIG8B	22	1S1	LOAN82	22
1C4	DUNG20	275	1L3	BUST21	275	1P8	BRIG8A	22	1S1	LOAN83	22
1C4	DUNG83	22	1L3	DERW8D	22	1P8	SAES8B	22	1S1	LOAN84	22
1C4	DUNG84	22	1L3	COVE20	275	1P8	BRIG8T	22	1S1	LOAN85	22
1C4	DUNG85	22	1L5	RUGE40	400	1P8	KEAD10	132	1S1	KINT2B	275
1C5	RAYL40	400	1L5	CELL40	400	1P8	CREB40	400	1S1	FOYE81	22
1C6	WARL20	275	1L5	IRON40	400	1P8	SAEN20	275	1S1	DRUM2B	275
1C9	SELL40	400	1L5	RUGE87	22	1P8	SAES20	275	1S1	DRUM2C	275
1D4	SUND42	400	1L5	RUGE86	22	1P8	SAES8A	22	1S1	ECCL40	400
1D4	ECLA40	400	1L5	IRON81	22	1Q2	HATL21	275	1S1	EERH20	275
1D4	SUND41	400	1L5	IRON82	22	1Q2	TEES8C	22	1S1	EKIS20	275
1D5	WYMO40	400	1L5	WILE40	400	1Q2	SALH20	275	1S1	ELVA20	275
1D5	PELH40	400	1L5	SHRE40	400	1Q2	HART20	275	1S1	KILS40	400
1D6	DIDC8A	22	1L7	RATS83	22	1Q2	TEES8T	22	1S1	FOYE20	275
1D6	LEIB4A	400	1L7	RATS41	400	1Q2	LACK22	275	1S1	KEIT2B	275
1D6	LEIB4B	400	1L7	RATS42	400	1Q2	LACK40	400	1S1	FOYE82	22
1D6	DIDC84	22	1L7	RATS81	22	1Q2	LACK4A	275	1S1	HUER81	22
1D6	COWL40	400	1L7	RATS82	22	1Q2	TEES8A	22	1S1	KAIM20	275
1D6	DIDC83	22	1L7	RATS84	22	1Q2	LACK4B	275	1S1	INKI40	400
1D6	DIDC8C	22	1L8	ENDE40	400	1Q2	HATL22	275	1S1	GIFF2B	275
1D6	DIDC81	22	1M5	CONQ8D	22	1Q2	LACK21	275	1S1	HUER82	22
1D6	DIDC42	400	1M5	SHOT8A	22	1Q2	TODP20	275	1S1	HUER40	400
1D6	DIDC8S	22	1M5	TREU4A	400	1Q2	HATL82	22	1S1	GRMO20	275
1D6	DIDC8D	22	1M5	CONQ12	132	1Q2	TEES8S	22	1S1	GLRO20	275
1D6	DIDC41	400	1M5	SHOT8C	22	1Q2	TEES8H	22	1S1	GLRB20	275
1D6	DIDC8B	22	1M5	CONQ8A	22	1Q2	TEES8G	22	1S1	GIFF2C	275
1D6	DIDC82	22	1M5	TREU4B	400	1Q2	TEES8F	22	1S2	TONG81	22
1D6	DIDC8T	22	1M5	DEES8A	22	1Q2	TEES8E	22	1S2	PEHE8A	22
1E6	MANN40	400	1M5	SHOT8B	22	1Q2	TEES8D	22	1S2	PEHE8B	22
1E6	AXMI40	400	1M5	CONQ8B	22	1Q2	TEES8B	22	1S2	PEHE8C	22

Area	Node	Voltage	Area	Node	Voltage	Area	Node	Voltage	Area	Node	Voltage
1E6	EXET40	400	1M5	LEGA4B	400	1Q2	HATL81	22	1S2	PEHE8G	22
1E7	HINP88	22	1M5	LEGA40	400	1Q4	OFFE20	275	1S3	WFIE81	22
1E7	HINP87	22	1M5	DEES8B	22	1Q4	SSHI20	275	1S3	BPGR81	22
1E7	HINP40	400	1M5	DEES8S	22	1Q4	NORT40	400			

Sending Node	Receiving Node	Index	Line Resistance *(pu)*	Line Reactance *(pu)*	Semi-shunt Conductance *(pu)*	Semi-shunt Susceptance *(pu)*	Rated Power
ABHA4A	EXET40	1	0.00103	0.00988	0	0.13801	1390
ABHA4B	EXET40	1	0.00103	0.00982	0	0.13726	1390
ABTH20	TREM2A	1	0.00256	0.02088	0	0.06129	625
ALDW20	BRIN21	1	0.0015	0.00783	0	0.02667	625
ALVE4A	TAUN4A	1	0.00153	0.01465	0	0.20461	1390
ALVE4B	TAUN4B	1	0.00153	0.01465	0	0.20461	1390
AMEM4A	ECLA40	1	0.00061	0.00665	0	0.10944	2010
AUCH20	COYL20	1	0.00493	0.03571	0	0.06682	690
AXMI40	CHIC42	1	0.00043	0.00627	0	0.14188	2780
AYRR2A	COYL20	1	0.00055	0.00385	0	0.0151	955
AYRR2A	KILS20	1	0.00068	0.00561	0	0.019	760
AYRR2B	KILS20	1	0.00068	0.00561	0	0.019	760
AYRR2B	COYL20	1	0.00008	0.001	0	0.00208	760
BAGB20	SWAN2B	1	0.00065	0.0077	0	0.02866	1650
BAGB20	MAGA20	1	0.00034	0.00344	0	0.03163	1650
BARK21	REBR21	1	0.00041	0.00436	0	0.01604	1380
BARK21	BARK2B	1	0.0001	0.00102	0	0.00376	1380
BARK22	REBR22	1	0.00041	0.00436	0	0.01604	1380
BARK22	BARK2A	1	0.0001	0.00102	0	0.00376	1380
BARY10	ABTH11	1	0.0062	0.03016	0	0	9999
BEAU20	FOYE20	1	0.0039	0.0206	0	0.04855	525
BEAU20	BLHI20	1	0.0123	0.0452	0	0.13935	525
BEAU20	DOUN20	1	0.0122	0.0836	0	0.16195	485
BEDD23	WIMB20	1	0.0004	0.00375	0	0.05882	860
BELL20	NEAR21	1	0.00022	0.00183	0	0.00609	955
BESW20	COVE20	1	0.00084	0.0076	0	0.02593	955
BESW20	CASD20	1	0.00268	0.02912	0	0.11088	955
BIRK20	CAPE20	1	0.0007	0.00665	0	0.02074	955
BIRK20	CAPE20	2	0.0007	0.00662	0	0.02062	955
BISW20	FECK20	1	0.00092	0.00912	0	0.0326	955
BISW20	KITW20	1	0.00109	0.00989	0	0.03373	955
BISW20	KITW20	2	0.00123	0.0111	0	0.03788	955
BLHI20	PEHE20	1	0.0042	0.0358	0	0.1081	1060
BLHI20	KINT20	1	0.006	0.0221	0	0.0683	525
BLVW1A	HARK11	1	0.00351	0.01101	0	0.00241	185
BLYT20	TYNE20	1	0.00072	0.00681	0	0.02318	1240
BLYT20	TYNE2A	1	0.00072	0.00684	0	0.0233	1240
BLYT20	STEW22	1	0.00148	0.01381	0	0.07134	525
BOLN40	NINF40	1	0.00057	0.00853	0	0.17421	2720
BOLN40	NINF40	2	0.00057	0.00853	0	0.17421	2720
BONN20	LAMB20	1	0.00181	0.01495	0	0.06504	650
BOTW40	LOVE40	1	0.00016	0.00246	0	0.05015	2780
BRAI40	BRFO40	1	0.00053	0.00798	0	0.16294	2780
BRAI40	RAYL40	1	0.00036	0.00551	0	0.11247	2780
BRED20	STAL22	1	0.00056	0.00593	0	0.02184	1380
BRFO40	NORW40	1	0.00129	0.01237	0	0.17286	1390
BRIG10	KEAD10	1	0.01221	0.04562	0	0.03681	260

Sending Node	Receiving Node	Index	Line Resistance	Line Reactance	Semi-shunt Conductance	Semi-shunt Susceptance	Rated Power
BRIG10	KEAD10	2	0.01441	0.05262	0	0.03832	260
BRIN21	CHTE20	1	0.00052	0.00788	0	0.0475	955
BRIN22	CHTE20	1	0.00051	0.00781	0	0.03557	955
BRIN40	FENW4A	1	0.00054	0.00758	0	0.14833	2010
BRLE40	WWEY4B	1	0.00104	0.00953	0	0.14592	1390
BRLE40	WWEY4A	1	0.00104	0.00953	0	0.14592	1390
BURW40	WALP40	1	0.00056	0.00849	0	0.17331	2780
BUSB20	STHA20	1	0.00078	0.00642	0	0.02176	955
BUSH20	OCKH2A	1	0.0005	0.00506	0	0.24782	760
BUST21	NECH20	1	0.00021	0.00285	0	0.41944	725
BUST21	DRAK22	1	0.0008	0.01215	0	0.05545	1130
BUST22	NECH20	1	0.00021	0.00286	0	0.42233	725
BUST22	DRAK21	1	0.0008	0.01214	0	0.05538	1130
CANT40	KEMS40	1	0.00051	0.00541	0	0.0833	1930
CANT40	KEMS40	2	0.00051	0.00541	0	0.0833	1930
CAPE4A	FROD40	1	0.0002	0.00307	0	0.06265	2780
CAPE4A	DEES40	1	0.00013	0.00192	0	0.03909	2780
CAPE4B	FROD40	1	0.00021	0.00314	0	0.06404	2780
CARE20	USKM2A	1	0.00109	0.01011	0	0.02304	695
CARR20	SMAN20	1	0.00046	0.00438	0	0.021	835
CARR20	SMAN20	2	0.00042	0.00396	0	0.01969	835
CELL40	DRAK41	1	0.00073	0.00844	0	0.14058	2180
CELL40	DRAK42	1	0.00073	0.00845	0	0.1408	2180
CELL40	MACC40	1	0.0005	0.00583	0	0.09716	3010
CHIC41	MANN40	1	0.00059	0.00893	0	0.18225	2780
CHIC42	MANN40	1	0.00059	0.00893	0	0.18225	2780
CHSI20	BEDD22	1	0.00083	0.00752	0	0.0401	760
CHSI20	BEDD21	1	0.00083	0.00748	0	0.03235	760
CHSI20	WWEY21	1	0.00069	0.00623	0	0.02125	955
CHSI20	WWEY22	1	0.00069	0.00624	0	0.02128	955
CHTE20	HIGM21	1	0.00101	0.01532	0	0.06983	1250
CHTE20	HIGM22	1	0.00101	0.01535	0	0.06997	1290
CITR40	WISD4A	1	0.007	0.008	0	0.20107	760
CITR40	WHAM4A	1	0.00009	0.001	0	0.8586	1410
CITR40	WHAM4B	1	0.00009	0.001	0	0.8586	1412
CLIF40	IMPP40	1	0.00028	0.00422	0	0.08529	2860
CLYM20	EERH20	1	0.00024	0.00321	0	0.01444	925
COSO40	TILB4B	1	0.00021	0.00227	0	0.03753	2010
COTT40	EASO4A	1	0.00148	0.02229	0	0.45502	2780
COTT40	EASO4B	1	0.00148	0.02229	0	0.45502	2780
COVE20	WILL20	1	0.00013	0.0014	0	0.02296	2010
COWB20	CARE20	1	0.00153	0.01425	0	0.03246	695
COWB20	ABTH20	1	0.00044	0.00471	0	0.01734	1380
COWB20	ABTH20	2	0.00044	0.00471	0	0.01734	1380
COWL40	MITY40	1	0.0013	0.01756	0	0.50266	1180
COWL40	ECLA40	1	0.0004	0.00604	0	0.1233	2770
CRUA2A	DALL20	1	0.0004	0.0036	0	0.0207	262

Sending Node	Receiving Node	Index	Line Resistance	Line Reactance	Semi-shunt Conductance	Semi-shunt Susceptance	Rated Power
CRUA2B	DALL20	1	0.0004	0.0036	0	0.0207	262
CULH40	COWL40	1	0.00007	0.00103	0	0.02101	2780
CULH40	DIDC41	1	0.00006	0.001	0	0.01765	2780
CURR20	GRMO20	1	0.00211	0.01731	0	0.0587	935
CURR20	COCK20	1	0.00138	0.01128	0	0.03825	920
DAIN40	CARR4A	1	0.00004	0.001	0	0.00625	870
DAIN40	CARR4B	1	0.00004	0.001	0	0.00602	870
DAIN40	MACC40	1	0.00054	0.0062	0	0.33494	2400
DAIN40	CELL40	1	0.00086	0.00991	0	0.39677	3010
DALK2A	COCK20	1	0.00046	0.0038	0	0.01287	920
DALK2B	POOB2B	1	0.00044	0.00339	0	0.03346	240
DALK2B	SMEA20	1	0.00002	0.01516	0	0.00054	920
DALK2B	COCK20	1	0.00046	0.0038	0	0.01287	920
DALL20	WIYH20	1	0.0039	0.033	0	0.1013	760
DALL20	WIYH20	2	0.0039	0.033	0	0.1013	760
DEES40	TREU4B	1	0.00024	0.00266	0	0.04381	2010
DEES40	TREU4A	1	0.00023	0.00265	0	0.0441	2180
DEES40	CAPE4B	1	0.00013	0.00192	0	0.03909	2770
DEES40	DAIN40	1	0.00096	0.01116	0	0.18575	3100
DEES40	DAIN40	2	0.00096	0.01116	0	0.18575	3100
DEVM40	WIYH4B	1	0.00055	0.00524	0	0.08958	1390
DIDC41	COWL40	1	0.00013	0.00189	0	0.03866	2780
DIDC41	DIDC42	5	0.00002	0.0107	0	0	2000
DIDC42	BRLE40	1	0.00048	0.00731	0	0.42786	2200
DIDC42	BRLE40	2	0.00048	0.00731	0	0.42786	2200
DINO40	PENT40	1	0.00007	0.00118	0	1.0762	1680
DINO40	PENT40	2	0.00009	0.00144	0	0.63375	1940
DRAK21	BUSH20	1	0.00146	0.01546	0	0.05689	1380
DRAK41	WILE40	1	0.00029	0.00316	0	0.05209	2010
DRAK41	RATS42	1	0.00052	0.00598	0	0.10339	2010
DRAK42	OLDB40	1	0.00084	0.00899	0	0.14667	2210
DRAX42	DRAX41	5	0.00006	0.02002	0	0.0145	1320
DUNG40	SELL40	1	0.00042	0.00461	0	0.15019	1850
DUNG40	SELL40	2	0.00042	0.00461	0	0.15019	1850
EALI20	WISD2A	1	0.00012	0.00139	0	0.3077	760
EASO40	WYMO40	1	0.0004	0.00606	0	0.12368	2720
EASO4A	LITB40	1	0.00002	0.001	0	0.24795	1100
EASO4A	WYMO40	1	0	0.001	0	0.00034	2780
EASO4A	EASO40	1	0	0.001	0	0	9999
EASO4B	EASO40	1	0.0004	0.00606	0	0.12368	2720
ECCL40	TORN40	1	0.0005	0.00653	0	0.3218	1250
ECCL40	TORN40	2	0.0005	0.00653	0	0.3218	1250
ECCL40	COCK4A	1	0.00156	0.01313	0	0.182	1110
ECCL40	COCK4B	1	0.00156	0.01313	0	0.182	1110
ECLA40	AMEM4B	1	0.00075	0.00686	0	0.10509	1390
EERH20	CLYM20	1	0.00024	0.00321	0	0.01444	762
EERH20	LOAN20	1	0.00118	0.01637	0	0.07478	925

Sending Node	Receiving Node	Index	Line Resistance	Line Reactance	Semi-shunt Conductance	Semi-shunt Susceptance	Rated Power
EERH20	NEAR21	1	0.00077	0.00632	0	0.02142	760
EGGB41	ROCH40	1	0.00146	0.01639	0	0.2965	1100
EGGB41	DRAX41	1	0.00013	0.00195	0	0.15252	2015
EGGB41	STSB40	1	0.00049	0.0074	0	0.15107	2780
EGGB42	DRAX42	1	0.00013	0.00194	0	0.0378	2520
EGGB42	PADI40	1	0.00109	0.01632	0	0.32131	2520
EGGB42	MONF40	1	0.00012	0.00173	0	0.03532	2780
EGRE1B	BLVW1A	1	0.0665	0.14815	0	0.01679	135
EKIS20	STHA20	1	0.00032	0.0026	0	0.00882	762
EKIS20	NEIL20	1	0.00145	0.01192	0	0.04042	1090
ELLA20	STAL22	1	0.00164	0.01606	0	0.05524	955
ELSE22	WARL20	1	0.00241	0.02374	0	0.09841	760
ELSE4A	SUND41	1	0.00072	0.00663	0	0.10146	1590
ELSE4B	SUND42	1	0.00072	0.00663	0	0.10146	1590
ELVA20	LINM20	1	0.00156	0.01431	0	0.04606	1380
ENDE40	RATS42	1	0.00041	0.00614	0	0.12537	2780
ENDE40	RATS41	1	0.00041	0.00615	0	0.12559	2780
EXET40	AXMI40	1	0.0004	0.00603	0	0.12305	2780
EXET40	CHIC41	1	0.00083	0.0123	0	0.26493	2780
FAWL40	LOVE40	1	0.00029	0.00402	0	0.37536	1100
FAWL40	BOTW40	1	0.00012	0.00152	0	0.29918	1100
FECK20	BESW20	1	0.0014	0.01427	0	0.05164	955
FECK40	HAMH40	1	0.00074	0.00806	0	0.13266	2010
FECK40	IRON40	1	0.00113	0.01234	0	0.20315	2010
FENW4A	DRAX41	1	0.00015	0.00224	0	0.04562	2770
FERR21	ELLA20	1	0.00171	0.01773	0	0.06651	1280
FERR21	SKLG20	1	0.00098	0.00957	0	0.04948	865
FERR22	MONF22	1	0.0001	0.00161	0	0.0129	1047
FERR23	MONF21	1	0.0001	0.00159	0	0.00725	1280
FERR23	SKLG20	1	0.00098	0.00958	0	0.05075	865
FFES2B	TRAW20	1	0.00077	0.00293	0	0.01029	550
FIDF21	FROD20	1	0.00021	0.00321	0	0.01465	1210
FIDF22	FROD20	1	0.00021	0.00321	0	0.01465	1210
FIDF23	FIDF22	5	0.00007	0.01037	0	0	750
FIDF24	FIDF21	5	0.00007	0.01041	0	0	750
FLEE40	BRLE40	1	0.00019	0.00292	0	0.0596	2780
FLEE40	BRLE40	2	0.00019	0.00292	0	0.0596	2780
FOUR20	BLYT20	1	0.00393	0.02935	0	0.10398	855
FOYE20	BLHI20	1	0.0122	0.051	0	0.1422	525
GLRB2A	GLRO20	1	0.0006	0.0053	0	0.01685	760
GLRB2A	TEAL20	1	0.0019	0.0167	0	0.051	760
GRAI41	KINO40	1	0.00013	0.00195	0	0.12877	2230
GRAI41	KEMS40	1	0.0001	0.00135	0	0.3213	2615
GRAI42	TILB4B	1	0.00031	0.00471	0	0.29192	2000
GRAI42	GRAI41	5	0.00002	0.0107	0	0	2000
GREN40	STAY42	1	0.00174	0.01909	0	0.31417	2010
GREN40	WBUR40	1	0.00226	0.02517	0	0.4643	2010

Sending Node	Receiving Node	Index	Line Resistance	Line Reactance	Semi-shunt Conductance	Semi-shunt Susceptance	Rated Power
GREY21	LACK22	1	0.0002	0.001	0	0.05728	230
GREY21	LACK4A	1	0.00005	0.001	0	0.00939	952
GREY21	LACK4B	1	0.00005	0.001	0	0.00939	952
GREY22	LACK21	1	0.00003	0.001	0	0.00898	952
GREY22	LACK21	2	0.00003	0.001	0	0.00898	952
GRIW40	KEAD42	1	0.00017	0.0027	0	0.05231	2470
GRMO20	KINC20	1	0.00072	0.00591	0	0.02005	935
GRNA20	ELVA20	1	0.00269	0.02551	0	0.08984	1000
HACK2A	TOTE22	1	0.00026	0.00243	0	0.02388	760
HACK2A	WHAM2B	1	0.00035	0.00326	0	0.01067	955
HACK2B	TOTE24	1	0.00026	0.00243	0	0.02388	760
HACK2B	WHAM2A	1	0.00035	0.00326	0	0.01067	955
HAMH20	BESW20	1	0.00095	0.00952	0	0.05424	760
HAMH20	COVE20	1	0.00046	0.00708	0	0.0323	1130
HAMH40	DRAK42	1	0.0005	0.0055	0	0.0905	2010
HARK20	GRNA20	1	0.00047	0.00498	0	0.02468	1000
HARK21	FOUR20	1	0.001965	0.014675	0	0.05199	855
HARK22	STEW21	1	0.00511	0.03433	0	0.25022	525
HARK40	STHA41	1	0.0023	0.02186	0	0.34466	2010
HART20	HATL22	1	0.00063	0.00581	0	0.01913	1090
HAWP20	NORT22	1	0.00064	0.00982	0	0.06889	900
HAWP20	HART20	1	0.00078	0.00702	0	0.02397	1090
HEYS40	QUER40	1	0.0002	0.00189	0	0.02644	1590
HEYS40	QUER40	2	0.0002	0.00193	0	0.02698	1590
HEYS40	STAN40	1	0.00021	0.00409	0	0.08646	3630
HEYS40	STAN40	2	0.00021	0.00409	0	0.08646	3630
HIGM21	THUR2A	1	0.00492	0.01873	0	0.06589	625
HIGM21	HIGM2A	5	0.00012	0.01012	0	0.0183	530
HIGM40	WBUR40	1	0.00025	0.00279	0	0.06844	2010
HIGM40	RATS41	1	0.00111	0.0121	0	0.22867	2010
HINP40	MELK40	1	0.00147	0.0161	0	0.26497	2010
HINP40	MELK40	2	0.00147	0.0161	0	0.265	2010
HUER40	NEIL4A	1	0.00077	0.00612	0	0.09482	797
HUER40	INKI40	1	0.00121	0.01157	0	0.2118	1320
HUER40	INKI40	2	0.00121	0.01157	0	0.2118	1320
HUER40	WIYH4A	1	0.00122	0.00984	0	0.16784	1320
HUER4A	KILL40	1	0.0011	0.01079	0	0.18832	1390
HUER4A	CREB40	1	0.00018	0.00264	0	0.05383	3180
HUER4B	KILL40	1	0.0011	0.01079	0	0.18832	1390
HUER4B	CREB40	1	0.00018	0.00264	0	0.05383	3180
HURS20	LITT2A	1	0.00029	0.00272	0	0.14186	840
HURS20	LITT2B	1	0.00029	0.00271	0	0.13953	840
HUTT40	HARK40	1	0.00163	0.01561	0	0.24342	1390
HUTT40	HARK40	2	0.00163	0.01561	0	0.24342	1390
INDQ40	LAND42	1	0.00104	0.00951	0	0.14568	1390
INDQ40	LAND41	1	0.00103	0.00939	0	0.14371	1390
INDQ40	ALVE4B	1	0.00205	0.01961	0	0.2739	1390

Sending Node	Receiving Node	Index	Line Resistance	Line Reactance	Semi-shunt Conductance	Semi-shunt Susceptance	Rated Power
INDQ40	ALVE4A	1	0.00205	0.01961	0	0.2739	1390
INKI40	DEVM40	1	0.00019	0.00269	0	0.05382	1593
INKI40	STHA40	1	0.00152	0.01614	0	0.29648	1390
IROA11	OLDS10	1	0	0.01147	0	0	9999
IROA12	OLDS10	1	0	0.01147	0	0	9999
IRON40	RUGE40	1	0.00111	0.01135	0	0.18226	1390
IRON40	PENN4A	1	0.00052	0.00475	0	0.07282	1390
IRON40	PENN4B	1	0.00056	0.0053	0	0.08261	1390
IRON40	LEGA4B	1	0.001	0.01151	0	0.19175	2400
IVER22	WATS22	1	0.00056	0.00595	0	0.04764	760
IVER4A	AMEM4A	1	0.00035	0.00378	0	0.06215	2010
IVER4B	AMEM4B	1	0.00043	0.0039	0	0.05969	1390
JORD20	BRIN21	1	0.00064	0.00569	0	0.0806	420
KAIM20	SMEA20	1	0.00044	0.0036	0	0.01218	935
KAIM20	CURR20	1	0.00046	0.00373	0	0.01264	935
KAIM20	COCK20	1	0.00092	0.00756	0	0.0256	935
KEAD41	HUER4A	1	0.00096	0.01412	0	0.25067	2780
KEAD41	WBUR40	1	0.0003	0.00451	0	0.09203	3320
KEAD41	KILL40	1	0.00044	0.00696	0	0.13219	3470
KEAD42	HUER4B	1	0.00018	0.00264	0	0.05383	3180
KEAD43	FENW4A	1	0.00036	0.00398	0	0.06556	2010
KEAD43	FENW4A	2	0.00036	0.00398	0	0.06556	2010
KEAD43	SPLN40	1	0.00123	0.01858	0	0.37613	2780
KEAD4A	COTT40	1	0.00054	0.00621	0	0.10666	2210
KEAD4B	COTT40	1	0.00054	0.00621	0	0.10666	2210
KEAR40	DAIN40	1	0.00026	0.00343	0	0.04681	2170
KEIT20	BLHI20	1	0.0001	0.001	0	0.0029	1060
KEIT20	KINT20	1	0.0029	0.0244	0	0.0736	1060
KEMS40	GRAI42	1	0.0001	0.00139	0	0.32199	2615
KIBY21	LISD20	1	0.00021	0.00187	0	0.40421	760
KIBY21	LISD20	2	0.00021	0.00185	0	0.3979	760
KIBY21	RAIN20	1	0.00025	0.00382	0	0.01745	1290
KIBY21	WASF2B	1	0.0004	0.0043	0	0.01583	1520
KIBY22	RAIN20	1	0.00025	0.00382	0	0.01745	1290
KIBY22	WASF2A	1	0.00041	0.00431	0	0.01588	1520
KILL40	SHBA40	1	0.00014	0.00221	0	0.04111	2780
KILS40	STHA40	1	0.00083	0.00678	0	0.10262	1390
KILS40	HUER40	1	0.0011	0.01079	0	0.18832	1390
KINB2A	TEAL20	1	0.0043	0.0371	0	0.11425	935
KINB2B	KINT20	1	0.0085	0.0731	0	0.2227	764
KINC20	LOAN20	1	0.00027	0.02124	0	0.03058	762
KINC20	LOAN20	2	0.00027	0.0212	0	0.02232	762
KINC20	KINB2B	1	0.0005	0.0043	0	0.0359	764
KINC20	KINB2A	1	0.0005	0.0043	0	0.01465	955
KINO40	TILB4A	1	0.00019	0.00281	0	0.23676	2000
KINO40	NFLE40	1	0.00031	0.0043	0	0.08335	2010
KINO40	SING40	1	0.00016	0.00215	0	0.04168	2010

Sending Node	Receiving Node	Index	Line Resistance	Line Reactance	Semi-shunt Conductance	Semi-shunt Susceptance	Rated Power
KINT20	PERS20	1	0.0014	0.0123	0	0.0371	1060
KINT20	PEHE20	2	0.0026	0.0219	0	0.0661	1060
KINT20	PEHE20	1	0.0036	0.0307	0	0.0924	1060
KINT20	BLHI20	1	0.006	0.0221	0	0.0683	525
KIRK20	BRAW20	1	0.00086	0.00832	0	0.27119	760
KIRK20	ELLA20	1	0.00162	0.01528	0	0.32146	762
KITW20	OLDB20	1	0.00036	0.00331	0	0.04316	670
KITW20	OCKH20	1	0.00061	0.00552	0	0.0307	760
LACK22	TODP20	1	0.00027	0.00243	0	0.00829	1090
LALE20	EALI20	1	0.00053	0.00392	0	0.83798	525
LALE20	EALI20	2	0.00053	0.00392	0	0.83798	525
LALE20	WWEY2A	1	0.00031	0.00334	0	0.0187	750
LALE20	IVER2A	1	0.00064	0.00684	0	0.06865	1380
LAMB20	BONN20	1	0.00181	0.01495	0	0.06504	795
LAMB20	LOAN20	1	0.00215	0.02073	0	0.09179	650
LAND41	ABHA4A	1	0.00049	0.00469	0	0.06557	1390
LAND42	ABHA4B	1	0.00049	0.00469	0	0.06557	1390
LEIB4A	SUND42	1	0.00016	0.00241	0	0.0492	2780
LEIB4A	COWL40	1	0.00057	0.00854	0	0.17427	2780
LEIB4B	SUND41	1	0.00016	0.00241	0	0.0492	2780
LEIB4B	ECLA40	1	0.00016	0.00241	0	0.0492	2780
LIDL1A	SEFI10	1	0.0478	0.10645	0	0.01369	115
LIDL1B	SEFI10	1	0.0478	0.10645	0	0.01369	115
LINM21	STHA20	1	0.00139	0.01274	0	0.04051	1380
LISD20	BIRK20	1	0.0002	0.00336	0	0.8503	831
LITT40	LITT4B	1	0.00017	0.00157	0	0.02399	1390
LITT4A	KEMS40	1	0.00064	0.00715	0	0.11489	1930
LITT4B	BEDD4B	1	0.00067	0.00615	0	1.1302	660
LITT4B	KEMS40	1	0.00064	0.00711	0	0.11412	1930
LOAN20	MOSM20	1	0.00132	0.01078	0	0.04501	760
LOAN20	TOWH20	1	0.00098	0.008	0	0.03143	620
LOVE40	FLEE40	1	0.00066	0.00725	0	0.11938	2010
LOVE40	FLEE40	2	0.00066	0.00725	0	0.11938	2010
LOVE40	BOLN40	1	0.00071	0.01078	0	0.22	2780
LOVE40	BOLN40	2	0.00071	0.01078	0	0.22	2780
MACC20	BRED20	1	0.00089	0.00804	0	0.02743	955
MAGA20	PYLE20	1	0.00015	0.00138	0	0.02649	1500
MANN40	FAWL40	1	0.00067	0.01007	0	0.20551	2780
MANN40	LOVE40	1	0.00067	0.01007	0	0.20551	2780
MELK20	IROA20	1	0.00182	0.01691	0	0.06087	865
MELK2A	IROA20	1	0.00181	0.01688	0	0.05445	865
MELK40	BRLE40	1	0.00172	0.01571	0	0.24055	1390
MELK40	BRLE40	2	0.00172	0.01571	0	0.24055	1390
MITY40	MELK40	1	0.00048	0.00522	0	0.08587	2010
MITY4A	FECK40	1	0.00135	0.01471	0	0.24149	1970
MITY4A	MELK40	1	0.0005	0.00538	0	0.08294	1970
MONF21	POPP20	1	0.00497	0.04126	0	0.10425	520

Sending Node	Receiving Node	Index	Line Resistance	Line Reactance	Semi-shunt Conductance	Semi-shunt Susceptance	Rated Power
MONF22	POPP20	1	0.0026	0.0191	0	0.04787	550
MONF22	BRAW20	1	0.00118	0.018	0	0.08213	1143
MOSM20	WFIE20	1	0.00015	0.00123	0	0.00409	955
NEAR22	BELL20	1	0.00022	0.00183	0	0.00609	955
NECH20	HAMH2A	1	0.00024	0.00367	0	0.01673	1130
NECH20	HAMH20	1	0.00024	0.00363	0	0.01657	1525
NEEP20	PITS20	1	0.00016	0.0012	0	0.13296	420
NEEP20	SHEC20	1	0.00021	0.00144	0	0.16218	420
NEIL20	BUSB20	1	0.001	0.0082	0	0.0278	1000
NEIL20	WIYH20	1	0.0013	0.01028	0	0.03559	749
NEWX20	HURS20	1	0.00042	0.00487	0	1.07662	760
NEWX20	HURS20	2	0.00044	0.00498	0	1.10098	760
NFLE40	SING40	1	0.00016	0.00215	0	0.04168	2010
NFLW4A	BARK40	1	0.00038	0.00412	0	0.06754	2010
NFLW4A	NFLE40	1	0.00002	0.001	0	0.00422	1750
NFLW4B	BARK40	1	0.00038	0.00412	0	0.06754	2010
NFLW4B	NFLE40	1	0.00002	0.001	0	0.00422	1750
NFLW4B	LITT40	1	0.00018	0.00168	0	0.02563	1110
NINF40	DUNG40	1	0.00048	0.00719	0	0.14683	2780
NINF40	DUNG40	2	0.00048	0.00723	0	0.14762	2780
NORL2A	BRIN21	1	0.0007	0.00586	0	0.12449	420
NORL2B	PITS20	1	0.00046	0.00275	0	0.36278	420
NORL2B	JORD20	1	0.00011	0.001	0	0.10062	420
NORT21	SPEN22	1	0.00222	0.00846	0	0.02974	625
NORT21	LACK21	1	0.00013	0.0014	0	0.02296	2010
NORT21	LACK21	2	0.00013	0.0014	0	0.02296	2010
NORT40	THTO41	1	0.00131	0.01805	0	0.32123	2010
NORT40	HAWP40	1	0.0003	0.00456	0	0.09301	2780
NORT40	LACK40	1	0.00041	0.00417	0	0.10537	1590
NORW40	SIZE40	1	0.00176	0.01946	0	0.31752	1390
NURS40	FAWL40	1	0.00022	0.0034	0	0.06946	2780
NURS40	LOVE40	1	0.00044	0.00668	0	0.13632	2780
OCKH20	HAMH20	1	0.00056	0.0061	0	0.10048	9999
OFFE20	HAWP20	1	0.00043	0.00388	0	0.01322	1090
OSBA40	NORT40	1	0.00112	0.01524	0	0.26406	2010
OSBA40	THTO42	1	0.00019	0.0028	0	0.05716	2780
PADI40	KEAR40	1	0.00057	0.00697	0	0.12494	2170
PADI40	BRAW40	1	0.00069	0.0103	0	0.19857	2520
PAFB40	ECLA40	1	0.00076	0.00828	0	0.13626	2010
PAFB40	ECLA40	2	0.00076	0.00828	0	0.13626	2010
PAFB40	ENDE40	1	0.00067	0.00757	0	0.12794	2010
PAFB40	ENDE40	2	0.00068	0.00762	0	0.12865	2010
PELH40	WALP40	1	0.00103	0.0156	0	0.31851	2780
PELH40	SUND42	1	0.00049	0.00745	0	0.15206	2780
PELH40	RYEH40	1	0.00026	0.00388	0	0.0793	2780
PELH40	RYEH4A	1	0.00025	0.00381	0	0.07782	2780
PELH40	BURW40	1	0.00047	0.00709	0	0.14475	2780

Sending Node	Receiving Node	Index	Line Resistance	Line Reactance	Semi-shunt Conductance	Semi-shunt Susceptance	Rated Power
PELH40	RAYL40	1	0.00109	0.0164	0	0.3348	2220
PEMB40	CLIF40	1	0.0016	0.0242	0	0.49387	2500
PEMB40	CLIF40	2	0.0016	0.0242	0	0.49387	2500
PEMB40	SWAN40	1	0.00093	0.01404	0	0.2866	3070
PENN20	BUSH20	1	0.00081	0.00861	0	0.03847	1040
PENN20	BISW20	1	0.00121	0.01209	0	0.04963	1040
PENT40	DEES40	1	0.00096	0.01412	0	0.25067	2780
PENT40	DEES40	2	0.00096	0.01412	0	0.25067	2780
PENT40	TRAW40	1	0.00061	0.00959	0	1.18195	2320
PENW21	WASF2B	1	0.00087	0.00922	0	0.03392	1520
PENW40	QUER40	1	0.00055	0.00597	0	0.09833	2010
PENW40	QUER40	2	0.00054	0.00595	0	0.09787	2010
PENW40	DAIN40	1	0.00101	0.01114	0	0.20598	3010
PENW40	PADI40	1	0.00054	0.00666	0	0.11986	3010
PERS20	PEHE20	1	0.0024	0.0208	0	0.0626	1060
PITS20	WIBA20	1	0.00009	0.001	0	0.0828	420
PYLE20	COWB20	1	0.00122	0.0114	0	0.02597	865
PYLE20	COWB20	2	0.00122	0.0114	0	0.02597	865
QUER40	HUTT40	1	0.00072	0.00663	0	0.10113	1390
QUER40	HUTT40	2	0.00058	0.00641	0	0.10546	2010
RAIN20	FIDF23	1	0.00018	0.00279	0	0.01273	1210
RAIN20	FIDF24	1	0.00018	0.00279	0	0.01273	1210
RASS40	CLIF40	1	0.0032	0.04837	0	0.98349	2470
RATS20	CASD20	1	0.00019	0.00282	0	0.03673	1000
RATS42	STAY41	1	0.00074	0.00805	0	0.13256	2010
RAYL40	COSO40	1	0.00023	0.00255	0	0.042	2010
RAYL40	TILB4A	1	0.00035	0.00381	0	0.06267	2010
ROCH20	WHGA20	1	0.00053	0.00478	0	0.03531	905
ROCH20	WHGA20	2	0.00052	0.00476	0	0.02998	840
ROOS10	LIDL1A	1	0.00861	0.01908	0	0.0021	154
ROOS10	LIDL1B	1	0.00861	0.01908	0	0.0021	154
ROWD2A	BEDD21	1	0.00021	0.00245	0	0.58638	760
ROWD2B	BEDD23	1	0.0002	0.0023	0	0.53564	760
ROWD40	LITT4A	1	0.00057	0.0052	0	0.07943	1590
RUGE40	DRAK42	1	0.00035	0.00387	0	0.06374	2010
RYEH40	WALX4A	1	0.00006	0.001	0	0.0179	2780
SAES20	SAEN20	1	0.00002	0.001	0	0.00101	1730
SALH20	HATL22	1	0.00039	0.00363	0	0.01171	1090
SALH20	NORT22	1	0.00046	0.00496	0	0.01752	1380
SEAB40	MELK40	1	0.00059	0.00876	0	0.17392	2550
SEFI10	EGRE1B	1	0.01198	0.02669	0	0.00302	135
SELL40	CANT40	1	0.00048	0.00513	0	0.11296	1930
SELL40	CANT40	2	0.00048	0.00513	0	0.12867	1930
SERX10	BOLN10	1	0.0079	0.0271	0	0.00507	9999
SERX10	BOLN10	2	0.0079	0.0271	0	0.00507	9999
SHBA40	GRIW40	1	0.00014	0.00221	0	0.04111	2780
SHEC20	NORL2A	1	0.00019	0.00112	0	0.14624	420

Sending Node	Receiving Node	Index	Line Resistance	Line Reactance	Semi-shunt Conductance	Semi-shunt Susceptance	Rated Power
SHRE40	IRON40	1	0.00024	0.00277	0	0.0461	2400
SHRE40	LEGA4A	1	0.00076	0.00875	0	0.14565	2400
SIZE40	BRFO40	1	0.00046	0.00672	0	0.15213	2780
SIZE40	BRFO40	2	0.00046	0.00672	0	0.15213	2780
SIZE40	PELH40	1	0.00123	0.01854	0	0.37839	2780
SJOW20	TOTE21	1	0.0003	0.0036	0	0.8896	785
SJOW20	TOTE23	1	0.0003	0.00363	0	0.89721	785
SKLG20	KIRK2A	1	0.00015	0.0024	0	0.46784	760
SMAN20	BRED20	1	0.00047	0.00412	0	0.23308	850
SMEA20	DALK2A	1	0.00002	0.01516	0	0.00054	920
SMEA4A	TORN40	1	0.00078	0.01008	0	0.37342	1250
SPEN21	NORT22	1	0.00221	0.00841	0	0.02959	625
SPEN22	STEW22	1	0.00107	0.01547	0	0.0562	795
SSHI20	WBOL20	1	0.0002	0.00178	0	0.00605	1090
STAL21	ROCH20	1	0.0012	0.01256	0	0.0444	1320
STAN40	PENW40	1	0.00032	0.0041	0	0.06662	2400
STAN40	PENW40	2	0.00032	0.0041	0	0.06662	2400
STAY41	COTT40	1	0.00041	0.00485	0	0.08556	2010
STAY42	COTT40	1	0.00048	0.0052	0	0.08563	2010
STEW21	BLYT20	1	0.00151	0.01391	0	0.04021	680
STEW21	BLYT20	2	0.00161	0.01384	0	0.05362	855
STEW21	SPEN21	1	0.00108	0.01549	0	0.06156	1040
STEW4A	ECCL40	1	0.0006	0.00476	0	0.07202	1390
STEW4B	ECCL40	1	0.0006	0.00476	0	0.07202	1390
STHA20	CLYM20	1	0.00052	0.00438	0	0.01386	770
STHA20	CLYM20	2	0.00052	0.00438	0	0.01386	770
STHA20	WISH20	1	0.00062	0.00504	0	0.01709	762
STHA40	TORN40	1	0.00253	0.02444	0	0.61052	1105
STSB40	NEEP40	1	0.00027	0.00251	0	0.03683	840
STSB4A	MACC40	1	0.00108	0.01236	0	0.58835	1040
SUND41	GREN40	1	0.00068	0.0074	0	0.12175	2010
SUND42	GREN40	1	0.00068	0.00743	0	0.12235	2010
SWAN2A	BAGB20	1	0.00065	0.0077	0	0.02866	1650
SWAN40	CLIF40	1	0.00067	0.01014	0	0.2069	3180
TAUN4A	HINP40	1	0.00045	0.00496	0	0.08172	2010
TAUN4A	EXET40	1	0.00065	0.00711	0	0.11705	2010
TAUN4B	HINP40	1	0.00045	0.00496	0	0.08172	2010
TAUN4B	EXET40	1	0.00065	0.00711	0	0.11705	2010
TEAL20	KINT20	1	0.0061	0.0536	0	0.11071	675
TEAL20	KINT20	2	0.0059	0.051	0	0.1536	935
TEAL20	KINT20	3	0.0061	0.0536	0	0.11071	675
TEMP21	PITS20	1	0.00029	0.00173	0	0.22732	420
TEMP21	BRIN21	1	0.00013	0.00119	0	0.004	857
TEMP22	BRIN21	1	0.00013	0.00119	0	0.004	857
THOM40	BRIN40	1	0.00041	0.00619	0	0.12555	2520
THOM40	DRAX42	1	0.00028	0.0037	0	0.12704	2210
THOM40	EGGB42	1	0.00031	0.00466	0	0.17045	2220

Sending Node	Receiving Node	Index	Line Resistance	Line Reactance	Semi-shunt Conductance	Semi-shunt Susceptance	Rated Power
THOM40	STAL40	1	0.00084	0.01271	0	0.60626	1040
THTO41	CREB40	1	0.00032	0.00489	0	0.09979	3180
THTO42	DRAX41	1	0.00024	0.00368	0	0.07509	2780
THTO43	DRAX42	1	0.00024	0.00368	0	0.07509	2780
THTO43	CREB40	1	0.00032	0.00489	0	0.09979	3180
THUR20	BRIN22	1	0.0006	0.00229	0	0.00804	625
THUR2A	THUR20	1	0.00049	0.00186	0	0.00654	625
TODP20	HATL21	1	0.00076	0.00703	0	0.02319	955
TOTE21	BRIM2D	1	0.00034	0.00314	0	0.03121	1090
TOTE22	BRIM2A	1	0.00034	0.00311	0	0.02722	1090
TOTE22	REBR21	1	0.00017	0.00201	0	0.55265	1380
TOTE23	BRIM2B	1	0.00034	0.00308	0	0.03149	1090
TOTE24	BRIM2C	1	0.00034	0.0031	0	0.02312	1090
TOTE24	REBR22	1	0.00016	0.00199	0	0.53971	1380
TOWH20	WFIE20	1	0.00049	0.004	0	0.01572	620
TRAW20	FFES2A	1	0.00077	0.00296	0	0.01474	420
TRAW40	TREU4A	1	0.00135	0.01234	0	0.18898	1710
TRAW40	TREU4B	1	0.00135	0.01234	0	0.18898	1710
TREU4A	LEGA40	1	0.00013	0.00225	0	0.03739	2860
TREU4B	LEGA40	1	0.00013	0.00225	0	0.03739	2860
TYNE20	WBOL20	1	0.0005	0.00469	0	0.01596	1090
TYNE2A	SSHI20	1	0.0003	0.00284	0	0.00967	1240
UPPB21	ABTH20	1	0.00124	0.01129	0	0.06772	786
UPPB21	CLIF2B	1	0.00032	0.00287	0	0.0098	955
UPPB22	ABTH20	1	0.00125	0.01133	0	0.03865	955
UPPB22	CLIF2A	1	0.00031	0.00284	0	0.0097	955
USKM2A	WHSO20	1	0.0003	0.0028	0	0.00638	695
USKM2B	TREM2A	1	0.00115	0.0069	0	0.01895	625
USKM2B	WHSO20	1	0.0003	0.0028	0	0.00638	695
USKM2C	WHSO20	1	0.00062	0.00235	0	0.00826	550
USKM2D	WHSO20	1	0.00062	0.00235	0	0.00826	550
WALH40	COWL40	1	0.00112	0.01554	0	0.46983	1180
WALH40	RASS40	1	0.00082	0.01243	0	0.45603	1230
WALH40	FECK40	1	0.00114	0.01252	0	0.20609	1970
WALH40	PEMB40	1	0.00201	0.03038	0	0.71765	1320
WALP11	KINL1A	1	0.00028	0.00267	0	0.03735	1390
WALP40	SPLN40	1	0.00034	0.00515	0	0.10194	2780
WALP40	SUTB4A	1	0.00008	0.001	0	0.01132	1450
WALP40	WBUR40	1	0.00056	0.00849	0	0.17331	2780
WALP40	NORW40	1	0.00166	0.01591	0	0.22229	1390
WALP40	NORW40	2	0.00166	0.01591	0	0.22229	1390
WALX21	BRIM2A	1	0.00026	0.00238	0	0.00814	1090
WALX21	BRIM2B	1	0.00027	0.00244	0	0.00832	1090
WALX22	BRIM2C	1	0.00027	0.00243	0	0.00829	1090
WALX22	BRIM2D	1	0.00027	0.00243	0	0.00829	1090
WARL20	ELSE21	1	0.00242	0.02385	0	0.11636	760
WARL20	TILB21	1	0.00061	0.00552	0	0.01883	1180

Sending Node	Receiving Node	Index	Line Resistance	Line Reactance	Semi-shunt Conductance	Semi-shunt Susceptance	Rated Power
WARL20	TILB22	1	0.00061	0.00552	0	0.01884	1180
WASF2A	PENW22	1	0.00087	0.0092	0	0.03388	1520
WATS21	IVER22	1	0.00055	0.00593	0	0.04508	760
WATS21	ELSE21	1	0.00025	0.00226	0	0.01956	760
WATS22	ELSE22	1	0.00025	0.00231	0	0.02918	760
WBOL20	OFFE20	1	0.00037	0.00339	0	0.01155	1090
WBOL20	HATL21	1	0.00222	0.02016	0	0.06808	1090
WFIB2A	TEAL20	1	0.0019	0.0167	0	0.051	760
WFIE20	GLRO20	1	0.00061	0.00496	0	0.01656	955
WFIE20	WFIB2A	1	0.0011	0.0093	0	0.0295	760
WHAM40	BARK40	1	0.00018	0.00185	0	0.02917	2010
WHAM40	BARK40	2	0.00018	0.00186	0	0.05322	2010
WHGA20	KEAR20	1	0.00066	0.00598	0	0.02729	830
WHGA20	KEAR20	2	0.00066	0.00601	0	0.03338	830
WHSO2A	IROA20	1	0.00364	0.01386	0	0.04874	550
WHSO2B	IROA20	1	0.00364	0.01386	0	0.04874	550
WHSO4A	SEAB40	1	0.00033	0.00496	0	0.47668	1425
WHSO4A	CLIF40	1	0.00044	0.00667	0	0.13504	2860
WIBA20	TEMP22	1	0.00016	0.001	0	0.12065	420
WILE40	RATS42	1	0.00036	0.0041	0	0.08542	1310
WILE40	RATS41	1	0.00035	0.00397	0	0.06588	2010
WIMB20	WISD2B	1	0.00041	0.00473	0	1.04689	760
WIMB20	NEWX20	1	0.00027	0.00309	0	0.68271	795
WIMB20	NEWX20	2	0.00027	0.00309	0	0.68271	795
WIMB20	BEDD21	1	0.00039	0.00366	0	0.0427	953
WISD4A	SJOW4A	1	0.007	0.008	0	0.20107	760
WISD4B	SJOW4B	1	0.007	0.008	0	0.20107	760
WISD4B	CITR40	1	0.007	0.008	0	0.20107	760
WISH20	NEAR22	1	0.00079	0.00646	0	0.0219	955
WISH20	NEAR21	1	0.00079	0.00646	0	0.0219	955
WISH20	KAIM20	1	0.00268	0.02196	0	0.07446	935
WIYH20	LAMB20	1	0.0009	0.00738	0	0.02501	955
WIYH20	LAMB20	2	0.0009	0.00738	0	0.02501	955
WMEL20	ALDW20	1	0.00041	0.00377	0	0.01235	714
WMEL20	THOM20	1	0.00112	0.01026	0	0.0815	764
WMEL20	THOM20	2	0.00112	0.01028	0	0.08692	764
WMEL20	THUR2A	1	0.0008	0.0074	0	0.02426	955
WWEY22	IVER21	1	0.00096	0.01021	0	0.05582	915
WYLF40	PENT40	1	0.00039	0.00585	0	0.11933	2220
WYLF40	PENT40	2	0.00039	0.00585	0	0.11933	2220
WYMO40	PELH40	1	0.0003	0.00446	0	0.09097	2780
WYMO40	SUND41	1	0.0002	0.00302	0	0.06158	2780

Simple Transformers

Sending Node	Recieving Node	Index	Rated Power *(MVA)*	Resistance (pu sending)	Reactance (pu sending)	Lateral Shunt Conductance (pu)	Lateral Shunt Susceptance (pu)	Transformer Ratio (pu/pu)
BRAW20	BRAW40	1	1000	0.00017	0.01587	0	-0.00232	1
BARK40	BARK21	1	750	0.00023	0.0267	0	0.00204	1
BARK40	BARK22	1	750	0.00023	0.0267	0	0.00204	1
BARY8A	BARY10	1	190	0.00263	0.10526	0	0	0.98587
BARY8S	BARY10	1	95	0.00526	0.16842	0	0	0.98929
BRIG10	BRIG8A	1	55	0.00582	0.21818	0	0	0.94013
BRIG10	BRIG8B	1	55	0.00582	0.21818	0	0	0.94013
BRIG10	BRIG8C	1	55	0.00582	0.21818	0	0	0.94013
BRIG10	BRIG8D	1	55	0.00582	0.21818	0	0	0.94013
BRIG10	BRIG8S	1	55	0.00582	0.21818	0	0	0.94014
BRIG10	BRIG8T	1	55	0.00582	0.21818	0	0	0.94014
BRIN21	BRIN40	1	1000	0.00015	0.01609	0	0.00705	1
BRIN22	BRIN40	1	1000	0.00014	0.01677	0	0.00705	1
CAPE20	CAPE4A	1	750	0.00014	0.01597	0	0.0172	1
CAPE20	CAPE4B	1	750	0.0002	0.016	0	-0.0023	1
CARR4A	CARR20	1	750	0.00017	0.01597	0	-0.00285	1
CARR4B	CARR20	1	750	0.00021	0.016	0	-0.00287	1
CLIF40	CLIF2B	1	750	0.00021	0.01603	0	-0.00287	1
CLIF40	CLIF2A	1	750	0.00017	0.01613	0	-0.00287	1
CORB8S	GREN12	1	145	0.00257	0.11586	0	0	1
DRAK41	DRAK22	1	750	0.00021	0.01604	0	0.00575	1
DRAK41	DRAK22	2	750	0.0002	0.01601	0	0.01565	1
DRAK41	DRAK21	1	1000	0.00017	0.0159	0	-0.0009	1
DUNG40	DUNG20	1	750	0.00026	0.016	0	-0.00144	1
DUNG40	DUNG20	2	750	0.00027	0.01604	0	-0.00134	1
ELSE4A	ELSE21	1	900	0.00021	0.0152	0	-0.00287	1
ELSE4B	ELSE22	1	1000	0.00017	0.016	0	-0.00232	1
FECK20	FECK40	1	1000	0.00018	0.01685	0	-0.0019	1
FERR40	FERR21	1	1000	0.00017	0.016	0	-0.00232	1
FERR40	FERR22	1	1000	0.00018	0.01507	0	0.01545	1
FFES81	FFES2A	1	180	0.00278	0.09811	0	0	1.00165
FFES82	FFES2B	1	180	0.00278	0.09811	0	0	0.97654
FROD20	FROD40	1	1000	0.00019	0.01597	0	-0.0023	1
FROD20	FROD40	2	900	0.00014	0.01684	0	0.0172	1
GREN11	CORB8A	1	145	0.00257	0.11586	0	0	0.95746
GREN12	CORB8B	1	145	0.00257	0.11586	0	0	0.95746
HARK21	HARK40	1	500	0.00029	0.02319	0	0.00605	1
HARK21	HARK40	2	500	0.00038	0.0237	0	-0.0017	1
HARK40	HARK22	1	500	0.00029	0.02402	0	-0.0017	1
HARK22	HARK40	2	500	0.00032	0.0238	0	0.00405	1
HIGM2A	HIGM40	1	500	0.00028	0.02379	0	-0.0017	1
HUER4A	HUER87	1	776	0.00021	0.02061	0	0	0.96749
HUER4A	HUER88	1	776	0.00021	0.02061	0	0	0.96749
IVER21	IVER4A	1	1000	0.00017	0.016	0	-0.00232	1

Sending Node	**Recieving Node**	**Index**	**Rated Power** *(MVA)*	**Resistance** (pu sending)	**Reactance** (pu sending)	**Lateral Shunt Conductance** (pu)	**Lateral Shunt Susceptance** (pu)	**Transformer Ratio** (pu/pu)
IVER21	IVER4B	1	500	0.00032	0.02404	0	0.00645	1
KEAR20	KEAR40	1	1000	0.00012	0.016	0	0.0001	1
KEAR20	KEAR40	2	1000	0.00012	0.016	0	0.0001	1
KINL1A	KINL8A	1	438	0.00066	0.03244	0	0	0.98
KINL1A	KINL8S	1	438	0.00066	0.03244	0	0	0.98
LITT2A	LITT40	1	750	0.00032	0.02619	0	0.00204	1
LITT2B	LITT40	1	750	0.00031	0.0259	0	-0.00246	1
MACC40	MACC20	1	750	0.00021	0.016	0	-0.00285	1
MELK2A	MELK40	1	750	0.00021	0.016	0	-0.00287	1
NORT21	NORT40	1	1000	0.00012	0.016	0	-0.0023	1
NORT40	NORT22	1	1000	0.00017	0.0151	0	0.02285	1
OLDS10	OLDS81	1	345	0.00132	0.03536	0	0	0.94054
OLDS10	OLDS82	1	345	0.00127	0.03449	0	0	0.94166
PENN4A	PENN20	1	1000	0.00016	0.0157	0	-0.00232	1
PENN4B	PENN20	1	1000	0.00017	0.016	0	-0.00232	1
RATS20	RATS41	1	1000	0.00017	0.016	0	-0.00232	1
ROCH20	ROCH40	1	1000	0.00018	0.01592	0	-0.00232	1
ROOS8A	ROOS10	1	210	0.0015	0.05952	0	0	0.98
ROOS8S	ROOS10	1	80	0.0032	0.12162	0	0	0.98
ROWD2A	ROWD40	1	750	0.00023	0.0267	0	-0.00246	1
ROWD2B	ROWD40	1	750	0.00023	0.0267	0	-0.00246	1
SIZE81	SIZE11	1	340	0.00136	0.04529	0	0	0.92325
SWAN40	SWAN2B	1	750	0.00022	0.01511	0	-0.00097	1
SWAN40	SWAN2A	1	750	0.0002	0.01601	0	-0.00097	1
THOM40	THOM20	1	750	0.00018	0.01622	0	0.00596	1
THOM40	THOM20	2	750	0.00019	0.01605	0	-0.00251	1
TILB21	TILB4A	1	750	0.00021	0.01645	0	-0.00265	1
TILB22	TILB4B	1	1000	0.0003	0.0161	0	-0.00088	1
TRAW20	TRAW40	1	750	0.00021	0.01606	0	0.00816	1
TRAW20	TRAW40	2	985	0.00021	0.01606	0	0.00854	1
USKM11	FIFP8A	1	144	0.001	0.1174	0	0	0.96014
USKM11	FIFP8B	1	144	0.001	0.1174	0	0	0.96014
USKM11	FIFP8C	1	144	0.001	0.1174	0	0	0.96014
WALX21	WALX4B	1	1000	0.00017	0.016	0	-0.00232	1
WALX4A	WALX22	1	1000	0.00017	0.016	0	-0.00232	1
WALX4B	WALX22	1	1000	0.00017	0.016	0	-0.00232	1
WHAM40	WHAM2A	1	750	0.00023	0.0267	0	-0.0025	1
WHAM40	WHAM2B	1	750	0.00023	0.0267	0	-0.0025	1
WHSO4A	WHSO20	1	750	0.00018	0.01613	0	-0.00081	1
WILL10	DERW8A	1	45	0.00582	0.24444	0	0	0.96776
WILL10	DERW8B	1	45	0.00582	0.24444	0	0	0.96776
WILL10	DERW8C	1	45	0.00542	0.24444	0	0	0.96794
WILL10	DERW8D	1	65	0.00375	0.16923	0	0	1
WILL10	DERW8S	1	65	0.0074	0.24444	0	0	1
WWEY2A	WWEY4B	1	750	0.00021	0.01603	0	0.00365	1
WWEY4B	WWEY21	1	750	0.00021	0.01603	0	0.00278	1
WWEY4A	WWEY22	1	750	0.00021	0.016	0	-0.00287	1

Sending Node	Recieving Node	Index	Rated Power *(MVA)*	Resistance (pu sending)	Reactance (pu sending)	Lateral Shunt Conductance (pu)	Lateral Shunt Susceptance (pu)	Transformer Ratio (pu/pu)
WWEY4A	WWEY21	1	750	0.00021	0.01606	0	0.00795	1
TILB80	TILB21	1	706	0.0003	0.0297	0	0	0.94838
TILB87	TILB21	1	706	0.0003	0.0297	0	0	0.94838
TILB88	TILB21	1	706	0.0003	0.0297	0	0	0.94838
TILB89	TILB21	1	706	0.0003	0.0297	0	0	0.94838
WALP12	PETE8A	1	190	0.00263	0.10526	0	0	0.98587
WALP12	PETE8B	1	190	0.00263	0.10526	0	0	0.98587
WALP12	PETE8S	1	190	0.00263	0.10526	0	0	0.98587
SIZE82	SIZE11	1	340	0.00136	0.04529	0	0	0.92325
FFES83	FFES2A	1	180	0.00278	0.09811	0	0	1.00165
FFES84	FFES2B	1	180	0.00278	0.09811	0	0	0.97654
GREY8A	NORW10	1	449	0	0.03118	0	0	0.95636
HAMH40	HAMH2A	1	1000	0.00018	0.0156	0	-0.00232	1
HIGM22	HIGM40	1	1000	0.00019	0.01574	0	-0.00232	1
MELK40	MELK20	1	750	0.00021	0.016	0	-0.00287	1
MONF21	MONF40	1	750	0.00021	0.016	0	-0.00285	1
NEEP40	NEEP20	1	750	0.00022	0.01655	0	-0.00287	0.93
OLDB20	OLDB40	1	1000	0.00017	0.0161	0	-0.00232	1
WALX4A	WALX21	1	1000	0.00017	0.016	0	-0.00232	1
STAL21	STAL40	1	1000	0.00017	0.01559	0	-0.00169	1
BRWA2A	HINP40	1	500	0.00036	0.02439	0	0.0295	1
BRWA2B	HINP40	1	500	0.00038	0.02433	0	0.0295	1
BEDD22	BEDD4B	1	660	0.00021	0.02587	0	-0.0015	1
IVER22	IVER4B	1	500	0.00018	0.024	0	-0.0017	1
IVER4A	IVER2A	1	500	0.00032	0.024	0	-0.0017	1
SHOT8A	CONQ12	1	160	0	0.097	0	0	0.97168
SHOT8B	CONQ12	1	160	0	0.097	0	0	1
SHOT8C	CONQ12	1	160	0	0.097	0	0	1
SHOR8A	SERX10	1	450	0	0.03745	0	0	0.9408
STEW4A	STEW21	2	1000	0.00023	0.01645	0	-0.00232	1
STEW4A	STEW21	1	1000	0.00023	0.01645	0	-0.00232	1
STEW4B	STEW22	1	1000	0.00023	0.01645	0	-0.00232	1
STEW4B	STEW22	2	1000	0.00023	0.01645	0	-0.00232	1
PENW21	PENW40	1	750	0.00021	0.01604	0	0.0055	1
PENW40	PENW21	2	1000	0.00017	0.016	0	-0.00232	1
PENW40	PENW22	1	750	0.00018	0.01599	0	0.01344	1
PENW40	PENW22	2	750	0.00019	0.01605	0	0.008	1
SJOW4A	SJOW20	1	750	0.00022	0.02573	0	-0.00246	1
SJOW4B	SJOW20	1	750	0.00022	0.02573	0	-0.00246	1
LACK40	LACK21	1	1000	0.00017	0.016	0	-0.0023	1
LACK4A	LACK40	1	1000	0.00012	0.016	0	-0.0023	1
LACK4B	LACK40	1	1000	0.00018	0.01595	0	-0.0023	1
CREB40	SAEN20	1	750	0.00021	0.016	0	-0.00285	1
CREB40	SAEN20	2	750	0.00021	0.016	0	-0.00285	1
CREB40	SAES20	1	750	0.00021	0.016	0	-0.00285	1
CREB40	SAES20	2	750	0.00021	0.016	0	-0.00285	1
DRAK21	DRAK81	1	706	0.0003	0.0297	0	0	0.94838

Sending Node	Recieving Node	Index	Rated Power *(MVA)*	Resistance (pu sending)	Reactance (pu sending)	Lateral Shunt Conductance (pu)	Lateral Shunt Susceptance (pu)	Transformer Ratio (pu/pu)
DRAK82	DRAK22	1	706	0.0003	0.0297	0	0	0.94838
DRAK89	DRAK22	1	706	0.0003	0.0297	0	0	0.94838
WILE40	WILL20	2	1000	0.00023	0.01645	0	-0.00232	1
WILE40	WILL20	1	1000	0.00023	0.01645	0	-0.00232	1
NFLW4A	NFLW20	1	750	0.00021	0.016	0	-0.00285	1
NFLW4B	NFLW20	1	750	0.00021	0.016	0	-0.00285	1
COCK4B	COCK21	1	1000	0.0001	0.016	0	0	1
COCK4A	COCK21	1	1000	0.0001	0.016	0	0	1
CRUA2A	CRUA81	1	111	0.00189	0.09153	0	0	0.96969
CRUA2A	CRUA82	2	111	0.00189	0.09108	0	0	0.96971
HUER40	HUER81	1	776	0.00021	0.02061	0	0	0.96749
HUER40	HUER82	1	776	0.00021	0.02061	0	0	0.96749
KILS40	KILS20	1	1000	0.00018	0.01607	0	0	1
KILS40	KILS20	2	1000	0.00013	0.01665	0	0	1
LOAN20	LOAN81	1	706	0.0003	0.0297	0	0	0.94975
LOAN20	LOAN82	1	706	0.0003	0.0297	0	0	0.94838
LOAN20	LOAN83	1	706	0.0003	0.0297	0	0	0.94838
LOAN20	LOAN84	1	706	0.0003	0.0297	0	0	0.94838
NEIL4A	NEIL20	1	1000	0.00018	0.01617	0	0	1
PEHE20	PEHE81	1	776	0.00021	0.02061	0	0	0.96387
PEHE20	PEHE82	1	776	0.00021	0.02061	0	0	0.96358
SMEA4A	SMEA20	1	1000	0.0001	0.016	0	0	1
STHA40	STHA20	1	1000	0.00018	0.01706	0	0	1
TORN40	TORN81	1	777	0.00021	0.02021	0	0	0.96669
TORN40	TORN82	1	777	0.00021	0.02021	0	0	0.96669
WIYH4A	WIYH20	1	1000	0.00013	0.0167	0	0	1
WIYH4B	WIYH20	1	1000	0.00013	0.016	0	0	1
FOYE81	FOYE21	1	170	0.0012	0.1174	0	0	0.96014
FOYE82	FOYE21	1	170	0.0012	0.1174	0	0	0.96014
WFIE81	WFIE20	1	80	0.00526	0.16842	0	0	0.98929
BPGR81	GRMO20	1	160	0.0014	0.1278	0	0	0.96014

Quad Boosters

Sending Node	Receiving Node	Index	Rated Power (MVA)	Copper Losses %	Iron Losses %	Magnetising Current %	Saturation Exponent	Nominal Tap	Initial Tap	Regulation Node	Target Volts	Tap No.	Sending Volts	Receiving Volts	Leakage Impedance %	Phase Shift °	Tap No.	Sending Volts	Receiving Volts	Leakage Impedance %	Phase Shift °	Tap No.	Sending Volts	Receiving Volts	Leakage Impedance %	Phase Shift °
WHSO2A	WHSO20	1	750	0.0375	0	0.04667	9	10	10			1	275	275	7.0054	-11.3	10	275	275	3.5027	0	19	275	275	7.0054	11.3
WHSO20	WHSO2B	1	750	0.0375	0	0.04667	9	10	10			1	275	275	7.0054	-11.3	10	275	275	3.5027	0	19	275	275	7.0054	11.3
WISD2A	WISD4A	1	750	0.05475	0	0.04667	9	10	10			1	275	275	10.3761	-11.3	10	275	275	5.188	0	19	275	275	10.3761	11.3
WISD2B	WISD4B	1	750	0.05475	0	0.04667	9	10	10			1	275	275	10.3641	-11.3	10	275	275	5.182	0	19	275	275	10.3641	11.3
KEAD4A	KEAD42	1	2750	0	0	0.01273	9	20	20			1	400	400	16.5	-11.3	20	400	400	8.25	0	39	400	400	16.5	11.3
KEAD4B	KEAD42	1	2750	0	0	0.01273	9	20	20			1	400	400	16.5	-11.3	20	400	400	8.25	0	39	400	400	16.5	11.3
STSB4A	STSB40	1	2000	0.034	0	0.0175	9	20	20			1	400	400	14.0002	-11.3	20	400	400	7.0001	0	39	400	400	14.0002	11.3
OCKH2A	OCKH20	1	760	0.22792	0	0.04605	9	10	10			1	275	275	9.8905	-11.3	10	275	275	4.9453	0	19	275	275	9.8905	11.3
LEGA40	LEGA4A	1	2400	0	0	0.01458	9	20	20			1	400	400	16.8	-11.3	20	400	400	8.4	0	39	400	400	16.8	11.3
LEGA40	LEGA4B	1	2400	0	0	0.01458	9	20	20			1	400	400	16.8	-11.3	20	400	400	8.4	0	39	400	400	16.8	11.3
KIRK20	KIRK2A	1	760	0	0	0.04605	9	10	10			1	275	275	14.896	-11.3	10	275	275	7.448	0	19	275	275	14.896	11.3
WHAM40	WHAM4A	1	2000	0.3398	0	0.0175	9	20	20			1	400	400	14.0165	-11.3	20	400	400	7.0082	0	39	400	400	14.0165	11.3
WHAM4B	WHAM40	1	2000	0.3598	0	0.0175	9	20	20			1	400	400	14.0185	-11.3	20	400	400	7.0092	0	39	400	400	14.0185	11.3
TONG10	TONG1A	1	90	0	0	0.38889	9	10	10			1	132	132	4.5	-11.3	10	132	132	2.25	0	19	132	132	4.5	11.3

Detailed Transformers

DUNG40	DUNG85	1	775	0.15578	0	0	9	10	6			1	440	22	15.8309	0	19	356	22	15.8309	0
DUNG40	DUNG86	1	775	0.15578	0	0	9	10	6			1	440	22	15.8309	0	19	356	22	15.8309	0
DUNG81	DUNG40	1	200	0.2558	0	0	9	10	8			1	22	440	20.8124	0	19	22	356	20.8124	0
DUNG82	DUNG40	1	200	0.2558	0	0	9	10	8			1	22	440	20.8124	0	19	22	356	20.8124	0
DUNG83	DUNG40	1	200	0.2558	0	0	9	10	8			1	22	440	20.8124	0	19	22	356	20.8124	0
DUNG40	DUNG84	1	200	0.2558	0	0	9	10	8			1	440	22	20.8124	0	19	356	22	20.8124	0
BOLN10	BOLN40	1	276	0.48328	0	0.11486	9	11	13	BOLN10	132	1	151.8	400	23.005	0	15	125.4	400	23.005	0
FAWL40	FAWL8C	1	570	0.18183	0	0	9	12	6			1	440	22	16.8707	0	19	356	22	16.8707	0
FAWL40	FAWL8A	1	570	0.18183	0	0	9	12	6			1	440	22	16.8707	0	19	356	22	16.8707	0
FAWL40	FAWL8B	1	570	0.18183	0	0	9	12	6			1	440	22	16.8707	0	19	356	22	16.8707	0

Transformer Parameters

Sending Node	Receiving Node	Index	Rated Power (MVA)	Copper Losses %	Iron Losses %	Magnetising Current %	Saturation Exponent	Nominal Tap	Initial Tap	Regulation Node	Target Volts	Tap No.	Sending Volts	Receiving Volts	Leakage Impedance %	Phase Shift °	Tap No.	Sending Volts	Receiving Volts	Leakage Impedance %	Phase Shift °	Tap No.	Sending Volts	Receiving Volts	Leakage Impedance %	Phase Shift °
HINP40	HINP87	1	783	0.16913	0	0	9	10	5			1	440	22	16.7007	0	19	356	22	16.7007	0					
HINP40	HINP88	1	783	0.17931	0	0	9	10	6			1	440	22	16.101	0	19	356	22	16.101	0					
SEAB40	SEAB8A	1	300	0.219	0	0	9	10	5			1	440	22	13.8017	0	19	360	22	13.8017	0					
SEAB40	SEAB8B	1	300	0.219	0	0	9	10	5			1	440	22	13.8017	0	19	360	22	13.8017	0					
SEAB40	SEAB8C	1	300	0.219	0	0	9	10	5			1	440	22	13.8017	0	19	360	22	13.8017	0					
SEAB8S	SEAB40	1	300	0.219	0	0	9	10	5			1	22	440	13.8017	0	19	22	360	13.8017	0					
ABTH20	ABTH87	1	590	0.26019	0	0	9	12	11			1	321.75	22	17.5019	0	19	244.75	22	17.5019	0					
ABTH20	ABTH88	1	590	0.26019	0	0	9	12	11			1	321.75	22	17.5019	0	19	244.75	22	17.5019	0					
ABTH20	ABTH89	1	590	0.26019	0	0	9	12	11			1	321.75	22	17.5019	0	19	244.75	22	17.5019	0					
ABTH11	ABTH20	1	180	0.2682	0	0.19167	9	10	7	ABTH11	132	1	151.8	275	14.4997	0	19	112.2	275	14.4997	0					
BAGB20	BAGB8A	1	590	0.26019	0	0	9	12	11			1	321.75	22	17.5019	0	19	244.75	22	17.5019	0					
BAGB20	BAGB8C	1	590	0.26019	0	0	9	12	11			1	321.75	22	17.5019	0	19	244.75	22	17.5019	0					
DINO81	DINO40	1	340	0.23766	0	0	9	10	10			1	22	440	15.9019	0	19	22	360	15.9019	0					
DINO84	DINO40	1	340	0.23766	0	0	9	10	10			1	22	440	15.9019	0	19	22	360	15.9019	0					
DINO85	DINO40	1	340	0.23766	0	0	9	10	10			1	22	440	15.9019	0	19	22	360	15.9019	0					
DINO86	DINO40	1	340	0.23766	0	0	9	10	10			1	22	440	15.9019	0	19	22	360	15.9019	0					
DINO83	DINO40	1	340	0.23766	0	0	9	10	10			1	22	440	15.9019	0	19	22	360	15.9019	0					
DINO82	DINO40	1	340	0.23766	0	0	9	10	10			1	22	440	15.9019	0	19	22	360	15.9019	0					
WYLF40	WYLF81	1	346	0.33043	0	0	9	14	11			1	460	22	16.5933	0	19	376	22	16.5933	0					
WYLF40	WYLF82	1	346	0.33389	0	0	9	14	11			1	460	22	17.0033	0	19	376	22	17.0033	0					
WYLF40	WYLF83	1	346	0.31936	0	0	9	14	11			1	460	22	16.4429	0	19	376	22	16.4429	0					
WYLF40	WYLF84	1	346	0.20241	0	0	9	14	11			1	460	22	15.9813	0	19	376	22	15.9813	0					
CONQ8D	DEES40	1	420	0.1911	0	0	9	10	5			1	22	440	15.7612	0	19	22	360	15.7612	0					
CONQ8C	DEES40	1	420	0.1911	0	0	9	10	5			1	22	440	15.7612	0	19	22	360	15.7612	0					
CONQ8B	DEES40	1	420	0.1911	0	0	9	10	5			1	22	440	15.7612	0	19	22	360	15.7612	0					
CONQ8A	DEES40	1	420	0.1911	0	0	9	10	5			1	22	440	15.7612	0	19	22	360	15.7612	0					
RUGE86	RUGE40	1	570	0.51015	0	0	9	10	7			1	22	440	14.1993	0	19	22	360	14.1993	0					
RUGE87	RUGE40	1	570	0.51015	0	0	9	10	7			1	22	440	14.1993	0	19	22	360	14.1993	0					
ROCK8A	FROD40	1	330	0	0	0	9	10	7			1	22	440	13.13	0	19	22	360	13.13	0					
ROCK8B	FROD40	1	330	0	0	0	9	10	7			1	22	440	13.13	0	19	22	360	13.13	0					

Transformer Parameters

Sending Node	Receiving Node	Index	Rated Power (MVA)	Copper Losses %	Iron Losses %	Magnetising Current %	Saturation Exponent	Nominal Tap	Initial Tap	Regulation Node	Target Volts	Tap No.	Sending Volts	Receiving Volts	Leakage Impedance %	Phase Shift °	Tap No.	Sending Volts	Receiving Volts	Leakage Impedance %	Phase Shift °	Tap No.	Sending Volts	Receiving Volts	Leakage Impedance %	Phase Shift °
ROCK8S	FROD40	1	330	0	0	0	9	10	7			1	22	440	13.13	0	19	22	360	13.13	0					
DEES8S	DEES40	1	190	0.247	0	0	9	10	6			1	22	440	12.5724	0	19	22	360	12.5724	0					
DEES8B	DEES40	1	190	0.247	0	0	9	10	6			1	22	440	12.5724	0	19	22	360	12.5724	0					
DEES8A	DEES40	1	190	0.247	0	0	9	10	6			1	22	440	12.5724	0	19	22	360	12.5724	0					
WILE40	WILL10	1	240	0.26256	0	0.13208	9	11	9	WILL10	132	1	400	151.8	20.1816	0	15	400	125.4	20.1816	0					
WILE40	WILL10	2	240	0.24456	0	0.13208	9	11	9	WILL10	132	1	400	151.8	19.0024	0	15	400	125.4	19.0024	0					
WILE40	WILL10	3	240	0.24456	0	0.13208	9	11	9	WILL10	132	1	400	151.8	19.1008	0	15	400	125.4	19.1008	0					
RATS41	RATS84	1	800	0.1552	0	0	9	14	11			1	460	22	15.7112	0	19	380	22	15.7112	0					
RATS81	RATS41	1	600	0.2514	0	0	9	12	10			1	22	468	16.1918	0	19	22	356	16.1918	0					
RATS41	RATS83	1	800	0.1552	0	0	9	14	11			1	460	22	15.7112	0	19	380	22	15.7112	0					
RATS82	RATS41	1	800	0.1704	0	0	9	14	12			1	22	460	15.6913	0	19	22	380	15.6913	0					
STAY41	STAY8B	1	490	0.48265	0	0	9	10	5			1	440	22	13.0093	0	19	360	22	13.0093	0					
STAY41	STAY8A	1	490	0.48265	0	0	9	10	5			1	440	22	13.0093	0	19	360	22	13.0093	0					
COTT40	CDCL8A	1	610	0	0	0	9	10	5			1	440	22	16.0003	0	19	356	22	16.0003	0					
COTT40	COTT81	1	610	0	0	0	9	10	5			1	440	22	16.0003	0	19	356	22	16.0003	0					
COTT40	COTT82	1	610	0	0	0	9	10	5			1	440	22	16.0003	0	19	356	22	16.0003	0					
COTT40	COTT83	1	610	0	0	0	9	10	5			1	440	22	16.0003	0	19	356	22	16.0003	0					
COTT40	COTT84	1	610	0	0	0	9	10	5			1	440	22	16.0003	0	19	356	22	16.0003	0					
WBUR40	WBUR81	1	600	0.4398	0	0	9	10	2			1	440	22	16.1658	0	19	360	22	16.1658	0					
WBUR40	WBUR82	1	600	0.45	0	0	9	14	7			1	460	22	16.286	0	19	376	22	16.286	0					
WBUR40	WBUR83	1	600	0.4302	0	0	9	14	7			1	460	22	16.3557	0	19	376	22	16.3557	0					
WBUR40	WBUR84	1	600	0.4398	0	0	9	10	2			1	440	22	16.1658	0	19	360	22	16.1658	0					
SPLN40	SPLN8A	1	306	0.20012	0	0	9	10	6			1	440	22	10.0021	0	19	360	22	10.0021	0					
SPLN40	SPLN8B	1	306	0.20012	0	0	9	10	6			1	440	22	10.0021	0	19	360	22	10.0021	0					
SPLN40	SPLN8S	1	306	0.20012	0	0	9	10	8			1	440	22	10.0021	0	19	360	22	10.0021	0					
SUTB8A	SUTB4A	1	345	0.2001	0	0	9	10	6			1	22	460	14.3099	0	19	22	340	14.3099	0					
SUTB8B	SUTB4A	1	345	0.2001	0	0	9	10	6			1	22	460	14.3099	0	19	22	340	14.3099	0					
SUTB8S	SUTB4A	1	345	0.2001	0	0	9	10	6			1	22	460	14.3099	0	19	22	340	14.3099	0					
WALP40	WALP11	1	240	0.432	0	0.13208	9	11	12	WALP11	133.32	1	400	151.8	20.1946	0	15	400	125.4	20.1946	0					
WALP40	WALP11	2	240	0.3552	0	0.13208	9	11	12	WALP11	133.32	1	400	151.8	20	0	15	400	125.4	20	0					
WALP40	WALP12	1	240	0.384	0	0.13208	9	11	10	WALP12	133.32	1	400	151.8	20.7136	0	15	400	125.4	20.7136	0					

Transformer Parameters

Sending Node	Receiving Node	Index	Rated Power (MVA)	Copper Losses %	Iron Losses %	Magnetising Current %	Saturation Exponent	Nominal Tap	Initial Tap	Regulation Node	Target Volts	Tap No.	Sending Volts	Receiving Volts	Leakage Impedance %	Phase Shift °	Tap No.	Sending Volts	Receiving Volts	Leakage Impedance %	Phase Shift °	Tap No.	Sending Volts	Receiving Volts	Leakage Impedance %	Phase Shift °
WALP40	WALP12	2	240	0.288	0	0.10458	9	11	10	WALP12	133.32	1	400	151.8	20.7136	0	15	400	125.4	20.7136	0					
NORW10	NORW40	1	240	0.3672	0	0.13208	9	11	12	NORW10	133.32	1	151.8	400	20.0191	0	15	125.4	400	20.0191	0					
NORW10	NORW40	2	240	0.97464	0	0.13208	9	11	12	NORW10	133.32	1	151.8	400	20.3034	0	15	125.4	400	20.3034	0					
NORW10	NORW40	3	240	0.36048	0	0.13208	9	11	12	NORW10	133.32	1	151.8	400	19.3034	0	15	125.4	400	19.3034	0					
NORW10	NORW40	4	240	0.2592	0	0.13208	9	11	12	NORW10	133.32	1	151.8	400	20.0489	0	15	125.4	400	20.0489	0					
SIZE11	SIZE40	1	240	0.2496	0	0.13208	9	11	14	SIZE11	134.64	1	151.8	400	19.1008	0	15	125.4	400	19.1008	0					
SIZE11	SIZE40	2	240	0.3672	0	0.13208	9	11	14	SIZE11	134.64	1	151.8	400	19.1075	0	15	125.4	400	19.1075	0					
SIZE84	SIZE40	1	800	0.1784	0	0	9	14	9			1	22	460	15.741	0	19	22	376	15.741	0					
SIZE40	SIZE83	1	800	0.1768	0	0	9	14	9			1	460	22	15.701	0	19	376	22	15.701	0					
COSO40	COSO8A	1	346	0.22421	0	0	9	10	5			1	440	22	11.2818	0	19	360	22	11.2818	0					
COSO40	COSO8B	1	346	0.22421	0	0	9	10	5			1	440	22	11.2818	0	19	360	22	11.2818	0					
COSO40	COSO8S	1	346	0.22421	0	0	9	10	8			1	440	22	11.2818	0	19	360	22	11.2818	0					
KINO40	KINO83	1	600	0.3	0	0	9	10	4			1	440	22	16.8327	0	19	360	22	16.8327	0					
KINO40	KINO84	1	600	0.3	0	0	9	10	4			1	440	22	16.8327	0	19	360	22	16.8327	0					
KINO40	DAMC8A	1	312	0	0	0	9	10	5			1	440	22	14.5579	0	19	356	22	14.5579	0					
KINO40	DAMC8B	1	312	0	0	0	9	10	5			1	440	22	14.5579	0	19	356	22	14.5579	0					
KINO40	DAMC8C	1	324	0	0	0	9	10	8			1	440	22	14	0	19	356	22	14	0					
KINO40	KINO81	1	600	0.3	0	0	9	10	4			1	440	22	16.8327	0	19	360	22	16.8327	0					
KINO40	KINO82	1	600	0.3	0	0	9	10	4			1	440	22	16.8327	0	19	360	22	16.8327	0					
GRAI81	GRAI41	1	800	0.3104	0	0	9	10	5			1	22	440	15.8134	0	19	22	356	15.8134	0					
GRAI82	GRAI41	1	800	0.3104	0	0	9	10	5			1	22	440	15.8134	0	19	22	356	15.8134	0					
GRAI83	GRAI41	1	800	0.3104	0	0	9	10	5			1	22	440	15.8134	0	19	22	356	15.8134	0					
GRAI84	GRAI41	1	800	0.3104	0	0	9	10	5			1	22	440	15.8134	0	19	22	356	15.8134	0					
MEDW8A	GRAI42	1	290	2.16514	0	0	9	14	9			1	22	460	15.8684	0	19	22	376	15.8684	0					
MEDW8B	GRAI42	1	290	2.16891	0	0	9	14	9			1	22	460	15.8293	0	19	22	376	15.8293	0					
MEDW8S	GRAI42	1	290	2.18167	0	0	9	14	9			1	22	460	15.9597	0	19	22	376	15.9597	0					
BARK2A	BARK8A	1	155	0.33	0	0	9	12	9			1	321.75	22	17.753	0	19	244.75	22	17.753	0					
BARK2A	BARK8B	1	155	0.33	0	0	9	12	9			1	321.75	22	17.7831	0	19	244.75	22	17.7831	0					
BARK2A	BARK8S	1	170	0.32997	0	0	9	12	9			1	321.75	22	18.553	0	19	244.75	22	18.553	0					
BARK2B	BARK8C	1	155	0.33	0	0	9	12	8			1	321.75	22	17.643	0	19	244.75	22	17.643	0					

Sending Node	Receiving Node	Index	Rated Power (MVA)	Copper Losses %	Iron Losses %	Magnetising Current %	Saturation Exponent	Nominal Tap	Initial Tap	Regulation Node	Target Volts	Tap No.	Sending Volts	Receiving Volts	Leakage Impedance %	Phase Shift °	Tap No.	Sending Volts	Receiving Volts	Leakage Impedance %	Phase Shift °	Tap No.	Sending Volts	Receiving Volts	Leakage Impedance %	Phase Shift °
BARK2B	BARK8D	1	155	0.32008	0	0	9	12	8			1	321.75	22	17.7629	0	19	244.75	22	17.7629	0					
BARK2B	BARK8E	1	155	0.32008	0	0	9	12	8			1	321.75	22	17.8128	0	19	244.75	22	17.8128	0					
BARK2B	BARK8T	1	250	0.25	0	0	9	12	11			1	321.75	22	20.9915	0	19	244.75	22	20.9915	0					
RYEH8S	RYEH40	1	305	0.30012	0	0	9	10	10			1	22	440	13.4935	0	19	22	360	13.4935	0					
RYEH40	RYEH8A	1	180	0.30006	0	0	9	10	7			1	440	22	12.7835	0	19	360	22	12.7835	0					
RYEH40	RYEH8B	1	205	0.25994	0	0	9	10	7			1	440	22	13.1025	0	19	360	22	13.1025	0					
RYEH40	RYEH8C	1	180	0.30006	0	0	9	10	7			1	440	22	12.8535	0	19	360	22	12.8535	0					
LITB8S	LITB40	1	307	0.10407	0	0	9	10	5			1	22	440	15.2702	0	19	22	360	15.2702	0					
LITB40	LITB8B	1	247	0.11708	0	0	9	10	5			1	440	22	15.3804	0	19	360	22	15.3804	0					
LITB40	LITB8A	1	247	0.11807	0	0	9	10	5			1	440	22	15.4906	0	19	360	22	15.4906	0					
GREN40	GREN12	1	240	0.384	0	0.13208	9	11	13	GREN12	132	1	400	151.8	19.1239	0	15	400	125.4	19.1239	0					
GREN40	GREN12	2	240	0.384	0	0.13208	9	11	13	GREN12	132	1	400	151.8	19.499	0	15	400	125.4	19.499	0					
GREN40	GREN11	1	240	0.3744	0	0.13208	9	11	8	GREN11	132	1	400	151.8	20.0987	0	15	400	125.4	20.0987	0					
GREN11	GREN40	2	240	0.384	0	0.13208	9	11	8	GREN11	132	1	151.8	400	19.8037	0	15	125.4	400	19.8037	0					
EGGB81	EGGB41	1	570	0.18183	0	0	9	12	6			1	22	440	16.8707	0	19	22	356	16.8707	0					
EGGB82	EGGB41	1	570	0.18183	0	0	9	12	6			1	22	440	16.8707	0	19	22	356	16.8707	0					
EGGB83	EGGB42	1	570	0.18183	0	0	9	12	6			1	22	440	16.8707	0	19	22	356	16.8707	0					
EGGB84	EGGB42	1	570	0.18183	0	0	9	12	6			1	22	440	16.8707	0	19	22	356	16.8707	0					
FERR22	FERR83	1	570	0.18183	0	0	9	12	6			1	321.75	22	16.8707	0	19	244.75	22	16.8707	0					
FERR84	FERR22	1	570	0.18183	0	0	9	12	6			1	22	321.75	16.8707	0	19	22	244.75	16.8707	0					
FERR22	FERR81	1	570	0.35169	0	0	9	17	10			1	330	22	15.6242	0	19	269.5	22	15.6242	0					
FERR22	FERR82	1	570	0.18183	0	0	9	12	6			1	321.75	22	16.8707	0	19	244.75	22	16.8707	0					
DRAX41	DRAX81	1	800	0.3104	0	0	9	10	5			1	440	22	15.8134	0	19	356	22	15.8134	0					
DRAX82	DRAX41	1	800	0.3104	0	0	9	10	5			1	22	440	15.7335	0	19	22	356	15.7335	0					
DRAX42	DRAX84	1	800	0.36	0	0	9	14	7			1	460	22	15.3242	0	19	376	22	15.3242	0					
DRAX42	DRAX85	1	800	0.36	0	0	9	14	7			1	460	22	15.4546	0	19	376	22	15.4546	0					
DRAX41	DRAX83	1	800	0.3104	0	0	9	10	5			1	440	22	15.7335	0	19	356	22	15.7335	0					
DRAX42	DRAX86	1	800	0.36	0	0	9	14	7			1	460	22	15.4546	0	19	376	22	15.4546	0					
HEYS40	HEYS88	1	800	0.1664	0	0	9	14	9			1	460	22	15.8009	0	19	376	22	15.8009	0					
HEYS40	HEYS81	1	800	0.184	0	0	9	14	8			1	460	22	16.1914	0	19	376	22	16.1914	0					

Sending Node	Receiving Node	Index	Rated Power (MVA)	Copper Losses %	Iron Losses %	Magnetising Current %	Saturation Exponent	Nominal Tap	Initial Tap	Regulation Node	Target Volts	Tap No.	Sending Volts	Receiving Volts	Leakage Impedance %	Phase Shift °	Tap No.	Sending Volts	Receiving Volts	Leakage Impedance %	Phase Shift °	Tap No.	Sending Volts	Receiving Volts	Leakage Impedance %	Phase Shift °
HEYS40	HEYS82	1	800	0.1952	0	0	9	14	8			1	460	22	16.4212	0	19	376	22	16.4212	0					
HEYS40	HEYS87	1	800	0.1664	0	0	9	14	9			1	460	22	15.8009	0	19	376	22	15.8009	0					
SAES20	SAES8A	1	412	0.05356	0	0	9	12	8			1	321.75	22	19.1993	0	19	244.75	22	19.1993	0					
SAES20	SAES8B	1	412	0.05356	0	0	9	12	8			1	321.75	22	19.1993	0	19	244.75	22	19.1993	0					
SAES20	SAES8C	1	412	0.05356	0	0	9	12	8			1	321.75	22	19.1993	0	19	244.75	22	19.1993	0					
HATL81	HATL22	1	735	0.25799	0	0	9	12	8			1	22	321.75	16.0023	0	19	22	244.75	16.0023	0					
HATL82	HATL22	1	735	0.25799	0	0	9	12	8			1	22	321.75	16.0023	0	19	22	244.75	16.0023	0					
SHBA40	SHBA8T	1	210	0.2709	0	0	9	10	8			1	440	22	13.9046	0	19	360	22	13.9046	0					
SHBA40	SHBA8S	1	320	0.20704	0	0	9	10	8			1	440	22	14.9016	0	19	360	22	14.9016	0					
SHBA8E	SHBA40	1	190	0.2508	0	0	9	10	8			1	22	440	12.6185	0	19	22	360	12.6185	0					
SHBA8D	SHBA40	1	190	0.2508	0	0	9	10	8			1	22	440	12.5805	0	19	22	360	12.5805	0					
SHBA8C	SHBA40	1	190	0.23199	0	0	9	10	8			1	22	440	12.6121	0	19	22	360	12.6121	0					
SHBA8B	SHBA40	1	190	0.24605	0	0	9	10	8			1	22	440	12.6824	0	19	22	360	12.6824	0					
SHBA8A	SHBA40	1	190	0.24795	0	0	9	10	8			1	22	440	12.6424	0	19	22	360	12.6424	0					
KILL40	KILL8C	1	180	0.30006	0	0	9	10	7			1	440	22	12.9035	0	19	360	22	12.9035	0					
KILL40	KILL8D	1	180	0.30006	0	0	9	10	7			1	440	22	12.8035	0	19	360	22	12.8035	0					
KILL40	KILL8T	1	205	0.25994	0	0	9	10	7			1	440	22	13.0027	0	19	360	22	13.0027	0					
KILL40	KILL8A	1	180	0.30006	0	0	9	10	7			1	440	22	12.9035	0	19	360	22	12.9035	0					
KILL40	KILL8B	1	180	0.30006	0	0	9	10	7			1	440	22	12.8035	0	19	360	22	12.8035	0					
KILL40	KILL8E	1	165	0.26994	0	0	9	14	8			1	460	22	11.5032	0	19	376	22	11.5032	0					
KILL8F	KILL40	1	165	0.26994	0	0	9	14	8			1	22	460	11.5032	0	19	22	376	11.5032	0					
KILL40	KILL8G	1	165	0.26994	0	0	9	14	8			1	460	22	11.5032	0	19	376	22	11.5032	0					
KILL40	KILL8H	1	404	0	0	0	9	14	11			1	460	22	15.0001	0	19	376	22	15.0001	0					
KILL40	KILL8I	1	404	0	0	0	9	14	11			1	460	22	15.0001	0	19	376	22	15.0001	0					
KILL40	KILL8S	1	205	0.25994	0	0	9	10	7			1	440	22	13.0027	0	19	360	22	13.0027	0					
KILL40	KILL8U	1	270	0.31995	0	0	9	14	8			1	460	22	13.0039	0	19	376	22	13.0039	0					
KILL40	KILH8A	1	90	0	0	0	9	14	9			1	460	22	11.997	0	19	380	22	11.997	0					
KILL40	KILH8B	1	90	0	0	0	9	14	9			1	460	22	11.997	0	19	380	22	11.997	0					
KILL40	KILH8C	1	90	0	0	0	9	14	9			1	460	22	11.997	0	19	380	22	11.997	0					
KILL40	KILH8S	1	150	0	0	0	9	14	9			1	460	22	12	0	19	380	22	12	0					

Sending Node	Receiving Node	Index	Rated Power	Copper Losses	Iron Losses	Magnetising Current	Saturation Exponent	Nominal Tap	Initial Tap	Regulation Node	Target Volts	Tap No.	Sending Volts	Receiving Volts	Leakage Impedance	Phase Shift	Tap No.	Sending Volts	Receiving Volts	Leakage Impedance	Phase Shift	Tap No.	Sending Volts	Receiving Volts	Leakage Impedance	Phase Shift
			(MVA)	%	%	%									%	°				%	°				%	°
KEAD41	KEAD8A	0	331	0.18999	0	0	9	10	3			1	440	22	17.3818	0	19	360	22	17.3818	0					
KEAD42	KEAD8B	1	331	0.18999	0	0	9	10	2			1	440	22	17.361	0	19	360	22	17.361	0					
KEAD42	KEAD8S	1	331	0.18999	0	0	9	10	4			1	440	22	17.3511	0	19	360	22	17.3511	0					
KEAD42	KEAD10	1	240	0.312	0	0.13208	9	11	12	KEAD10	132	1	400	151.8	20.2896	0	15	400	125.4	20.2896	0					
KEAD42	KEAD10	2	240	0.3528	0	0.13208	9	11	12	KEAD10	132	1	400	151.8	19.8007	0	15	400	125.4	19.8007	0					
KEAD42	KEAD10	3	240	0.264	0	0.13208	9	11	12	KEAD10	132	1	400	151.8	19.9889	0	15	400	125.4	19.9889	0					
USKM2A	USKM11	1	120	0.44664	0	0.59583	9	10	12	USKM11	132	1	275	151.8	13.9371	0	19	275	112.2	13.9371	0					
USKM2C	USKM11	1	120	0.45	0	0	9	10	12	USKM11	132	1	275	151.8	13.9672	0	19	275	112.2	13.9672	0					
USKM2D	USKM11	1	150	0.5682	0	0.528	9	10	11	USKM11	132	1	275	151.8	17.5127	0	19	275	112.2	17.5127	0					
USKM2B	USKM11	1	120	0.45	0	0	9	10	12	USKM11	132	1	275	151.8	13.9405	0	19	275	112.2	13.9405	0					
IROA20	IROA11	1	180	0.3474	0	0.19167	9	10	11	IROA11	132	1	275	151.8	14.1199	0	19	275	112.2	14.1199	0					
IROA20	IROA11	2	180	0.35298	0	0.19167	9	10	11	IROA11	132	1	275	151.8	13.9995	0	19	275	112.2	13.9995	0					
IROA12	IROA20	1	180	0.34434	0	0.19167	9	10	11	IROA12	132	1	151.8	275	13.9042	0	19	112.2	275	13.9042	0					
IROA20	IROA12	2	180	0.35298	0	0.19167	9	10	11	IROA12	132	1	275	151.8	14.1884	0	19	275	112.2	14.1884	0					
DIDC8S	DIDC41	1	600	0.4098	0	0	9	10	9			1	22	440	16.6352	0	19	22	360	16.6352	0					
DIDC8C	DIDC41	1	600	0.4098	0	0	9	10	9			1	22	440	16.6352	0	19	22	360	16.6352	0					
DIDC8D	DIDC41	1	600	0.4098	0	0	9	10	9			1	22	440	16.6352	0	19	22	360	16.6352	0					
DIDC8A	DIDC42	1	600	0.4098	0	0	9	10	9			1	22	440	16.6352	0	19	22	360	16.6352	0					
DIDC8B	DIDC42	1	285	0.24396	0	0	9	10	8			1	22	440	13.7021	0	19	22	360	13.7021	0					
DIDC8T	DIDC42	1	305	0.23394	0	0	9	10	6			1	22	440	13.802	0	19	22	360	13.802	0					
HARK21	HARK11	1	120	0.38292	0	0.59583	9	10	7	HARK11	134.904		1	275	151.8	14.0548		0	19	275	112.2	14.0548		0		
HARK22	HARK11	1	120	0.42348	0	0.59583	9	10	7	HARK11	134.904		1	275	151.8	14.0056		0	19	275	112.2	14.0056		0		
SEFI10	SEFI8C	1	50	0.44	0	0	9	10	9			1	151.8	22	12.2279	0	19	112.2	22	12.2279	0					
SEFI8B	SEFI10	1	50	0.45	0	0	9	10	9			1	22	151.8	12.2283	0	19	22	112.2	12.2283	0					
SEFI10	SEFI8A	1	50	0.44	0	0	9	10	9			1	151.8	22	12.2479	0	19	112.2	22	12.2479	0					
SEFI10	SEFI8S	1	65	0.42997	0	0	9	10	9			1	151.8	22	12.2576	0	19	112.2	22	12.2576	0					
SEFI10	CALD81	1	50	0.44	0	0	9	10	9			1	151.8	22	12.2479	0	19	112.2	22	12.2479	0					
SEFI10	CALD82	1	50	0.44	0	0	9	10	9			1	151.8	22	12.2479	0	19	112.2	22	12.2479	0					
SEFI10	CALD83	1	50	0.44	0	0	9	10	9			1	151.8	22	12.2479	0	19	112.2	22	12.2479	0					
SEFI10	CALD84	1	50	0.44	0	0	9	10	9			1	151.8	22	12.2479	0	19	112.2	22	12.2479	0					

Sending Node	Receiving Node	Index	Rated Power (MVA)	Copper Losses %	Iron Losses %	Magnetising Current %	Saturation Exponent	Nominal Tap	Initial Tap	Regulation Node	Target Volts	Tap No.	Sending Volts	Receiving Volts	Leakage Impedance %	Phase Shift °	Tap No.	Sending Volts	Receiving Volts	Leakage Impedance %	Phase Shift °	Tap No.	Sending Volts	Receiving Volts	Leakage Impedance %	Phase Shift °
SEFI10	CALD88	1	50	0.44	0	0	9	10	9			1	151.8	22	12.2479	0	19	112.2	22	12.2479	0					
SEFI10	CALD85	1	50	0.44	0	0	9	10	9			1	151.8	22	12.2479	0	19	112.2	22	12.2479	0					
SEFI10	CALD86	1	50	0.44	0	0	9	10	9			1	151.8	22	12.2479	0	19	112.2	22	12.2479	0					
SEFI10	CALD87	1	50	0.44	0	0	9	10	9			1	151.8	22	12.2479	0	19	112.2	22	12.2479	0					
INDQ40	INDQ81	1	190	0.24605	0	0	9	10	8			1	440	22	12.6824	0	19	360	22	12.6824	0					
IRON40	IRON81	1	570	0.18183	0	0	9	12	6			1	440	22	16.8707	0	19	356	22	16.8707	0					
IRON40	IRON82	1	570	0.18183	0	0	9	12	6			1	440	22	16.8707	0	19	356	22	16.8707	0					
LITT40	LITT81	1	800	0.3104	0	0	9	10	5			1	440	22	15.8134	0	19	356	22	15.8134	0					
LITT40	LITT82	1	800	0.3104	0	0	9	10	5			1	440	22	15.8134	0	19	356	22	15.8134	0					
LITT40	LITT83	1	800	0.3104	0	0	9	10	5			1	440	22	15.8134	0	19	356	22	15.8134	0					
DIDC42	DIDC81	1	600	0.4098	0	0	9	10	9			1	440	22	16.6352	0	19	360	22	16.6352	0					
DIDC42	DIDC82	1	600	0.4098	0	0	9	10	9			1	440	22	16.6352	0	19	360	22	16.6352	0					
DIDC41	DIDC83	1	600	0.4098	0	0	9	10	9			1	440	22	16.6352	0	19	360	22	16.6352	0					
DIDC41	DIDC84	1	600	0.4098	0	0	9	10	9			1	440	22	16.6352	0	19	360	22	16.6352	0					
FIDF82	FIDF22	1	570	0.26277	0	0	9	7	2			1	22	302.5	16.8319	0	19	22	220	16.8319	0					
FIDF81	FIDF21	1	570	0.25536	0	0	9	7	2			1	22	302.5	16.5622	0	19	22	220	16.5622	0					
FIDF21	FIDF83	1	570	0.25536	0	0	9	7	2			1	302.5	22	16.5622	0	19	220	22	16.5622	0					
FIDF22	FIDF84	1	570	0.26277	0	0	9	7	2			1	302.5	22	16.8319	0	19	220	22	16.8319	0					
CONQ12	DEES40	1	240	0.2544	0	0.13208	9	11	13	CONQ12	132	1	151.8	400	19.0025	0	15	125.4	400	19.0025	0					
CONQ12	DEES40	2	240	0.2544	0	0.13208	9	11	13	CONQ12	132	1	151.8	400	19.0025	0	15	125.4	400	19.0025	0					
BRIM2A	BRIM8A	1	240	0.38856	0	0.10458	9	10	10			1	316	22	19.7038	0	19	220	22	19.7038	0					
TEES8A	GREY21	1	200	0.2558	0	0	9	10	8			1	22	316.25	20.8124	0	19	22	233.75	20.8124	0					
TEES8B	GREY21	1	200	0.2674	0	0	9	10	8			1	22	316.25	20.9319	0	19	22	233.75	20.9319	0					
GREY21	TEES8C	1	200	0.279	0	0	9	10	8			1	316.25	22	20.9321	0	19	233.75	22	20.9321	0					
TEES8D	GREY21	1	200	0.2714	0	0	9	10	8			1	22	316.25	20.8126	0	19	22	233.75	20.8126	0					
TEES8S	GREY21	1	400	0.18	0	0	9	10	6			1	22	316.25	13.4262	0	19	22	233.75	13.4262	0					
TEES8E	GREY22	1	200	0.2558	0	0	9	10	6			1	22	316.25	20.6992	0	19	22	233.75	20.6992	0					
GREY22	TEES8F	1	200	0.2674	0	0	9	10	6			1	316.25	22	20.8125	0	19	233.75	22	20.8125	0					
TEES8G	GREY22	1	200	0.279	0	0	9	10	6			1	22	316.25	20.6995	0	19	22	233.75	20.6995	0					
GREY22	TEES8H	1	200	0.2666	0	0	9	10	6			1	316.25	22	20.6993	0	19	233.75	22	20.6993	0					

Sending Node	Receiving Node	Index	Rated Power (MVA)	Copper Losses %	Iron Losses %	Magnetising Current %	Saturation Exponent	Nominal Tap	Initial Tap	Regulation Node	Target Volts	Tap No.	Sending Volts	Receiving Volts	Leakage Impedance %	Phase Shift °	Tap No.	Sending Volts	Receiving Volts	Leakage Impedance %	Phase Shift °	Tap No.	Sending Volts	Receiving Volts	Leakage Impedance %	Phase Shift °
TEES8T	GREY22	1	400	0.1869	0	0	9	10	6			1	22	316.25	13.2763	0	19	22	233.75	13.2763	0					
CRUA2B	CRUA83	1	999	2.88711	0	0.19444	9	10	8		22	1	305.25	22	95.1486	0	19	247.5	22	95.1486	0					
CRUA2B	CRUA84	1	999	2.88711	0	0.19444	9	10	8		22	1	305.25	22	95.1486	0	19	247.5	22	95.1486	0					
PEHE20	PEHE8A	1	999	0.96903	0	0.19444	9	13	11		22	1	332.75	22	47.9618	0	19	247.5	22	47.9618	0					
PEHE20	PEHE8B	1	999	0.96903	0	0.19444	9	13	11		22	1	332.75	22	47.9618	0	19	247.5	22	47.9618	0					
PEHE20	PEHE8C	1	999	0.96903	0	0.19444	9	13	11		22	1	332.75	22	47.9618	0	19	247.5	22	47.9618	0					